Investigating Acuros BrachyVision dose calculation accuracy in various materials relevant to high dose rate brachytherapy using GATE

Tyrone Te Ruruku, BSc.

A thesis submitted for the Degree of Master of Science in Medical Physics

Physics and Astronomy
University of canterbury
New Zealand

May 2020

Investigating Acuros BrachyVision dose calculation accuracy in various materials relevant to high dose rate brachytherapy using GATE

Tyrone Te Ruruku

Abstract

The AAPM Task Group No.43 has provided a standardised dose calculation methodology that is now the international benchmark for all brachytherapy dosimetry publications and treatment planning systems (TPS). However, limitations of this methodology has seen the development of model-based dose calculation algorithms. In 2009, Varian Medical Systems released Acuros BrachyVision (ABV) which calculates doses by explicitly solving the Linear Boltzmann Transport Equation. This study aims to investigate the accuracy of ABV dose calculations in various materials relevant to high dose rate (HDR) brachytherapy with an Iridium-192 GammaMed Plus source. This study is comprised of two main parts:

1. Construct and validate a monte carlo model of an Iridium-192 GammaMed Plus HDR source. Energy spectrum and TG43 parameters were simulated and compared to results collated in studies conducted by Taylor and Rogers [1] and Ballester et al. [2].
2. Calculate and compare doses calculated within a series of phantoms using both GATE and ABV. Comparison techniques used were; (i) point-to-point profile comparison; (ii) 1D gamma analysis; and (iii) correlation and statistical significance analysis.

Source validation results yielded good agreement with published data. Spectrum and TG43 comparisons showed no major differences, with TG43 comparisons agreeing within 1%. Point-to-point comparisons showed large differences between GATE and ABV near the source and in low density materials. 1D gamma analysis pass criteria of 2%/2 mm and 2%/1 mm produced pass rates ranging between 59% - 100% and 45% - 100% respectively. Correlation analysis Showed statistically there is no significant difference between doses calculated in ABV and GATE. A critical analysis of this study's results suggest that ABV is unable to accurately calculate doses in low density materials. Furthermore, spatial distribution of dose near the source is within 2 mm.

Acknowledgements

I would like to extended my gratitude to my supervisors; Dr Felix Wong and Dr Steven Marsh who have provided guidance throughout this entire study.

I would also like to extend thanks to my work colleagues at the Waikato Regional Cancer center for their continuous support.

Finally, to my family and friends, for the love and morale support that is forever endless I thank you.

Contents

List of Figures

List of Tables

Chapter 1

Introduction

Cancer is a generic term used for a large number of diseases that are caused by normal cells progressively mutating, uncontrollably proliferating outside their usual boundaries, invading other areas of the body and spreading to other organs [3]. According to World Health Organisation statistics, cancer is the second leading cause of death worldwide. In 2018 cancer accounted for 9.6 million deaths, where the most common cases were lung (2.09 million cases), breast (2.09 million cases), colorectal (1.80 million cases), prostate (1.28 million cases), Non-melanoma skin cancer (1.04 million cases) and stomach (1.03 million cases) [3]. With the development of modern medicine, approximately 50 percent of all cases can benefit from radiation therapy (RT) [4].

RT is administered through multiple modalities, with the most common modality being external beam radiation therapy (EBRT) [5]. This modality aims to conform dose to a treatment volume by directing photons or electrons at a tumour from outside of the body. An alternative to EBRT is brachytherapy, which for the most part can be referred to as an internal RT technique. In contrast to EBRT, brachytherapy is capable of maximising dose to the treatment volume and minimising dose to neighbouring tissues [6] due to the rapid dose fall off with increasing distance from the seed [7].

Traditionally, Radium-226 (Ra226) was the isotope of choice in HDR brachytherapy applications. However, it posed major safety concerns as a ruptured Ra226 source would result in α particles and radon gas being absorbed by nearby tissue and bone. This isotope was therefore replaced with less hazardous radionuclides such as cobalt-60, gold-198, tantalum-182, and cesium-137 [8, 9]. In 1958 Iridium-192 (Ir-192) replaced all these isotopes and is now established as the preferred isotope for high dose rate (HDR) brachytherapy [10].

As brachytherapy sources evolved, so did the dosimetry systems used to plan brachytherapy treatments. Brachytherapy dosimetry systems established in the early 1900's included the Stockholm, Paris, Quimby, Paterson-Parker and Manchester system. Each system denoted a set of rules that defined the geometric arrangement, source strength and methodology to obtain a desired dose distribution [11]. Major limitations of early brachytherapy dosimetry systems are their inability to personalise treatment plans and the lack of consideration for attenuation and scatter effects [8].

In practice, scatter and attenuation cannot be ignored. Furthermore, personalised treatments plans are highly desirable. In 1995 the American Association of Physicists in Medicine (AAPM) Task Group No. 43 published their dosimetry protocol (TG43) which included a new brachytherapy dose calculation formalism. In contrast to earlier dosimetry systems, TG43 parameters incorporated measureable quantities that accounted for source-to-source differences in encapsulation and internal construction. Since the publication of TG43, the number of source models commercially available increased dramatically, the National Institute of Standards and Technology (NIST) introduced a new primary standard for air kinetic energy released per unit mass (kerma) strength and brachytherapy dosimetry literature substantially grew [12, 13]. In response, the AAPM published an updated version of TG43 and it was termed TG43U1. Improvements presented in TG43U1 included quantity revisions and eliminations, guidance on interpolating and extrapolating tabulated parameters, and corrections for inconsistencies and omissions in TG43 and its implementation. TG43U1 has provided a standardised dose calculation methodology and is now the international benchmark for all brachytherapy sources in brachytherapy dosimetry publications and treatment planning systems (TPS) [14, 15].

TG43U1 parameters are based on a collection of simulations made in an infinite homogeneous water phantom. In clinical applications, where patients and applicators are not homogeneous and have finite dimensions, these parameters may lead to inaccurate dose calculations. Studies have shown that clinically accepted parameters can be over- or under- by at least 5% [16]. A possible solution to improve on TG43U1 are model-based dose calculation algorithms (MBDCAs). Model-based approaches either explicitly simulate radiation transport or employ mathematical tools such as integration and point spread functions. In 2009, Varian Medical Systems released Acuros BrachyVision (ABV) which calculates dose by explicitly solving the Linear Boltzmann Transport Equation (LBTE) [17]. LBTE solvers are in their infancy but are expected to play an important role in future TPS dose calculation algorithms [18]. A large number of studies compare Monte Carlo (MC) and LBTE method results as they are both expected to converge to the same solution [19, 20].

1.1 Purpose

The aim of this study was to assess the dose calculation accuracy of ABV in various materials that are relevant to HDR brachytherapy. This was achieved by,

- Developing and validating a MC model of a GammaMed plus (GMP) HDR brachytherapy source
- Making comparisons between MC and ABV calculated doses

MC modelling of the GMP HDR brachytherapy source was done using the Geant4 Application for Emission Tomography (GATE). The MC model was validated by comparing simulated photon spectra and TG43 factors with published data [1, 2, 13].

Once the source model was validated, MC and ABV calculated doses were compared. This was done by completing the following tasks: **(i)** produce identical digital heterogeneous phantoms in both GATE and ABV, **(ii)** compare GATE and ABV calculated doses by comparing profiles that span across all materials in the phantom. Tasks (i) and (ii) were repeated for all anatomical materials defined in ABV and solid applicator materials stainless steel, peek and PMMA.

Chapter 2

Background

In this chapter I will begin by introducing some fundamental RT concepts that will provide a knowledge base for later sections. These concepts will include fundamental quantities and interactions that may occur when ionizing radiation(IR) penetrates through tissue. Following this, I will discuss the models used to determine the overall effect IR has on a single cell and a population of cells that make up living tissue. This will help the reader understand why, if used properly, radiation can be used for cancer treatment. Thereafter, I will provide an overview of how brachytherapy treatments are delivered. This study's main focus is HDR brachytherapy, however later sections will compare HDR and LDR to provide a holistic view of possible brachytherapy treatments. I will then provide overviews of TG43 and Varian's LBTE solver Acuros BrachyVision (ABV). Finally, I will introduce the Geant4 Application for Emission Tomography (GATE) MC package. Given that there is some uncertainty around the accuracy of ABV, GATE was used as the primary tool to investigate the dose calculation accuracy of ABV in various materials relevant to HDR brachytherapy.

2.1 Fundamental Concepts in Radiation Dosimetry

The primary quantity of concern in RT is absorbed dose, where the International Commission of Radiation Units and Measurements [21] define it as the mean energy $d\epsilon$ imparted by IR in a given mass dm.

$$\mathrm{D}=\frac{\mathrm{d}\epsilon}{\mathrm{dm}} \tag{2.1}$$

The first step towards calculating dose is to determine the photon fluence [8],

$$\phi=\frac{\sum \delta \mathrm{s}}{\mathrm{dV}} \tag{2.2}$$

where $\sum \delta$s is the sum of all photon track lengths that pass through volume dV.

Following this we must calculate the kinetic energy released per unit mass (kerma) [8],

$$K = \frac{dE_{tr}}{dm} \tag{2.3}$$

where dE_{tr} is the sum of the initial kinetic energies of all electrons liberated in a mass dm. Additionally kerma must be separated into collisional kerma (K_{col}) and radiative kerma (K_{rad}), where both these quantities will quantify the amount of energy lost by ionizing particles due to collisional and radiative energy losses [8].

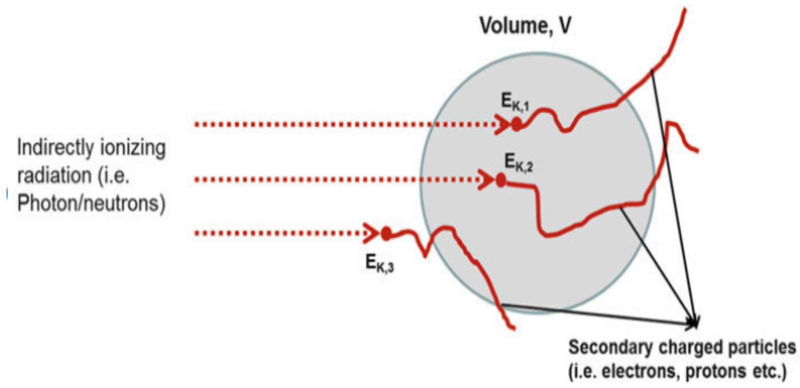

Figure 2.1: Schematic of kerma [22].

Under charged particle equilibrium (CPE) we can then estimate dose as follows [8, 23],

$$D \approx K_{col} = \int_0^{Emax} E\phi_E E\Big(\frac{\mu_{en}(E)}{\rho}\Big)_{med} dE \tag{2.4}$$

where $\frac{\mu_{en}(E)}{\rho}$ and ϕ_E are the mass energy absorption coefficient and photon fluence respectively, for photons with energy E.

In the process of dose deposition, photons and electrons undergo countless interactions. The interactions of primary interest in this study are presented in the following sections.

2.1.1 Photon Interaction Processes

Photons penetrating through tissue are attenuated through a countless number of interactions with atoms that make up the medium. Photon-atom interactions may be between the photon and a loosely bound electron, a tightly bound electron or the nucleus [23].

The probability or cross-section of a photon interacting with an electron or atom is proportional to photon energy hv, and the atomic number Z of the medium. [23]. An iridium-192 source has a max energy of 1.378 MeV [24], which means the dominant photon interactions will be the Photoelectric effect and Compton Scattering [23]. This is illustrated in figure 2.2

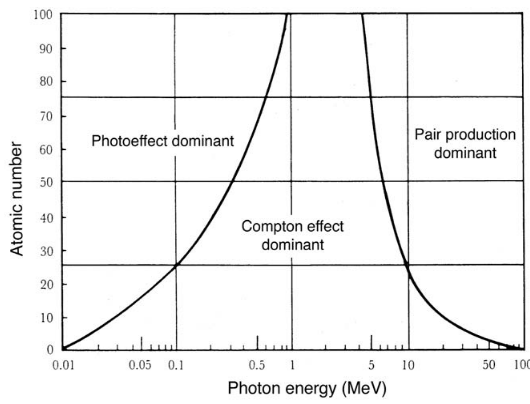

Figure 2.2: Dominant physical processes of photon interactions in matter as a function of photon energy and atomic number Z.

The Photoelectric Effect

The photoelectric effect (PE) refers to an interaction between a photon and a tightly bound electron [25]. The tightly bound electron absorbs the incoming photon, providing it with a sufficient amount of energy to be ejected from the atom as a photoelectron with a kinetic energy T,

$$\mathrm{T}{=}\mathrm{hv} - \mathrm{E_B} \tag{2.5}$$

where hv is the incident photon energy and $\mathrm{E_B}$ is the electron binding energy. The ejected photoelectron will produce a vacancy in the atom which will then result result in the emission of characteristic x-rays or Auger electrons [23].

The PE cross section (i.e. the probability that a photon will interact with an atom via the photoelectric effect) is inversely proportional to the third power of the energy and increases with the fourth power of the attenuators atomic number.

$${}_{\mathrm{a}}\tau \propto \frac{\mathrm{Z}^4}{(\mathrm{hv})^3} \tag{2.6}$$

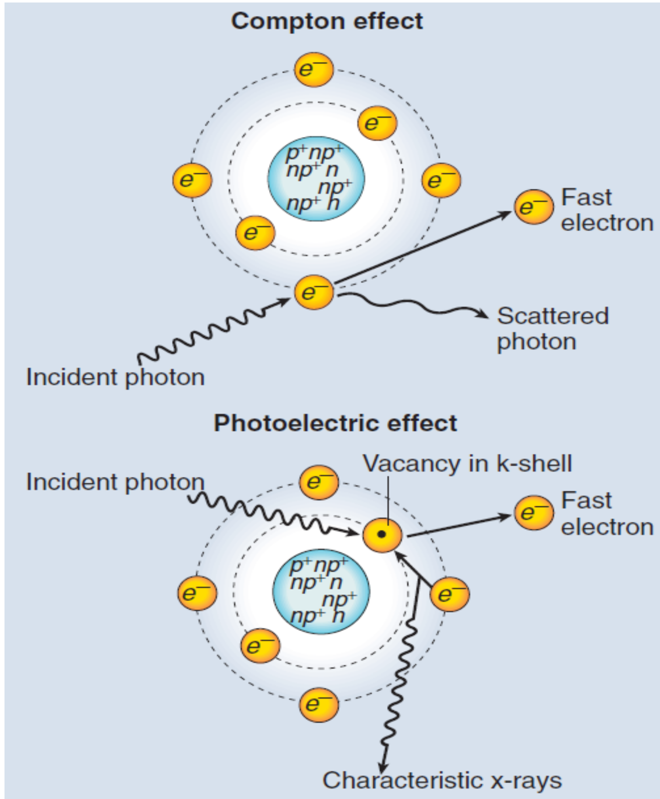

Figure 2.3: Schematic of Compton scattering and the photoelectric effect.

Compton Scattering

Also known as incoherent scattering, Compton scattering refers to the interaction of a photon with a free electron (Figure 2.3) [23]. The incident photon, carrying energy hv, will impart a fraction of its energy to the orbital electron and eject it from the atom. The incident photon will be scattered with a kinetic energy of hv' at an angle ϕ, where ϕ is the angle between the initial and final propagation directions (equation 2.7). The electron will be ejected with a kinetic E_k (equation 2.8) at an angle θ, where θ is the angle between the incident direction and the direction of the recoil electron.

$$\mathrm{hv'}{=}\mathrm{hv}\frac{1}{1+\epsilon(1-\mathrm{Cos}(\phi)} \tag{2.7}$$

$$\mathrm{E_k}{=}\mathrm{hv}\frac{\epsilon(1-\cos\phi)}{1+\epsilon(1-\mathrm{Cos}(\phi))} \tag{2.8}$$

$$\epsilon{=}\frac{\mathrm{hv}}{\mathrm{m_e c^2}} \tag{2.9}$$

The Compton scattering cross section is expressed using the Klein-Nishina differential equation (equation 2.10) [8]. Integrating equation 2.10 will provide an expression for the total Klein-Nishina cross section per electron (equation 2.11). The total cross section per atom is ${}_{\mathrm{a}}\sigma_{\mathrm{KN}}{=}\mathrm{Z_e}\sigma_{\mathrm{KN}}$ [8].

$$\frac{\mathrm{d_e}\sigma_{\mathrm{KN}}}{\mathrm{d}\sigma}=\frac{\mathrm{r_e^2}}{2}\left(\frac{\mathrm{hv'}}{\mathrm{hv}}\right)^2\left(\frac{\mathrm{hv'}}{\mathrm{hv}}+\frac{\mathrm{hv}}{\mathrm{hv'}}-\mathrm{Sin}^2\phi\right) \tag{2.10}$$

$$_{\mathrm{e}}\sigma_{\mathrm{KN}}=2\pi\mathrm{r_e^2}\left(\frac{1+\epsilon}{\epsilon^2}\left[\frac{2(1+\epsilon)}{1+2\epsilon}-\frac{\ln(1+2\epsilon)}{\epsilon}\right]+\frac{\ln(1+2\epsilon)}{2\epsilon}-\frac{1+3\epsilon}{(1+2\epsilon)^2}\right) \tag{2.11}$$

2.1.2 Electron Interaction Processes

The outcome of photoelectric and compton interactions is the liberation of electrons, and it is these electrons that deposit energy (i.e. dose) to the medium. Electrons will interact with atomic nuclei and orbital electrons through direct Coulomb interactions. Through these interactions, they will lose kinetic energy through collisional or radiative losses and change their direction of travel (i.e. scattered). The energy lost by an electron as it is scattered through a medium is described by the stopping power of the medium.

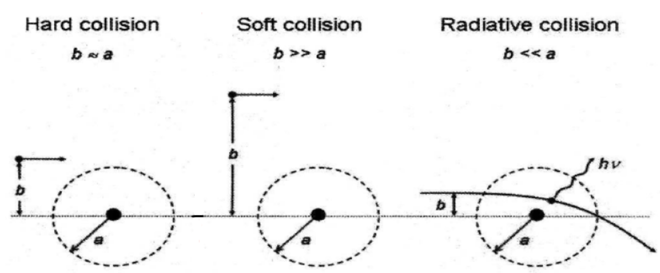

Figure 2.4: Schematic for hard, soft and radiative collisions.

Electron interactions are for the most part inelastic and are termed soft, hard and radiative collisions. The type of collision an electron will have with an atom of radius **a** is determined by the impact parameter **b**, where the impact parameter is the perpendicular distance to closest approach between the incident electron and the nucleus of the target atom before an interaction (figure 2.4 [26]). Soft collisions will occur when **b**»**a**. The incident electron will interact with the entire atom and only transfer a small fraction of its energy to orbital electrons. Hard collisions will occur when **b** $\approx$ **a**. The incident electron will interact with an orbital electron and in doing so will transfer a large fraction of it energy. Lastly there are radiative collisions, which occur when **b** « **a**. The incident electron will divert from its original direction and emit a bremsstrahlung photon in the process. The energy of the bremsstrahlung photon is determined by the magnitude of **b**.

Stopping Power

The energy lost through hard, soft and radiative are described by the total stopping power of the medium [23]. The total stopping power is defined as the amount of energy lost by an electron per unit length and therefore carries units of MeV/cm. Inelastic electron interactions have two outcomes; (i) energy transfer to orbital electrons; or (ii) electron scatter resulting in the emission of a bremsstrahlung photon. Given these two outcomes, the total stopping power can be separated into two components: collisional stopping power, which describes the amount of energy transferred to orbital electrons, and radiative stopping power which describes the amount of energy lost through bremsstrahlung photon emission. Ultimately, stopping powers will determine the range of an electron in any given medium.

Electron stopping powers are calculated using the Bethe theory [23, 26],

$$-\frac{\mathrm{dE}}{\mathrm{dx}}=\frac{4\pi \mathrm{z}^2\mathrm{e}^4\mathrm{n}}{\mathrm{mc}^2\beta^2}\left[\ln\frac{2\mathrm{mc}^2\beta^2}{\mathrm{I}(1-\beta^2)}-\beta^2\right] \tag{2.12}$$

where z is the atomic number of the incident particle, e is the magnitude of electron charge, n is the number of electrons per unit volume of the medium, m is electron mass, c is the speed of light in vacuum, β is the speed of the electron relative to c and I is the mean excitation energy of the medium.

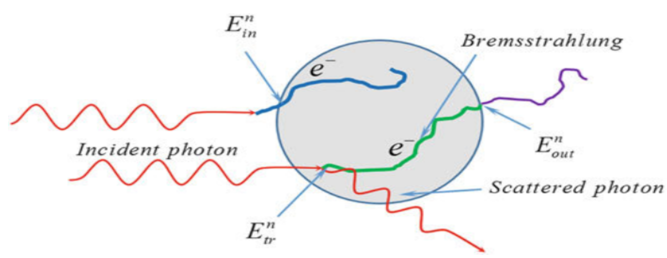

Figure 2.5: Schematic of photon and electron interactions resulting in dose deposition [22].

2.2 Radiobiology

With a basic understanding of dose and how IR deposits energy in a medium, this section will discuss the overall effect IR has on both a single cell and population of cells.

Photoelectric and Compton interaction inside or nearby a cell will result in interactions with a cells deoxyribonucleic acid (figure 2.6) [27]. These interactions may inflict single (sub-lethal) and/or double (lethal) strand breaks [28]. A single cell's response to these breaks may include damage repair, apoptosis, mitosis delay, mitotic death, mutation, genomic instability, transformation, increased radioresistance and induced damage to unexposed cells surrounding exposed cells via the bystander effect. The probability of inducing cell death after being exposed to IR is based on the number of double strand breaks [29].

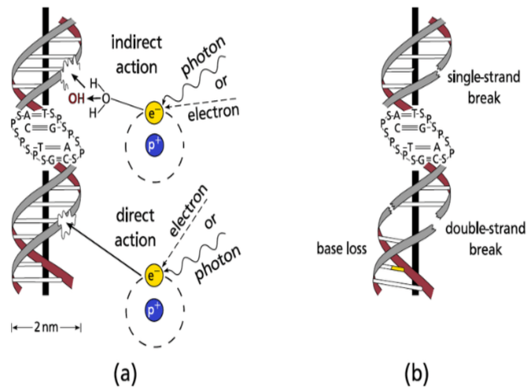

Figure 2.6: Direct and indirect interactions of IR with DNA resulting in single and double strand breaks.

Given that a tumour is a population of cells, we must consider them as a whole. The most common tool used to quantify the effects of IR on a population of cells is the Linear quadratic (LQ) model [30]. It is a model that describes the relationship between absorbed dose and the fraction of clonogenic cells surviving a single exposure,

$$\mathrm{SF}{=}\mathrm{e}^{-\alpha\mathrm{D}-\beta\mathrm{D}^2} \tag{2.13}$$

where SF is the surviving fraction of cells, D is the dose delivered to the cells, and α and β are numerical constants that quantify cell radiosensitivity [28, 31]. An example of an LQ model plot is shown in figure 2.7

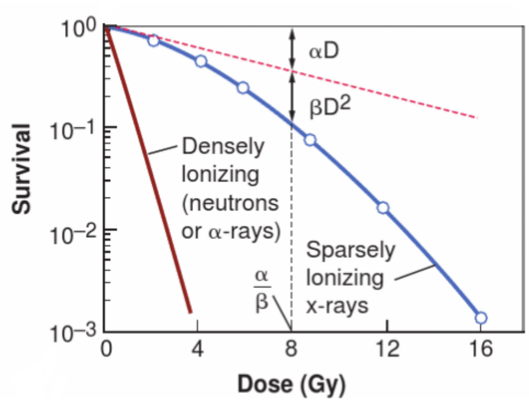

Figure 2.7: A linear quadratic model plot [28].

The shape of the LQ plot is determined by the α (linear) and β (quadratic) constants, where α (linear) and β (quadratic) are constants that vary from tissue to tissue and are presented in literature as a ratio, α/β.

In general, most tumours will have high α/β ratio and can be termed early responding tissues, whereas most normal tissues will have low α/β ratio and can be termed late responding tissues [32]. A comparison of early and late responding tissue using the LQ model is shown in figure 2.8. This figure highlights that at lower doses, a larger fraction of healthy tissue cells (i.e. late responding) can be spared than for cancerous tissue cells (i.e. early responding).

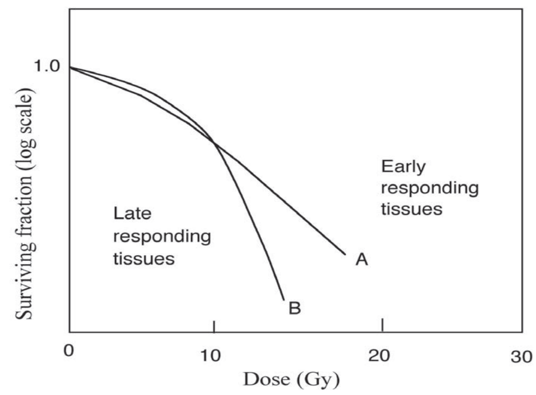

Figure 2.8: A comparison of early and late responding tissues using an LQ plot [23].

The efficacy of all RT techniques can be expressed using two probabilities: (i) tumour control probability, TCP, and (ii) the normal tissue complication probability, NTCP [33]. The TCP-NTCP model is a theoretical model based on a sigmoidal response (figure 2.9). The disparity between the TCP and NTCP curves are governed by α/β ratios and fractionation regimens used for treatment [34]. In a clinical situation, an optimal treatment plan will present a NTCP$\leq$ 5% and a TCP$\geq$ 50% [28].

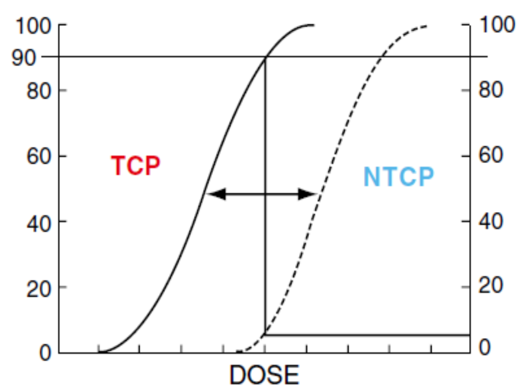

Figure 2.9: TCP-NTCP model plot.

Given brachytherapy is capable of minimising dose to normal healthy tissue, the disparity between the NTCP and TCP curves can be pushed further apart. Furthermore, with respect to the LQ model, SF will approach zero more rapidly for cancer cells as there is minimal dose deposited in healthy tissue. However, It should be noted that dose to healthy tissue is only minimised, not eliminated. Therefore measures such as fractionation must be used to avoid healthy tissue complication. Additionally, fractionation will allow for the SF of cancer cells to increase their radiosensitivity.

2.2.1 The Four R's of Radiobiology

The efficacy of fractionation is based on radiobiological experiments that gave birth to the 'Four R's of radiobiology'. Fractionation allows sub-lethal cell damage to **repair**, **repopulate**, **re-oxygenate** and **redistribute** through the mitotic cell cycle [28]. A summary of the four R's of radiobiology are as follows:

Repair: IR may inflict lethal or sub-lethal cell DNA damage. The ability to repair damage varies between normal tissue cells and tumour cells [29]. Time between fractions allows critical healthy tissues to repair and minimise NTCP.

Redistribution: Cells display differential radiosensitivity in different phases of the mitotic cycle. Radiosensitivity is high in the late G2 and M phase, less radiosensitive during the G1 phase and most resistant during the S phase [29]. Time between fractions allows for surviving cells in more radio resistant phases to redistribute into less radiosensitive phases [28].

Repopulation: Time between fractions will allow repaired tumour and normal tissue cells to repopulate [28, 29]. Even though this means tumour size will increase in this time, the LQ model suggests that more tumour cells than normal tissue cells are killed in any given fraction [25]. Therefore SF will approach zero more rapidly for tumour cells than for normal tissue cells.

Reoxygenation: Studies have shown that cell radiosensitivty depends heavily on the oxygen levels within the cell. The reason for this is that the extent of damage caused by free radicals is proportional to the amount of oxygen in the cell. The presence of oxygen in a cell that has been exposed to IR will result in free radicals inflicting non-restorable damage to the chemical composition of the cell DNA [28]. Oxygen levels will vary throughout the mitotic cycle and the separation between a cell and its nearest blood supply. Normoxic, hypoxic and anoxic cells refer to cells with high, medium and low oxygen levels, respectively. Eradicating cells close to a blood supply may result in an increase in blood flow to hypoxic and anoxic cells. Either from an increase in blood flow and/or redistribution, time between fractions allows for radiosensitvity to increase and therefore improve the efficacy of the treatment.

2.3 Brachytherapy

A comparison between EBRT and brachytherapy would show that, relative to the TCP-NTCP model, brachytherapy may achieve superior TCP values [35]. Minimising dose to healthy tissue and maximising dose to the tumour is highly desirable. A complete comparison covering all variables shows that brachytherapy is best suited for small and localised tumours at specific anatomical sites. Brachytherapy will often be used to treat cancers in the head and neck region, breast, cervix, prostate and eye [36].

Given that both LDR and HDR brachytherapy can be used to treat similar types of cancer, the following section will provide a brief overview of both HDR and LDR, and thereafter will highlight some of the key advantages and disadvantages of HDR when compared to LDR.

2.3.1 LDR

Uniform dose distributions in LDR are achieved by implanting a large number of radioactive seeds in or near the target volume for long periods of time [37]. Traditionally physicists were required to manually load all needles and applicators. This was followed by a physician manually implanting the seeds into their planned locations. In some cases the physician was also tasked with fixing the applicator in place for the duration of the treatment, where treatments could last several hours to several days [38].

Radionuclides used in LDR include palladium-103, caesium-131 and iodine-125, with the most commonly used being the latter. Iodine-125 decays to Tellurium-125 via electron capture, emits characteristic x-rays with energies of 27.4 and 31.4 keV and has a half life of 59.6 days.

2.3.2 HDR

In contrast to LDR, uniform dose distributions are achieved in HDR by placing a single source at multiple dwell positions for dwell times as small as 0.1 sec. In preparation for an HDR procedure, a physician's task is to insert and stabilize all applicators and needles required for treatment inside the patient. Transfer guide tubes are used to connect each needle or applicator to a remote afterloader (RAL) system (figure 2.10 [39]). Following this, everyone except for the patient will exit the room and treatment will commence.

Figure 2.10: Varian's GammaMed iX remote afterloader.

Radionuclides used in HDR include Caesium-137, Cobalt-60 and iridium-192, with the most favoured isotope being the latter [40]. Iridium-192 decays via beta minus decay (95.6%) to excited states of Platinum-192 and electron capture (4.4%) to excited states of Osmium-192 [9]. It has a half life of 73.8 days and emits photons with an average energy of 380 keV [40].

2.3.3 HDR Vs LDR

Given that HDR is more commonly used, the following section will present some of the advantages and disadvantages of HDR when compared to LDR.

Advantages that HDR has over LDR include,

Stable applicator positioning: For intracavitary HDR procedures (e.g. gynaecological brachytherapy), treatments will typically require the patient to be immobilized in the lithotomy position using straps and stirrups. This results in less movement of the patient and the applicator. Studies have reported applicators will move on average 2mm throughout the procedure, where as in LDR on average they will move up to 2 cm [37].

Outpatient treatment: HDR procedures are typically outpatient based, and therefore allowing the patient to return home after each fraction of treatment is complete.

Reduced radiation exposure to staff: A major advantage of HDR is that all involved in the procedure is required to leave the treatment room before patient radiation exposure can commence. With sufficiently shielded walls and doors, radiation exposure to all personnel are kept to a minimum.

Disadvantages of HDR when compared to LDR include,

Treatment Unit complexity: Compared with traditional LDR processes of manually loading sources, HDR requires more complex equipment. With transfer guide tubes to guide the source from the RAL to the applicator or needles inside the patient and treatment software that connects the TPS to the RAL, there are notably more parameters to consider in HDR when compared to LDR [37].

Radiobiology: The major disadvantage for HDR is a result of its radiobiological effects. When compared to LDR, HDR inflicts more damage to normal tissue cells and by doing so reduces the therapeutic ratio [28, 37].

Potential for high radiation exposure: An HDR source has the potential to get stuck in a position out side of its safe or break off its wire. In any case where the source is stuck outside its safe, the patient may be exposed to dangerously high levels of radiation. Furthermore, the physicist who enters the room to remove the source may potentially receive an exposure above the allowed limits.

2.4 Dose Calculation Algorithms

At the Waikato Regional Cancer Center (WRCC), all brachytherapy treatments are planned using BrachyVision treatment planning software (BV). BV is a subsystem within Varian's oncology information system ARIA and provides a comprehensive tool-set to increase consistency and efficiency in the brachytherapy planning process. BV is divided into different applications, each used for specific tasks within the the treatment planning process. Some of these tasks include, defining patient anatomy, planning applicator or source positions and computing dose [41]. In BV, the latter can be achieved using either the TG43 formalism or Acuros (ABV). The TG43 formalism calculates dose using multitude of predefined terms, where as ABV calculates dose by solving the Linear Boltzmann Transport Equation. The following sections will provide an overview of the TG43 formalism and how ABV solves the LBTE.

2.4.1 AAPM TG43 Dose Calculation Formalism

In 1995, the American Association of Physicists in Medical Physics Task group No. 43 published their report on dosimetry of interstitial brachytherapy sources [9], and is now globally referred to as TG43. Presented in this document was a recommended dose calculation formalism that progressively became the worldwide standard for brachytherapy dose calculations [12, 15]. It also provided dosimetry data sets for commercially available sources at the time of its publication. In 2004, the AAPM published a revised AAPM protocol for brachytherapy dose calculations [12] and was later termed TG43U1. TG43 protocol was updated for the following reasons:

- To eliminate inconsistencies and omissions in the original TG43 document.
- To recommend consensus datasets for iodine-125 and palladium-103 source models introduced before and after the publication of the TG43 protocol in 1995.
- To develop guidelines for experimental and MC determination of reference-quality dose distributions.
- To provide additional AAPM recommendations for acquiring dosimetry data and clinical implementation.

The general 2D formalism presented in TG43 was retained in TG43U1,

$$\mathrm{D}(\mathrm{r},\theta)=\mathrm{S_k}\Lambda\left(\frac{\mathrm{G_L}(\mathrm{r},\theta)}{\mathrm{G_L}(\mathrm{r_0},\theta_0)}\right)\mathrm{g_L}(\mathrm{r})\mathrm{F}(\mathrm{r},\theta) \tag{2.14}$$

where r is the distance to the point of interest in centimetres and θ is the angle with respect to the longitudinal axis of the source. The reference point to which the formula is normalised to is denoted by $(\mathrm{r_0}, \theta_0)$ and lies on the transverse bisector of the active core of the source at a distance of 1 cm, i.e., r = 1 cm and $\theta = 90$ deg. TG43 and TG43U1 assumes all seeds and dose distributions surrounding a source are cylindrically symmetrical, with the origin of the co-ordinate system at the center of the active core.

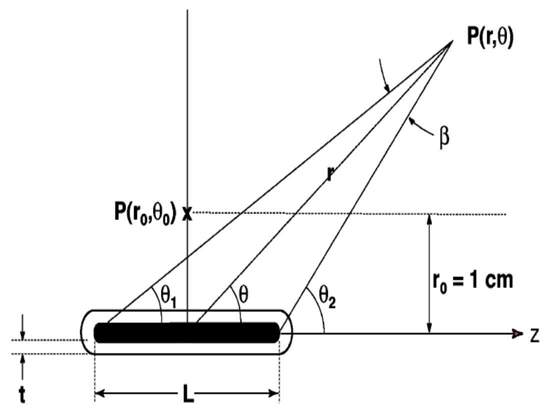

Figure 2.11: TG43 and TG43U1 dosimetry calculation co-ordinate system.

The first term in equation 2.14, S_K, is the air kerma Strength (AKS). AKS was first introduced in TG-32 Report No. 21 and is presented in TG43 as a measure of source strength. TG43 defines the air kerma strength as the product of the air kerma rate, $\dot{k}$, at the calibration point along the transverse bisector of the source in free space and the square of the distance, d, between the calibration point and the origin [42]. TG43U1 proposed minor revisions to this definition by explicitly stating experimental set up conditions and excluding photons that would increase air kerma rate without significantly contributing to dose at distances greater than 1 mm in tissue [12]. With these revisions, the current equation to be used for calculating air kerma strength is,

$$S_k = \dot{k}_\delta r^2 \tag{2.15}$$

where δ is the cut off energy. Air kerma strength carries units of $cGycm^2h^{-1}$. However, for simplicity, TG43 and TG43U1 denotes the units of S_K with the symbol U.

$$1U = 1cGycm^2h^{-1} = 1\mu Gym^2h^{-1} \tag{2.16}$$

The second term in equation 2.14, Λ, is the dose rate constant (DRC). This term is defined as the dose rate in water to a point 1 cm away from the source along the transverse axis (i.e. r = 1 cm, $\theta = 90$ deg) for a unit air kerma strength source. It is an absolute quantity that converts S_k, which is measured in air, to dose rate to water, in a water phantom.

$$\Lambda = \frac{\dot{D}(r_0, \theta_0)}{S_k} \tag{2.17}$$

The dose rate constant includes effects due to radionuclide distribution in the source, source geometry, encapsulation, filtration and scatter due to the capsule and the phantom. Λ has units of cGy $h^{-1}U^{-1}$.

The third term in equation 2.14, $\left(\frac{G_L(r,\theta)}{G_L(r_0,\theta_0)}\right)$, is a ratio of the geometry function calculated at both the reference point and the point of interest. The geometry function provides an effective inverse square law correction for a line source and neglects all scatter and absorption effects. For a point and a finite line source, the geometry function at all points can be modeled using the following equations,

$$G_P(\mathbf{r},\theta){=}\mathrm{r}^{-2} \tag{2.18}$$

$$\mathrm{G_L}(\mathbf{r},\theta){=}\begin{cases}\beta/(\mathrm{L r}\sin\theta) & \text{if } \theta \neq 0^o\\ \\ (\mathrm{r}^2-\mathrm{L}^2/4)^{-1} & \text{if } \theta{=}0^o\end{cases} \tag{2.19}$$

where β is the angle between two hypothetical lines starting at each end of the source and meeting at the point of interest, P(r,θ), and L is the active length of the source. TG43U1 recommends consistent use of the line source approximation models when evaluating 2D dose distributions.

The fourth term in equation 2.14, $\mathrm{g_L}(\mathrm{r})$, is the radial dose function. This function is a relative quantity that accounts for scatter and absorption effects across the transverse plane (i.e. $\theta_0{=}\pi/2$) caused by the medium and the encapsulation around the active core. TG43U1 made a minor revision to the radial dose function formalism, and added the subscript "X". This subscript was used to indicate whether a line source, "L", or a point source, "P", approximation model was used to calculate the geometry function. The radial dose function given in TG43U1 is as follows,

$$\mathrm{g_X}(\mathbf{r}){=}\frac{\dot{\mathrm{D}}(\mathbf{r},\theta_0)\mathrm{G_X}(\mathbf{r}_0,\theta_0)}{\dot{\mathrm{D}}(\mathbf{r}_0,\theta_0)\mathrm{G_X}(\mathbf{r},\theta_0)} \tag{2.20}$$

Consensus source data will typically present radial dose function values in tables for discrete values of $\mathbf{r}$ to allow for interpolation between data points. In contrast, some commercial treatment planning systems (e.g Vitesse and brachyvision) will fit a fifth order polynomial to the tabulated data [12].

Finally, the fifth term in equation 2.14, F(r,θ), is the 2D anisotropy function. This function describes the angular variation of dose due to self filtration, oblique filtration of primary photons through the encapsulating material and scattering of photons in the surrounding medium. The dose rate is lowest along the source axis due to the increased self absorption and filtration, and highest around θ=90 deg. The anisotropy function given in TG43U1 is as follows,

$$\mathrm{F}(\mathbf{r},\theta){=}\frac{\dot{D}(\mathbf{r},\theta)\mathrm{G_L}(\mathbf{r},\theta_0)}{\dot{\mathrm{D}}(\mathbf{r},\theta_0)\mathrm{G_L}(\mathbf{r},\theta)} \tag{2.21}$$

The TG43 formalism has provided a worldwide standard for brachytherapy dose calculations for may years. However, The design of this formalism does not accommodate for real patient geometry and materials introduced by the patient and applicators that may be used for treatment. In light of this, Varian have developed an algorithm that can explicitly account for heterogeneities.

2.4.2 Acuros BrachyVision

The Acuros BV (ABV) dose calculation algorithm was developed from a desire to provide a rapid and accurate alternative to MC simulations that is capable of accounting for finite patient dimensions, anatomical material differences and applicator materials. ABV achieves this by deterministically solving the Linear Boltzmann Transport Equation (LBTE). LBTE is a mathematical model that describes radiation conservation as energised particles traverse through a medium [18].

In the context of Ir192 HDR brachytherapy, secondary electrons ranges are much smaller that the voxel calculation size. Furthermore, the fraction of energy lost through radiative processes of charged particles is negligible. Therefore ABV does not track secondary electrons and employs the kerma approximation, $D=K_{coll} \approx K$ [17].

In order for ABV to calculate kerma, it must first solve the LBTE to determine the fluence. Photon fluence through a voxel has three components: (i) primary fluence (ii) fluence from photons being scattered in the surrounding voxels, and (iii) photons that interact inside the voxel and are either absorbed locally or scattered. The three components that contribute to the total fluence are accounted for in the general form of the LBTE,

$$\hat{\Omega} \cdot \vec{\nabla}\Psi(\vec{r}, E, \hat{\Omega}) = \overbrace{\frac{q_{primary}(E, \hat{\Omega})}{4\pi}\delta(\vec{r} - \vec{r_P})}^{(i)} + \overbrace{q_{scatter}(\vec{r}, E, \hat{\Omega})}^{(ii)} - \overbrace{\sigma_t(\vec{r}, E)\Psi(\vec{r}, E, \hat{\Omega})}^{(iii)} \tag{2.22}$$

where:

$\Psi(\vec{r}, E, \hat{\Omega})$ is the angular photon fluence,

$q_{scatter}(\vec{r}, E, \hat{\Omega})$ is the photon scattering source,

$q_{primary}(E, \hat{\Omega})$ is the primary photon source,

$\vec{r}$ is the position of interest,

$\vec{r_P}$ is the source position,

E is the energy of the particle,

$\hat{\Omega}$ is the particle motion direction,

$\delta(\vec{r} - \vec{r_P})$ is the Dirac delta function between the source location and the position of interest, and

σ_t is the macroscopic total cross section at the position of interest, $\sigma_t(\vec{r}, E)$.

Under charged particle equilibrium (CPE), the primary fluence can be analytically solved using ray-tracing [15, 17, 18, 43]. The scatter component however, cannot be solved analytically. The scatter component is a function of angular fluence and can be expressed as a double integral over energy and direction,

$$q_{scatter}(\vec{r}, E, \hat{\Omega}) = \int_0^\infty \int_{4\pi} \sigma_s(\vec{r}, E' \rightarrow E, \hat{\Omega} \cdot \hat{\Omega}')\Psi(\vec{r}, E', \hat{\Omega}')d\hat{\Omega}'dE' \quad (2.23)$$

where:

$\sigma_s(\vec{r}, E' \rightarrow E, \hat{\Omega} \cdot \hat{\Omega}')$ is the macroscopic differential scatter cross section.

The macroscopic differential scatter cross section can be expanded in Legendre polynomials, $P_L = \mu_0$, where $\mu_0 = \psi \cdot \psi'$, and the angular fluence is expanded into spherical harmonics, L=3 for within group scattering and L=2 for out of group scattering [17, 18]. Applying these expansions replaces the integrals with discrete summations, which make the scatter component of LBTE much easier to compute [18]. $q_{scatter}(\vec{r}, E, \hat{\Omega})$ can now be written as,

$$q_{scatter}(\vec{r}, E, \hat{\Omega}) = \sum_{l=1}^{L} \sum_{m=-l}^{l} \int_0^\infty \sigma_{s,l}(\vec{r}, E' \rightarrow E)\phi_{l,m}(\vec{r}, E')Y_{l,m}(\hat{\Omega})dE' \quad (2.24)$$

where:

$\sigma_{s,l}(\vec{r}, E' \rightarrow E)\phi_{l,m}$ is the macroscopic differential equation.

$\phi_{l,m}(\vec{r}, E')$ is the spherical harmonic moments,

$Y_{l,m}(\hat{\Omega})$ is the spherical harmonic functions, and

l,m are the angular indices.

ABV solves the resulting form of the LBTE by discretizing its six variables: three variables in space, (x, y ,z), using finite difference or finite element methods, two variables in angle, $\mu, \eta, \xi = \sqrt{1 - \mu^2 - \eta^2}$, using discrete ordinates method, and energy, E, using the multigroup approximation [17, 18, 44]. ABV's solution to the LBTE provides the angular and energy dependent photon fluence at every spatial degree of freedom within the computational domain, which can then be converted to dose [17],

$$D(\vec{r}) = \frac{1}{\rho(\vec{r})} \sum_{g=1}^{G} \sigma_{kerma.g}(\vec{r}) \Big\{ \sum_{p=1}^{P} \phi_{p,g}^{uncollided}(\vec{r}) \phi_{g}^{collided}(\vec{r}) \Big\} \quad (2.25)$$

where:

$D(\vec{r})$ is the dose at position $\vec{r}$,

$\rho(\vec{r})$ is the density at position $\vec{r}$,

$\sigma_{kerma.g}(\vec{r})$ is the macroscopic kerma cross section, and

$\sum_{p=1}^{P} \phi_{p,g}^{uncollided}(\vec{r}) \phi_{g}^{collided}(\vec{r})$ is the total scalar fluence at position $\vec{r}$.

Generally there are two methods that can be used to produce an LBTE solution. The first being explicitly solving the LBTE (i.e. ABV) and the second being MC. With sufficient refinement, both methods should converge on the same solution.

GammaMed Plus Source

Sources used in ABV are modelled as effective sources, where they are represented as one or more point sources located on the surface of the true source geometry. Photons are emitted from each point source with the energy and angular intensity that best represents where they are located relative to the true geometry of the source. Given that effective sources are a multitude of point sources, the LBTE must be solved for each point source located at $\vec{r_p}$ and summed to give the total fluence at position $\vec{r}$. The spectrum of photons emitted from each point source are binned into 37 groups and 10,000 angles.

The source of interest in this study is the GammaMed Plus HDR (GMP) source. Figure 2.12 shows the dimensions, in millimeters, and materials used to model the GMP source [45]. The core of the GMP source is a 3.5 mm long solid iridium cylinder with a diameter of 0.6 mm. Encapsulating the source core is a hollow AISI 316L stainless steel cylinder, with a density of 8.03 g/cm^3, an outer diameter of 0.9 mm and a truncated cone end. Source encapsulation is directly attached to an AISI 304 stainless steel cylinder, with a density of 5.6 g/cm^3, a diameter of 0.9 mm and a length of 2 mm. All effective sources in ABV are modelled with a source wire length of 2 mm. The reason for this is that a source wire length of 2 mm is the maximum length where significant bending of the wire doesn't occur [17].

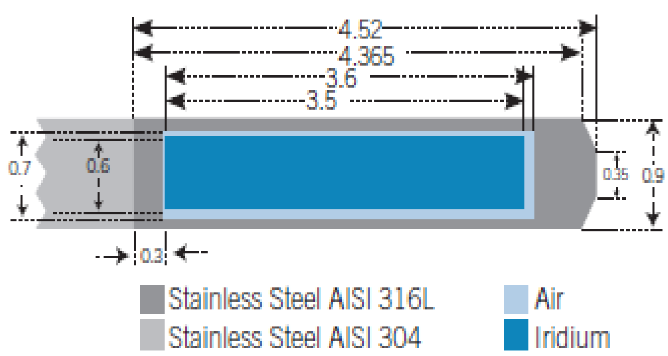

Figure 2.12: GammaMed Plus source geometry.

Evenly distributed through the active core of the GMP source is the radioisotope iridium-192 (Ir192). Ir192 has a half life of 74 days and decays into platinum-192 via electron capture (EC) 95.13% of the time and β^- into Osmium 192 the remaining 4.87%. The complicated photon spectrum ranges from 7.82 keV to 1.378 MeV and has an average energy of approximately 370 keV [9, 24]. Simulations for this study were performed using the Ir192 spectrum provided by the NNDC [46]

2.5 Monte Carlo

The MC method can be defined as a numerical method used to solve equations and calculate integrals through repeated random sampling [47]. MC simulations are capable of modelling physical processes and systems where the probability of different numerical results are not easily predictable. Furthermore, it is a tool capable of providing results for problems that cannot be attained analytically or experimentally. MC has many applications and is considered the gold standard for attaining numerical results when modelling radiation transport [19, 48]. It doesn't explicitly solve the LBTE, rather it indirectly produces an LBTE solution [17].

2.5.1 Random Number Generators

Random sampling is achieved in MC through random number generation. This is accomplished using a random number generator algorithm (RNG). By definition, computers are unable to produce numbers that are truly random and are therefore termed pseudorandom numbers [47]. RNG's will typically produce a uniform distribution of numbers between 0 and 1, either as large sequences of predetermined numbers or on the fly. Together with cross section modelling, these numbers will be used to determine the outcome of a particle interaction. Given that the number of histories executed in RT simulations are on the order of billions, the ideal RNG will have an extremely long period. This is to avoid any correlation in MC results [47].

2.5.2 Monte Carlo Statistics

Uncertainties presented in this study will be expressed using the methods recommended in the guide to the expression of uncertainty in measurement (GUM) [49]. The GUM defines the quantity to be measured as the measurand Y, and its associated standard uncertainty as the standard deviation u. In most cases, the best estimate of the measurand, denoted as y, will not be directly measured, and will be determined from N input estimate quantities $\mathrm{x_N}$ through a functional relationship f, where each input estimate will have its own standard uncertainty. Therefore the standard uncertainty of each input quantity must be combined to determine the combined standard uncertainty in y.

$$\mathrm{y}{=}\bar{\mathrm{Y}}{=}\mathrm{f}(\mathrm{x}_1, \mathrm{x}_2, ..., \mathrm{x}_N) \tag{2.26}$$

$$\mathrm{u_c(y)}{=}\sqrt{\sum_{\mathrm{i=1}}^{\mathrm{N}} \left(\frac{\mathrm{f}}{\mathrm{x_i}}\right)^2 \mathrm{u}^2(\mathrm{x_i})}{=}\sqrt{\sum_{\mathrm{i=1}}^{\mathrm{N}} \mathrm{u}_i^2(\mathrm{y})} \tag{2.27}$$

Uncertainties are separated into two types, type A and a type B. Type A uncertainties are evaluated using statistical methods, and type B uncertainties are evaluated by any means other than statistical analysis. In the context of absorbed dose measurements, GATE simulations provide the experimental standard deviation for each voxel. Given that the MC method is a stochastic process, the uncertainties provided by GATE are type A uncertainties. The uncertainties determined in GATE are calculated using the history-by-history method described by Chetty et al [50, 51],

$$\mathrm{S}_{\bar{\mathrm{d}}_\mathrm{k}}{=}\sqrt{\frac{1}{\mathrm{N}-1}\left(\frac{\sum_{\mathrm{i=1}}^{\mathrm{N}} \mathrm{d}_{\mathrm{k,i}}^2}{\mathrm{N}} - \left(\frac{\sum_{\mathrm{i=1}}^{\mathrm{N}} \mathrm{d_{k,i}}}{\mathrm{N}}\right)^2\right)} \tag{2.28}$$

where $S_{\bar{d}_k}$ is the experimental standard deviation of the dose deposited in voxel k, $d_{k,i}$ is the dose deposited in voxel k by an independent history i and N is the total number of incident photons.

2.6 Geant4 Application for Emission Tomography (GATE)

MC packages frequently used in medical physics applications include EGS4, EGSnrc, PENELOPE, MCNP, Geant4 and Gate. In this study, the MC package used was GATE and therefore the following sections will discuss the structure of GATE and the macro files executed in GATE, tools used to interact with GATE simulations, variance reduction techniques available in GATE and monte carlo statistics.

GEANT4 is a MC code that contains comprehensive physics models, libraries and tools capable of modelling a variety of complex scenarios [52]. Though it is versatile, it is a very complex code to use. Efficient use of GEANT4 requires a considerable level of experience with object-oriented codes written in C++ programming language. For new users to gain such a level of experience can be very time consuming. It is for this reason that applications such as GATE have been developed.

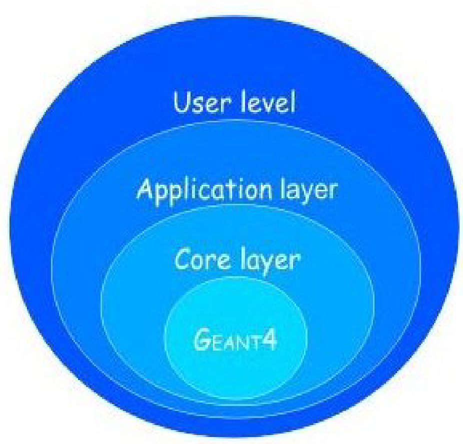

Figure 2.13: Layered architecture of GATE.

GATE is an advanced open source application software developed by the international OpenGate community. Well known for its widespread use in imaging simulations, GATE has also shown its potential when used in dosimetry applications [53]. The GATE application encapsulates all the complex functionalities of GEANT4 while providing a user friendly interface. It is a multilayered structure with the base of the structure being the Geant4 MC code (Figure 2.13) [54]; The core layer defines the main tools and features; The application layer is a subset of tools and features defined in the core layer; The user layer is the layer that end-users can interact with and call upon the functionalities of GEANT4 to simulate their experiments.

Gate simulations are run by executing primary macro files. Macro files contain a list of commands defining each component required to successfully run a simulation. In addition, secondary macro files may be written and executed within the primary macro file. The basic structure of a main macro file is shown in Table 2.1 [55].

Table 2.1: Basic structure of a primary macro file used in radiotherapy Gate simulations.

[Verbose macro]
[Visualisation macro]
1 - Geometry description macros
2 - Phantom description macros
3 - Physics related macros
4 - Output set up macros
/gate/run/initialize
6 - Source description macros
/gate/application/setTotalNumberofPrimaries 50 /gate/application/start

2.6.1 Actors

In order to draw information from a simulation, the user must include actors in their macro files. Actors are tools that allow the user to interact with their simulations by collecting information (e.g. absorbed dose, number of particles entering a volume etc.) or modifying the behaviour of their simulations (e.g. particle filtration/killing) [56].

Some actors, such as the DoseActor, will store information (i.e. energy deposited, dose, uncertainty) in a 3D scoring matrix. Within the main macro, the actor must be attached to a volume of interest. The user is able to set the size, resolution (i.e. voxel size) and position of the 3D scoring matrix relative to the origin of the volume of interest. It should be noted that, if the volume of interest is larger or smaller than the 3D scoring matrix, information will only be scored for hits occurring within their overlapping regions.

2.6.2 Variance Reduction Techniques (VRT's)

Variance informally describes how spread out a series of numbers are from their mean value. The variance in MC simulation results is proportional to 1/N, where N is the number of histories produced in the simulation [47]. The most obvious way to decrease the variance would be to increase the number of histories, although this will also increase simulation times. A major disadvantage of the MC method is that it can be very time consuming. Therefore, algorithm techniques such as variance reduction techniques are essential as they optimise transport parameters while maintaining a high level of accuracy. Variance reduction techniques used in this study include range/energy cuts and kerma approximation.

Range/Energy Cuts

Range/ energy cuts is a technique that terminates particle tracking once any given particle has gone below an energy or range threshold set by the user. Without range and energy cuts, particles are tracked until they reach the system boundary (i.e the world) or deposit all of their energy.

variables to consider when selecting range and energy thresholds include,

- are the particle ranges much smaller than the calculation volume, and therefore deposit all of its energy locally, and
- is the energy of the particle large enough to significantly contribute to the dose

When a particle is stopped due to its energy or range falling below the set thresholds, all of its energy is deposited locally [56].

Kerma approximation

Within the context of brachytherapy, the energy released by photons is absorbed directly in the neighbourhood of the photon ray [47]. Therefore, secondary electrons do not need to be tracked. As a result, kerma can be used as an approximation of dose. Photon fluence through any volume V can be estimated as,

$$\phi = \frac{\mathrm{L}}{\mathrm{V}} \tag{2.29}$$

where L is the distance travelled in the voxel between successive collisions. Following on from equation 2.29, an estimate of the absorbed dose under CPE is given by [45, 47, 57],

$$\mathrm{D} = \phi \mathrm{E} \frac{\mu_{\mathrm{en}}}{\rho} \tag{2.30}$$

Along with electron energy cut-offs, the kerma approximation is one of the most effective VRT's [51].

Chapter 3

Method

The primary purpose of this study was to assess the dose calculation accuracy of ABV in a variety of materials relevant to HDR brachytherapy. The following sections will present the methodologies used to achieve this.

First I will outline the settings used to build a GMP source model in GATE. These settings will include GMP source specification, physics, RNG's and VRT's. I will then present the phantom that was designed and modelled for making GATE versus ABV comparisons. Following this, I will detail the methodology used to verify the source model. Thereafter I will present the data analysis tools used to make GATE versus ABV comparisons.

3.1 GATE Setup

The primary tool used in this study was the GATE MC toolkit V8.0, with the base of this toolkit being the GEANT4 environment (V10.4). Both GEANT4 and the GATE tool kit were installed and built on a PC with an Intel® Xeon® E5620 processor. This processing unit is a 4 core processor with 2.4 GHz processor base frequency. Using a single processor resulted in simulation times ranging between 2 - 5 days.

GATE was used to model Varian's Ir192 GammaMedPlus HDR (GMP) source. Geometry and material information used to model this source was taken from work done by Lopez et al. 2.12 [45]. A screenshot of the GMP source modelled in GATE is given in figure 3.1. Following recommendations provided by Rivard et al. [24], the Ir192 spectrum attached to the active length of the source was that provided by the National Nuclear Data Center (NNDC) [46].

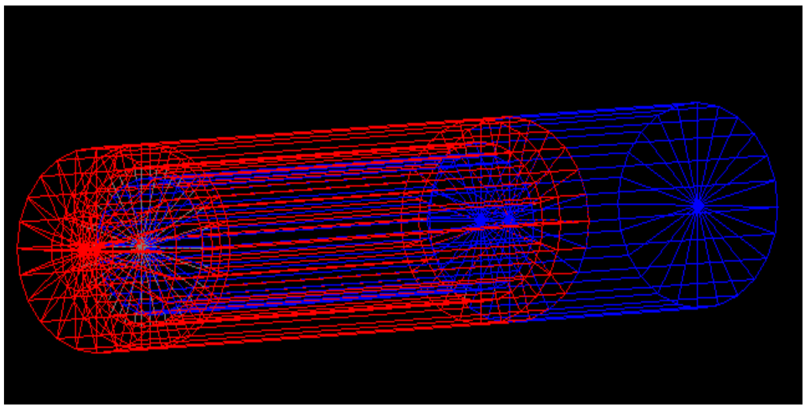

Figure 3.1: GMP source modelled in GATE.

NNDC's Ir192 spectrum has a maximum energy of approximately 1.38 MeV. Therefore the primary interactions to be considered when modelling the GMP source are Compton scattering and the photoelectric effect. Before the release of GATE V7.0, user guides instructed users to individually list the interaction processes of interest. However, since the release of GATE V7.0, developers highly recommend using the predefined physics lists, inherently available in GEANT4. Therefore for this study the emstandard package was used. For Ir192 energies, this package calculates cross sectional data using the Klein-Nishina and Livermore models for photon interactions, and the urban model for electron interactions [58].

GATE V8.0 has three different RNG's available for use, the Ranlux64, the James Random and the Mersenne Twister (MT). Studies have shown that of these three generators, the MT generator is favoured because of its extremely long period of $2^{19937} - 1$ [59, 60] and therefore was used in this study. In addition to MT's extremely long period, the MT generator preregenerates a pool of numbers to be used instead of generating random numbers on the fly, and as a result reduces simulation times [47].

Simulation times were further reduced by using VRT's such as energy cuts and kerma approximators. Following Perez et al. recommendations, a photon cut energy of 10 keV was used [13]. A cut-off energy of 10 keV will reduce simulation times while maintaining simulation accuracy. Perez et al. also provides recommendations for the use of kerma approximators, which will be provided in a later section.

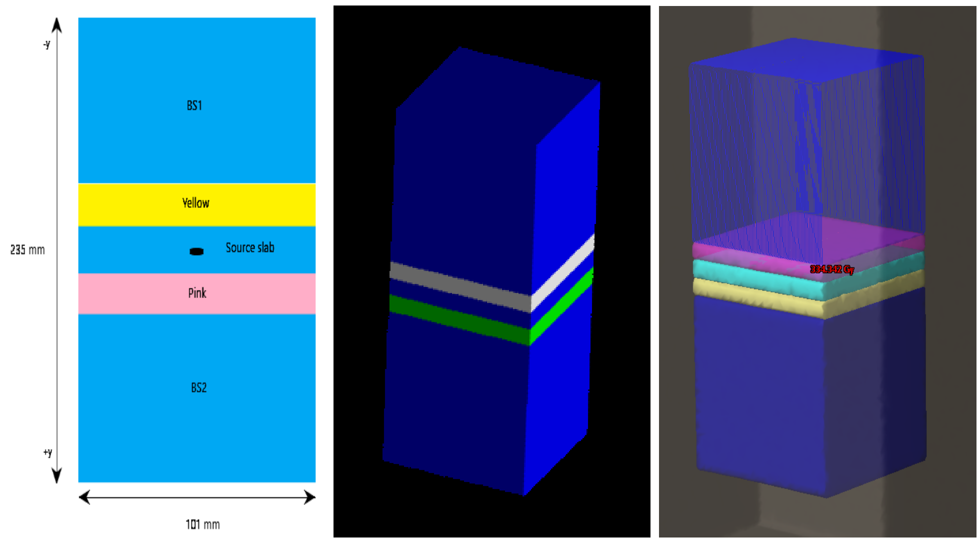

(a) (b) (c)

Figure 3.2: **(a)** Digital phantom design. **(b)** Digital phantom modelled in GATE. **(c)** Digital phantom modelled in ABV.

3.2 Digital Phantom

Dose calculation comparisons were made using a simple digital phantom with interchangeable slabs (figure 3.2). This phantom is comprised of 4 individual slabs of material, where BS1 and BS2 are 101 mm x 101 mm x 101 mm and 'Source slab', 'Pink' and 'Yellow' are 101 mm x 101 mm x 11 mm. The dose calculation grid across the entire system is made up of 1 mm x 1 mm x 1 mm voxels . These dimensions were selected so that the center of each slab coincided with the center of a voxel.

With the source centered in the 'source slab', this system is used to produce 6 individual phantoms with varying materials where dose was measured using the standard *DoseActor*. Presented in table 3.1 are the materials assigned to each slab for each phantom setup. All material composition data is given in appendix A.1.5.

Table 3.1: Phantom material combinations used for GATE vs Acuros BV comparisons.

Phantom material combinations					
Phantom	**BS1**	**Pink**	**Source Slab**	**Yellow**	**BS2**
1	water	Air	water	Peek	water
2	water	Bone	water	Cartilage	water
3	water	Lung	water	Titanium	water
4	water	Muscle	water	Adipose	water
5	water	Water	Stainless steel	water	water
6	water	Water	PMMA	Water	water

3.3 Source Validation

Before dose comparisons can be made between GATE and ABV, the GMP source modelled in GATE must be validated. This is to provide evidence that what is being simulated is a true reflection of what happens in the real world. Therefore simulated photon spectra and TG43 factor results were compared with well validated published data.

Recommended TG43 Consensus data for the GMP source was published by Perez et al. in their report "*Dose calculation for photon-emitting brachytherapy sources with average energy higher than 50 keV: report of the AAPM and ESTRO*" [13] and includes results published by Ballester et al. [2] and Taylor and Rogers [1]. Simulations in this study for all TG43 parameters were set up according to recommendations provided by Perez et al. [13], Lopez et al. [45] and Thiam et al. [61]. Recommendations for calculating TG43 parameters include,

- Minimise volume averaging effects to <0.1% when using the collisional kerma approximator by configuring voxel sizes to be 0.1 mm x 0.1 mm x 0.1 mm for distances in the range of $r_{source} \leq 1$ cm, 0.5 mm x 0.5 mm x 0.5 mm for distances in the range of 1 cm $< r \leq 5$ cm, 1 mm x 1 mm x 1 mm for distances in the range of 5 cm $< r \leq 10$ cm and 2 mm x 2 mm x 2 mm for distances in the range of 10 cm $< r \leq 20$ cm
- Simulations should be computed in a phantom that approximates full scatter conditions of an unbounded phantom. For Ir192, a spherical phantom with a radius of R = 40 cm should be used
- When feasible, type A uncertainties should be kept below <0.1%

With the exception of AKS and photon spectrum measurements, where the *EnergySpectrumActor* was used, all TG43 dose measurements were acquired using GATE's kerma approximator, the *TLEDoseActor*. The number of histories for all TG43 measurements was set to 2.1 x 10^9.

3.3.1 Energy Weighted Spectrum

With the GMP source located in the center of a vacuum, the *EnergySpectrumActor* was used to detect and store all photons emitted from the source (including the source wire). The *EnergySpectrumActor* builds a histogram based on the energy range and bin width defined by the user. In this study, the energy range and bin width was set to 0.001 - 1.38 MeV and 0.001 MeV respectively

Spectrum results from this study were compared to Taylor and Rogers results, where spectrum results were presented in their study as an energy weighted spectrum. Therefore the *EnergySpectrumActor* output was processed and presented using the following equation [1],

$$\frac{\mathrm{dR(E_j)}}{\mathrm{dE}} \Big/ \mathrm{R} = \sum_{\mathrm{i}} \mathrm{E_i} \Big/ (\Delta \mathrm{E} \cdot \mathrm{R}) \tag{3.1}$$

where E_j is the energy at the middle of a bin, E_i is the energy of the i^{th} photon escaping the the source with energies between $E_j \pm \Delta E/2$, ΔE is the bin width and R is the sum of the energies of all photons detected.

3.3.2 Air Kerma Strength S_k and Dose Rate Constant Λ

Following TG43U1, Γ was calculated by dividing the dose rate at the reference point ($\dot{D}(1, \pi/2)$) in a liquid water phantom by the AKS (equation 2.17), where AKS is the air kerma rate multiplied with the square of the distance from the origin to the point where the air kerma rate was measured (equation 2.15).

Assuming isotropic emission around the source in the transverse plane, $\dot{D}(1, \pi/2)$ was calculated as the mean dose rate scored at four representations of the reference point around the source,

$$\dot{D}(1, \pi/2) = \frac{\dot{D}(1, \pi/2, 0) + \dot{D}(1, \pi/2, \pi/2) + \dot{D}(1, \pi/2, \pi) + \dot{D}(1, \pi/2, 3\pi/2)}{4N} \tag{3.2}$$

where N is the total number of histories executed.

Following this, the air kerma was then calculated according to [8],

$$\text{kerma} = \int E\Phi_E \frac{\mu_{en}(E)}{\rho} dE \tag{3.3}$$

where Φ_E and $\frac{\mu_{en}}{\rho}(E)$ are the fluence and the mass energy absorption coefficient in air for photons with energy E respectively. Within the context an ^{192}Ir source and the materials considered, the fraction of energy lost through radiative processes is negligible (i.e. $K_{rad} \approx 0$) and therefore,

$$\frac{\mu_{en}}{\rho} = \frac{\mu_{tr}}{\rho}(1 - g) \approx \frac{\mu_{tr}}{\rho} \tag{3.4}$$

With the source origin positioned at the center of a spherical vacuum, the fluence was measured by attaching an *EnergySpectrumActor* to a thin cylindrical volume with an inner diameter of 50 mm and a width of 1 mm. The output spectrum was configured to store all photons between 0.001 MeV and 1.379 MeV into bins 0.001 MeV wide. Given that the output spectrum is a histogram, equation 3.3 was approximated using a Riemann sum approximation [62]. Therefore the air kerma rate at a distance of 5 cm from the source due to photons with $E \geq 0.001$ MeV was calculated as,

$$\dot{K}_{0.001MeV} = 1.602 \times 10^{-10} \frac{\sum_{i=0}^{n} \Phi_i i\Delta E \frac{\mu_{en}}{\rho}(i\Delta E)}{N} \tag{3.5}$$

where Φ_i is the fluence due to the photons in the i_{th} bin, ΔE is the bin width, $\frac{\mu_{en}}{\rho}(i\Delta E)$ is an approximation of the mass energy absorption coefficient for all photons in i^{th} bin[1], N is

[1] Values for $\frac{\mu_{en}}{\rho}(i\Delta E)$ were obtained by interpolating data published by NIST [63]. See figure A.1 of appendix A.2.1

the total number of histories and 1.602×10^{13} is the conversion factor to convert MeV/g to joules/kg.

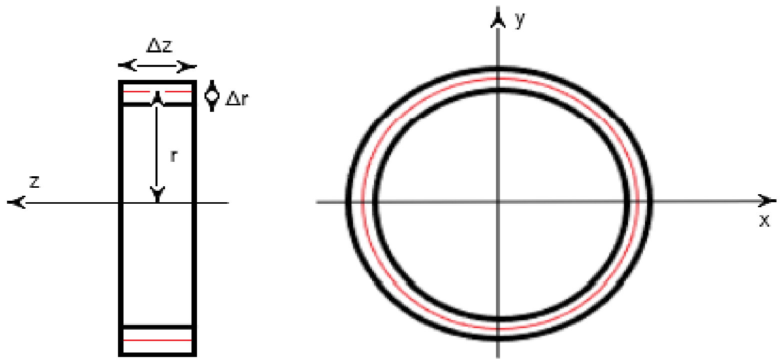

Figure 3.3: Ring geometry definition.

3.3.3 Radial Dose Function, g(r)

Following TG43U1, the radial dose function only requires measurements in the transverse bisector plane of the source (equation 2.20). Once again assuming isotropic emission around the source in the transverse plane, absorbed dose was measured using thin rings centred around the source origin. Dose measurements were produced for r = {0.2cm, 0.25cm, 0.5cm, 0.75cm 1cm, 1.5cm, 2cm, 3cm, 4cm, 5cm, 6cm, 7cm, 8cm, 10cm} using the cylinder dimensions shown in table A.1 of appendix A.2.3. Once the dose deposited in each ring was measured, the dose rate was then calculated as,

$$\dot{\mathrm{D}}(\mathrm{r}, \frac{\pi}{2}) = \frac{\mathrm{D}(\mathrm{r}, \frac{\pi}{2})}{\mathrm{N}} \tag{3.6}$$

where N is the total number of histories. TG43U1 recommends consistent use of a line-source approximation when deriving both the radial dose and anisotropy functions. It is for this reason that the geometry function values shown in figure A.2 of appendix A.2.2 were calculated as per equation 2.19.

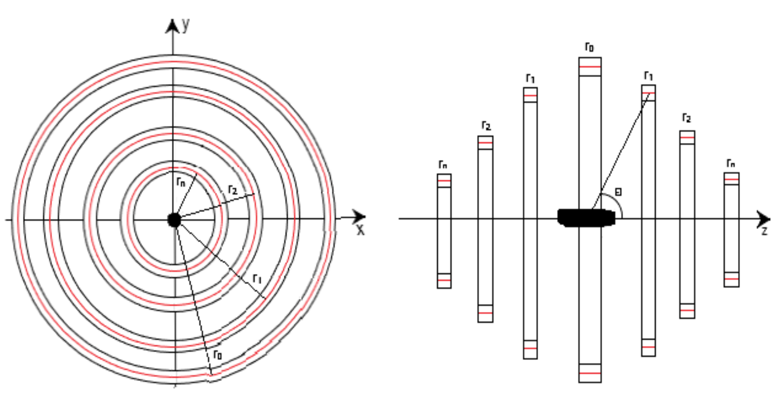

Figure 3.4: Anisotropy measurement setup.

3.3.4 2D Anisotropy Function, F(r,θ)

The system used to produce the required measurements is illustrated in figure 3.4. For any given value r_0, the 2D anisotropy function describes the variability in the dose distribution over $0 \leq \theta \leq \pi$. Therefore to calculate the anisotropy function for a single value of r_0, absorbed dose measurements at different points along the long axis of the source must be produced. The radius and position along the z axis of each ring was calculated as follows,

$$r_n = r_0 \mathrm{Sin}\theta \tag{3.7}$$

$$z(r_n) = \frac{r_n}{\mathrm{Tan}\theta} \tag{3.8}$$

where n represents the total number of rings on either side of source origin. Anisotropy function values were produced for $r_0 = \{4\text{mm}, 6\text{mm}, 10\text{mm}, 35\text{mm}, 60\text{mm}, 100\text{mm}\}$ using the cylinder dimensions shown in tables A.2 - A.7 of appendix A.2.4. It should be noted that at 0 and $\frac{\pi}{2}$, dose measurements were produced using cubes instead of rings. Once the dose deposited in each volume was measured, the dose rate was then calculated as,

$$\dot{D}(r_0, \theta) = \frac{D(r_0, \theta)}{N} \tag{3.9}$$

where N is the total number of histories.

3.4 Monte Carlo Calibration factor

The maximum number of histories executable in a single GATE simulation is approximately 2.1 x 10^9. For a 10 Ci source, 2.1 x 10^9 reflects a real dwell time of less than 0.01 sec. Given that the absolute minimum dwell time that is accepted in BrachyVision is 0.1 sec [64], a single GATE simulation executing 2.1 x 10^9 will not suffice. Multiple simulations can be executed to generate enough data to reflect an acceptable dwell time but will be very time consuming. This can be avoided by producing a MC calibration factor that can accurately convert GATE doses into doses that reflect dwell times larger than 0.1 sec.

A MC calibration factor was produced using the system described in section 3.2. With water as the material assigned to each slab and a source centered in the phantom with its long axis orthogonal to the y axis, the dose rate at y = 1 cm and y = -1 cm were estimated for a dwell time t (ABV) and histories N (GATE). Taking the average of these estimations, the MC calibration factor was calculated as,

$$f = \frac{\bar{\dot{D}}_{ABV}(r_0, \theta_0)}{\bar{\dot{D}}_{GATE}(r_0, \theta_0)} \tag{3.10}$$

where $\dot{D}_{ABV}(r_0, \theta_0)$, $\dot{D}_{GATE}(r_0, \theta_0)$ and f carry units of Gy/seconds, Gy/history and history/second respectively. This calibration factor was then applied in the following equation to convert GATE doses to doses that reflect practical dwell times in BV,

$$D_X(r,\theta) = f \cdot \frac{D_{GATE}(r,\theta) \cdot t}{N} \tag{3.11}$$

where X represents the algorithm used to estimate the dose at r and θ (i.e. TG43 or ABV), t is the planned dwell time, $D_{GATE}(r,\theta)$ is the dose estimated at r and θ in GATE, N is the number of simulated histories and f is the MC calibration factor.

3.5 Comparison Tools

Using the phantom setup described in section 3.2, GATE versus ABV dose to medium estimations were compared, with GATE being used as reference. In order to make confident conclusions about the accuracy of ABV, the following comparison techniques were used:

- Point-to-point profile comparisons
- 1D Gamma analysis
- Correlation and statistical significance analysis

Gamma Analysis

The gamma analysis technique compares all measurement points against the calculated dose distribution and assigns each point a quality index number γ. It is a pass-fail test that is based on discrete point dose differences and distance-to-agreement (DTA) tolerances (e.g δD=2%, δd=1mm respectively) [65, 66]. The magnitude of γ is determined by the distance between the measurement point and the calculated point that exhibits a dose within the specified point dose difference tolerance ΔD. A geometrical representation that considers the DTA and point dose difference tolerances of a 1D gamma analysis is shown in figure 3.5 [65, 67], where the circumference of the circle is defined by Equation 3.12.

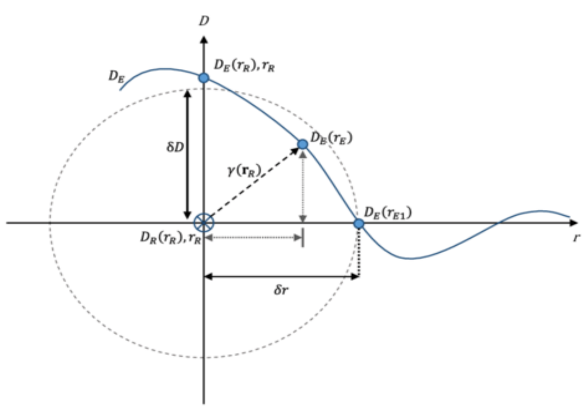

Figure 3.5: Geometric representation of a 1D gamma analysis.

$$1 = \sqrt{\frac{\Delta r^2(\mathbf{r}_R, \mathbf{r})}{\delta r^2} + \frac{\Delta D^2(\mathbf{r}_R, \mathbf{r})}{\delta D^2}} \tag{3.12}$$

where

$$\Delta \mathrm{r}(\mathbf{r}_{\mathrm{R}}, \mathbf{r}) = |\mathbf{r} - \mathbf{r}_{\mathrm{R}}| \tag{3.13}$$

and

$$\Delta \mathrm{D}(\mathbf{r}_{\mathrm{R}}, \mathbf{r}) = \mathrm{D}(\mathbf{r}) - \mathrm{D}_{\mathrm{R}}(\mathbf{r}_{\mathrm{R}}) \tag{3.14}$$

Figure 3.5 illustrates that the pass fail criteria is based on whether or not D_E lies within the circumference of the circle defined by Δd and ΔD. Taking the right hand side of equation 3.12 we can write,

$$\gamma(\mathrm{r}_{\mathrm{R}}, \mathrm{r}_{\mathrm{E}}) = \sqrt{\frac{\Delta \mathrm{r}^2(\mathbf{r}_{\mathrm{R}}, \mathbf{r}_{\mathrm{E}})}{\delta \mathrm{r}^2} + \frac{\Delta \mathrm{D}^2(\mathbf{r}_{\mathrm{R}}, \mathbf{r}_{\mathrm{E}})}{\delta \mathrm{D}^2}} \tag{3.15}$$

where

$$\Delta \mathrm{r}(\mathbf{r}_{\mathrm{R}}, \mathbf{r}_{\mathrm{E}}) = |\mathbf{r}_{\mathrm{R}}, \mathbf{r}_{\mathrm{E}}| \tag{3.16}$$

and

$$\Delta D(\mathbf{r}_{\mathrm{R}}, \mathbf{r}_{\mathrm{E}}) = \mathrm{D}_{\mathrm{E}}(\mathbf{r}_{\mathrm{E}}) - \mathrm{D}_{\mathrm{R}}(\mathbf{r}_{\mathrm{R}}) \tag{3.17}$$

From equation 3.5 we can then determine the quality index at $\mathbf{r}_{\mathrm{R}}$ as,

$$\Gamma(\mathbf{r}_{\mathrm{R}}) = \min\{\Gamma(\mathbf{r}_{\mathrm{R}}, \mathbf{r}_{\mathrm{E}}\} \forall \{\mathbf{r}_{\mathrm{E}}\} \tag{3.18}$$

where the pass-fail criteria becomes,

- $\gamma(\mathbf{r}_{\mathrm{R}}) \leq 1$, calculation passes
- $\gamma(\mathbf{r}_{\mathrm{R}}) > 1$, calculation fails.

One dimensional local gamma analyses were executed in this study using a Matlab code provided by M. Geurts [68]. Gamma analysis pass criterion used in this study was δr=2mm δD=2% and δr=1mm δD=2% with a pass rate of $\geq$ 99%.

Correlation Analysis

Correlation analysis is a statistical method used to analyse the strength of a relationship between two quantitative variables x and y. The correlation analysis method used to calculate the correlation between x and y in this study was the Pearson correlation coefficient method [69, 70]. This method produces a correlation coefficient r and is calculated using the following equation,

$$\mathrm{r} = \frac{\sum \mathrm{xy} - \frac{\sum \mathrm{x} \sum \mathrm{y}}{\mathrm{n}}}{\sqrt{(\sum \mathrm{x}^2 - \frac{(\sum \mathrm{x})^2}{\mathrm{n}})(\sum \mathrm{y}^2 - \frac{(\sum \mathrm{y})^2}{\mathrm{n}})}} \tag{3.19}$$

where n is the number of individuals. Illustrated in figure 3.6 are cases where x and y demonstrate strong correlation (i.e r = 1 and r = -1) and no correlation (i.e. r $\approx$ 0). The degree of correlation between variable x and y is determined by how close r is to 1 or -1.

A positive correlation coefficient means that x and y are positively correlated. Conversely, a negative correlation coefficient means that x and y are negatively correlated.

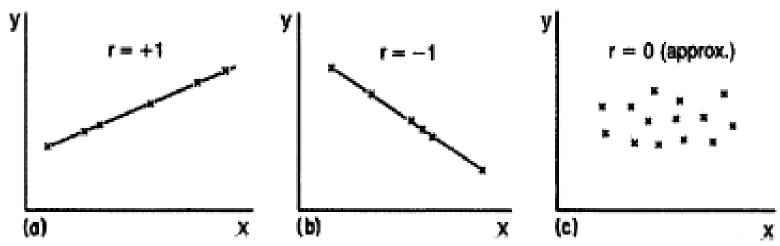

Figure 3.6: scatter diagrams for r = 1; r = -1; and r $\approx$ 0.

All Pearson correlation coefficients presented in this study are accompanied with their associated P-value. The purpose of a P-value is to firstly indicate the probability of encountering an alpha error and secondly to indicate whether or not the null hypothesis can be rejected or accepted [71]. The null hypothesis in this study is that statistically ABV and GATE calculated doses are significantly different. The null hypothesis can be rejected if P $\leq \alpha$, where α has been set to 5% which will provide a 95% level of confidence in avoiding an alpha error.

Chapter 4

Results

4.1 Source Validation

4.1.1 Energy Weighted Spectrum

Presented in figure 4.1 is a comparison of the energy weighted photon spectrum produced in this study with that published in Taylor and Rogers TG43 Parameter database for brachytherapy. In general there is good agreement, with both sets of data giving spikes for the same energies.

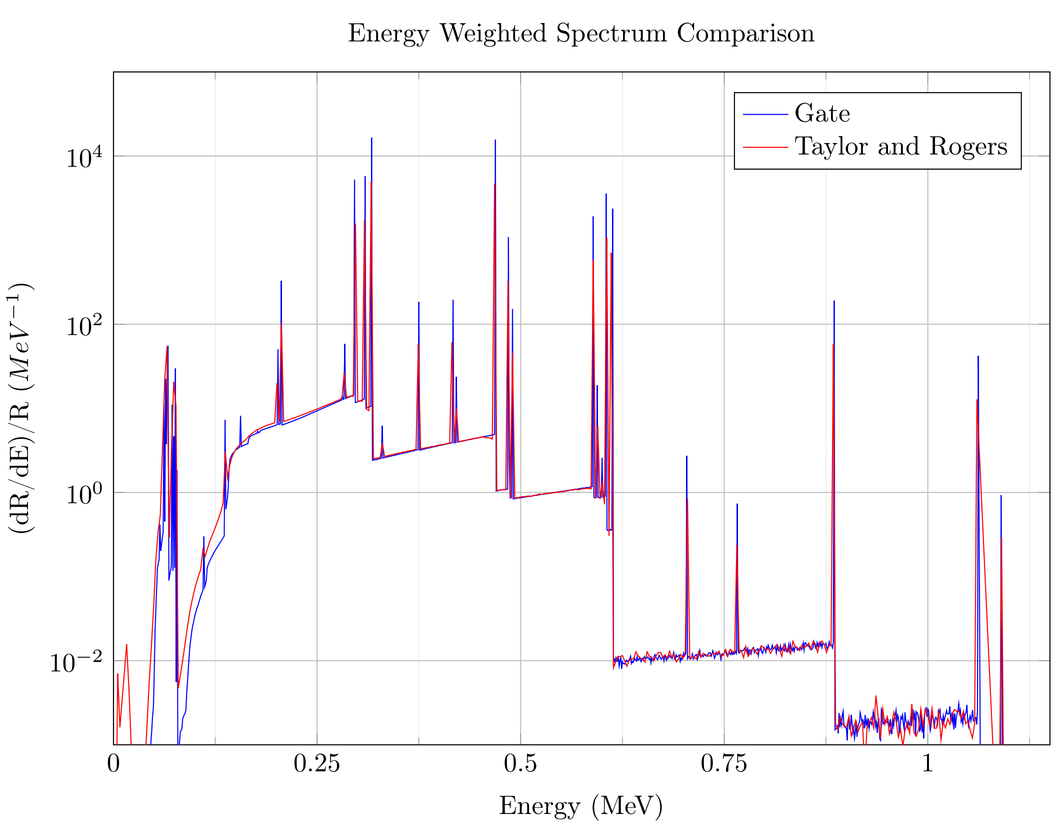

Figure 4.1: Energy weighted spectrum comparison between results produced in this study and work done by Taylor and Rogers.

4.1.2 TG43 Comparisons

Source validation is typically achieved by comparing simulated results with both experimental and published data. However, given that TG43 data for the GMP source is well validated within the medical physics community, simulated results were only compared with published data. Consensus TG43 data for the GMP source was published by Perez et al. [13] and was therefore used as the primary reference for comparisons.

Air KERMA Strength $\mathbf{S_k}$ and Dose Rate Constant Λ

Presented in figure A.1 of appendix A.2.1 is a plot of energy vs mass energy absorption coefficient for air [46] with their corresponding best fit equations. To reduce uncertainties when interpolating between data points, all best fit equations were determined such that their corresponding determination coefficients (r^2) were close to 1. This study's best estimation of $\mathrm{S_k}(1\mathrm{cm}, \frac{\pi}{2})$ was,

$$\mathrm{S_k} = 9.027 \text{ x } 10^{-12} \text{ cm}^2 \text{ cGy history}^{-1}$$

With this this value, the DRC could be estimated and is presented in table 4.1. With a combined standard uncertainty of 2.17%, this study's best estimate of the DRC is in excellent agreement with consensus data.

Table 4.1: MC and consensus DRC comparison.

$_{\mathrm{GATE}}\mathbf{\Lambda}$ (cGy h^{-1} U^{-1})	$_{\mathrm{consensus}}\mathbf{\Lambda}$ (cGy h^{-1} U^{-1})	**Difference**
1.123 ± 0.033	1.117 ± 0.004	0.57%

Radial Dose Function

Radial dose function values produced in this study are presented in table 4.2 and figure 4.2. All data points are in agreement within 1% with consensus data and Taylor and Rogers results. The combined standard uncertainties for all data points are no larger than 0.06% (k=1). Error bars are included in figure 4.2 but are too small to be evident on the plot.

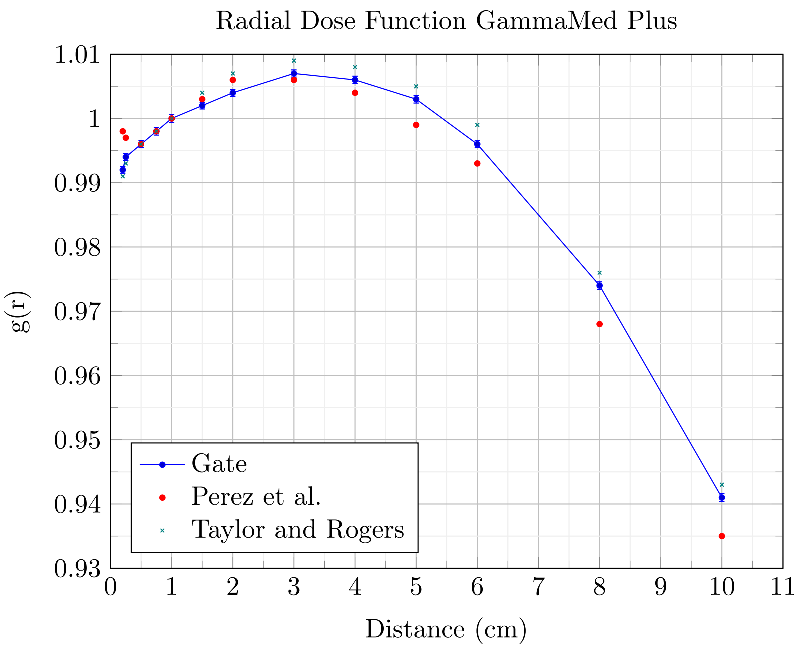

Figure 4.2: Radial dose function comparisons between Perez eat al., Taylor and Rogers, and this study's results.

Table 4.2: Discrete point comparisons of this study's radial dose function values with consensus data.

r(cm)	${}_{\text{GATE}}G_L(r)$	U (k=1)	${}_{\text{Con}}G_L(r)$	difference	${}_{\text{T\&R}}G_L(r)$	difference
0.20	0.992	0.05%	0.998	0.61%	0.991	-0.08%
0.25	0.994	0.05%	0.997	0.36%	0.993	0.06%
0.50	0.996	0.06%	0.996	0.06%	0.996	-0.06%
0.75	0.998	0.06%	0.998	-0.05%	0.998	0.01%
1.00	1.000	0.06%	1.000	0.00%	1.000	0.00%
1.50	1.002	0.05%	1.003	0.10%	1.004	0.16%
2.00	1.004	0.06%	1.006	0.13%	1.007	0.23%
3.00	1.007	0.06%	1.006	-0.09%	1.009	0.22%
4.00	1.006	0.06%	1.004	-0.21%	1.008	0.23%
5.00	1.003	0.06%	0.999	-0.34%	1.005	0.24%
6.00	0.996	0.06%	0.993	-0.34%	0.999	0.29%
8.00	0.974	0.06%	0.968	-0.57%	0.976	0.23%
10.0	0.941	0.06%	0.935	-0.61%	0.943	0.19%

Anisotropy Function

The 2D anisotropy function values produced in this study for r = {0.4cm, 0.6cm, 1cm, 3.5cm, 6cm, 10cm} are presented in figure 4.3. These figures show good agreement with consensus data. Notable differences can be seen at data points close to the long axis of the source. The combined standard uncertainty for all data points are no larger than 1.47% (k=1). Error bars are included in figure 4.3 but are too small to be evident on the plot.

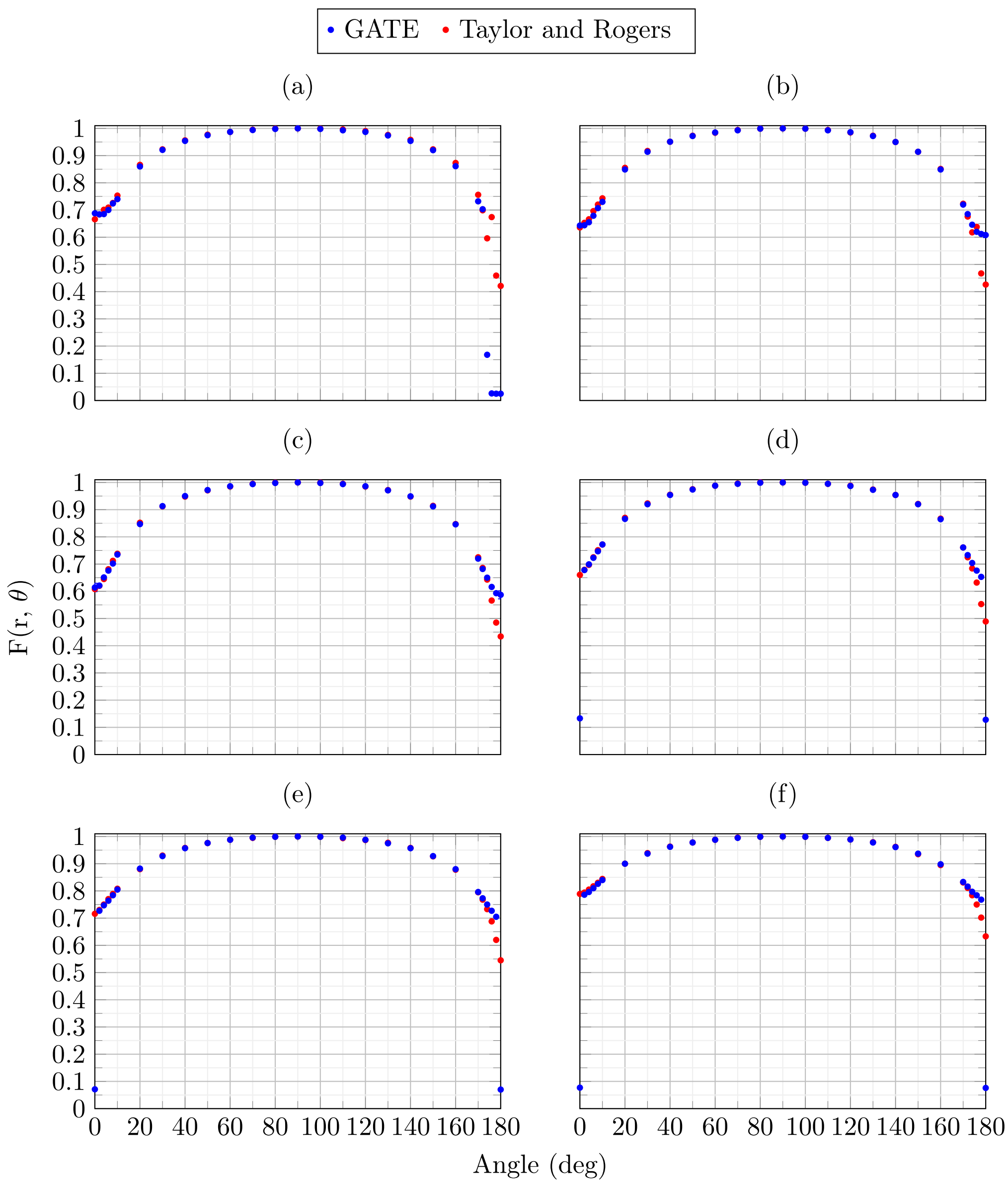

Figure 4.3: Anisotropy comparisons for (a) r = 0.4 cm, (b) r = 0.6 cm, (c) r = 1 cm, (d) r = 3.5 cm, (e) r = 6 cm and (f) r = 10 cm.

4.2 Monte Carlo Calibration factor

Presented in table 4.3 are dose rates estimations at two representations of P(r_0, θ_0) determined in GATE and ABV. Using these values and equation 3.10, the monte carlo calibration factor calculated and applied in this study was,

$$f=1.15 \text{ x } 10^{12} \text{ histories/second}$$

where the combined uncertainty in f is 2.92% (k=2)

Table 4.3: Dose rate measured at multiple representations of P(r_0, θ_0) in GATE and ABV.

	GATE			ABV	
	D (Gy)	U (k=1)	$\dot{D}$ (Gy/history)	D (Gy)	$\dot{D}$ (Gy/second)
P(r, θ, ϕ)	2.34x10^{-4}	1.03%	1.11 x 10^{-13}	1.288	0.1288
P(r, θ, ϕ)	2.35x10^{-4}	1.03%	1.11 x 10^{-13}	1.288	0.1288
		Mean	1.12x10^{-13}	**Mean**	0.1288

4.3 GATE Vs Acuros BrachyVision Comparison

4.3.1 Point-to-Point Profile Comparison

Figures 4.4 - 4.9 present direct dose to medium profile comparison for each phantom setup and differences at each data point as a ratio. The combined standard uncertainty for all data points ≤16.7% (k=2). Profiles generated in ABV between -0.2 cm≤y≤0.2 cm are flat and therefore comparisons were not made in this region.

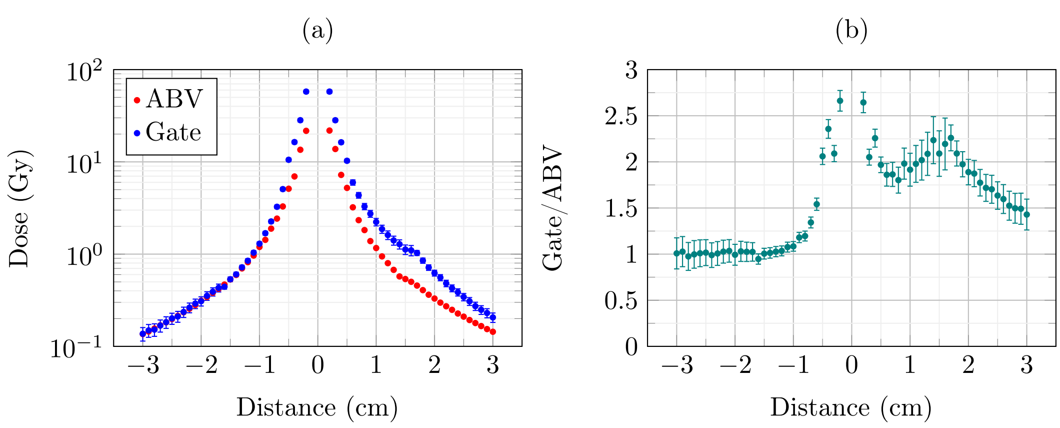

Figure 4.4: GATE versus ABV profile comparison for phantom 1, with (a) showing a direct point-to-point comparison and (b) displaying the dose difference at each point as a ratio.

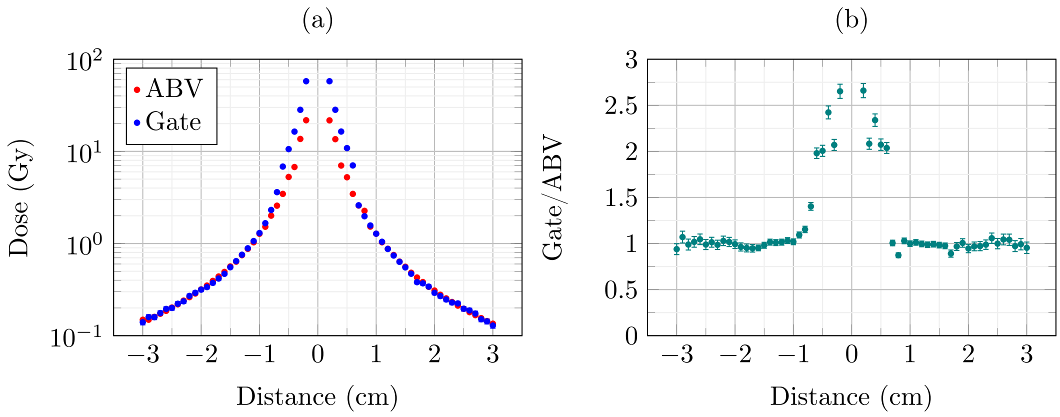

Figure 4.5: GATE versus ABV profile comparison for phantom 2, with (a) showing a direct point-to-point comparison and (b) displaying the dose difference at each point as a ratio.

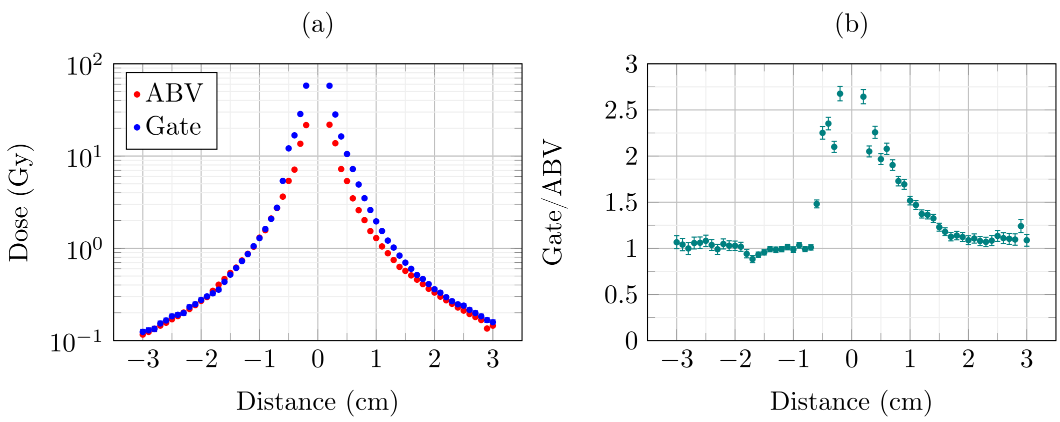

Figure 4.6: GATE versus ABV profile comparison for phantom 3, with (a) showing a direct point-to-point comparison and (b) displaying the dose difference at each point as a ratio.

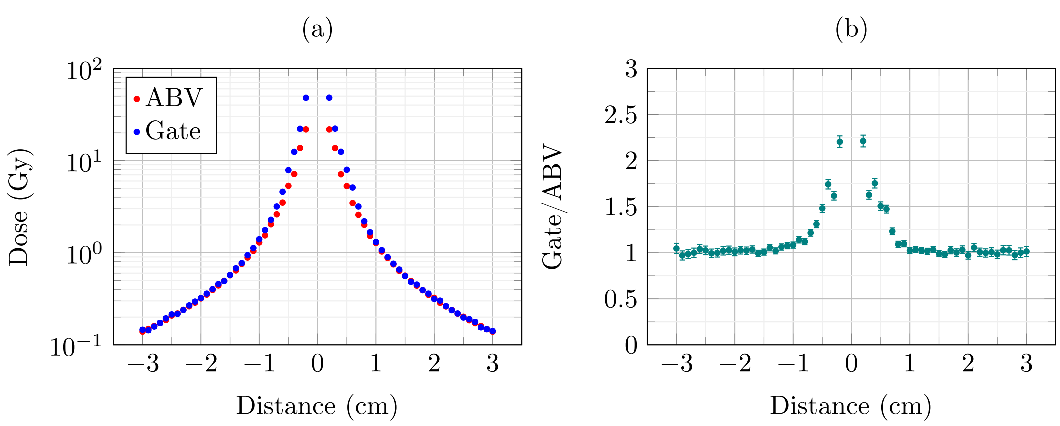

Figure 4.7: GATE versus ABV profile comparison for phantom 4, with (a) showing a direct point-to-point comparison and (b) displaying the dose difference at each point as a ratio.

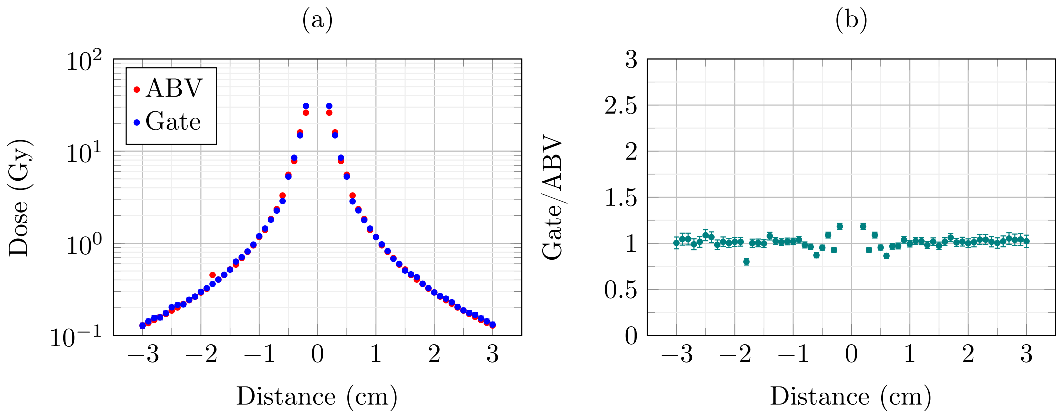

Figure 4.8: GATE versus ABV profile comparison for phantom 5, with (a) showing a direct point-to-point comparison and (b) displaying the dose difference at each point as a ratio.

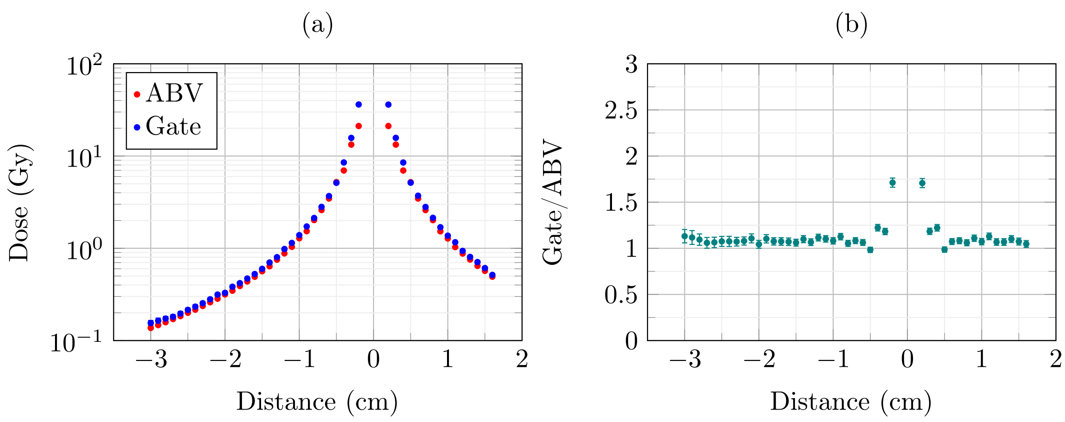

Figure 4.9: GATE versus ABV profile comparison for phantom 6, with (a) showing a direct point-to-point comparison and (b) displaying the dose difference at each point as a ratio.

4.3.2 1D Gamma Analysis

Presented in figure 4.10 are the gamma index values calculated at every point. A gamma index pass criteria of 2%/1 mm gave pass rates of 43% for phantom 1, 86% for phantom 2, 57% for phantom 3 and 100% for phantoms 4, 5 and 6. A gamma index pass criteria of 2%/2 mm gave pass rates of 59%, 98% for phantom 2, 89% for phantom 3 and 100% for phantoms 4, 5 and 6.

4.3.3 Correlation Analysis

For correlation analysis, profiles in all phantoms were separated and analysed as two separate profiles (i.e. +y and -y). By doing this, comparisons were made only between points in the same material. Pearson correlation coefficients (r) for all profiles are shown in table 4.4 with corresponding p values. To visualize the Pearson correlation coefficients, plots of ABV doses versus GATE doses have been provided in figure 4.11.

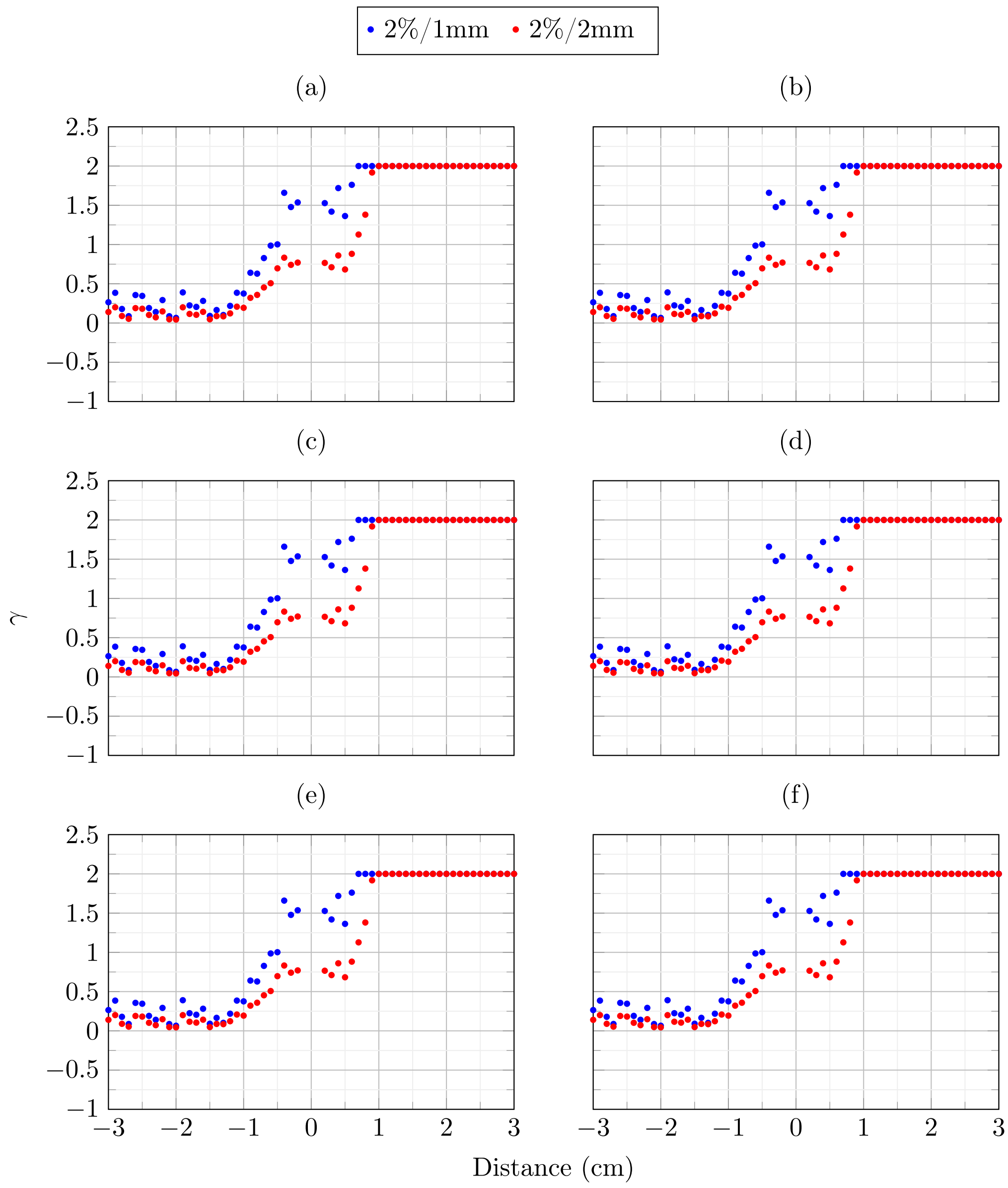

Figure 4.10: 1D gamma analysis results for phantoms 1(a), 2(b), 3(c), 4(d), 5(e) and 6(f) using a gamma criteria of 2%/1 mm and 2%/2 mm.

Table 4.4: Pearson correlation coefficients for correlation analyses done on every phantom, with corresponding p values.

	+Y		-Y	
Phantom	Pearson correlation coefficient	P-value	Pearson correlation coefficient	P-value
1	0.9786	< 0.05	0.9816	< 0.05
2	0.9915	< 0.05	0.9924	< 0.05
3	0.9930	< 0.05	0.9908	< 0.05
4	0.9888	< 0.05	0.9883	< 0.05
5	0.9940	< 0.05	0.9940	< 0.05
6	0.9831	< 0.05	0.9831	< 0.05

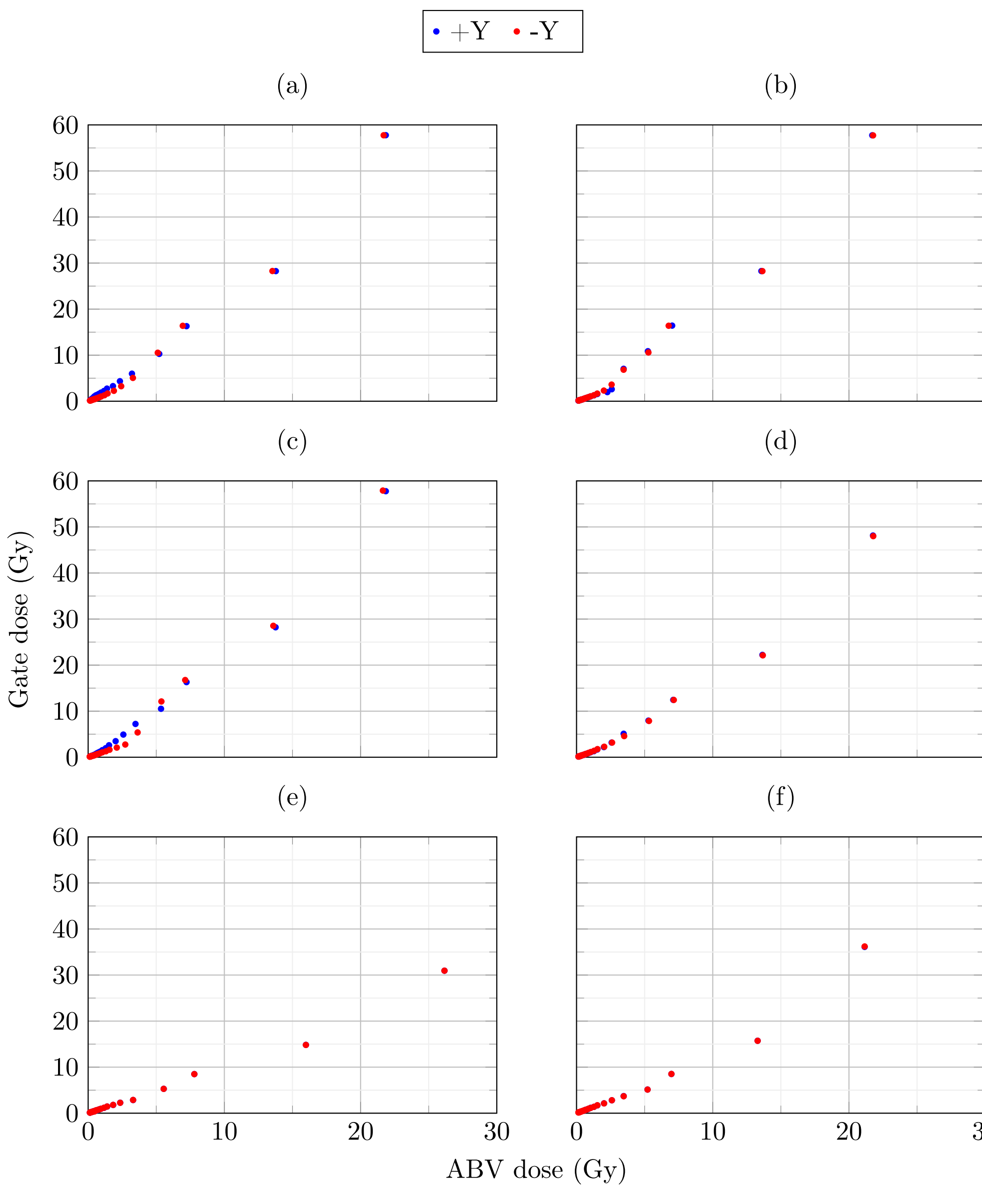

Figure 4.11: Visualisations of the Pearson Correlation Coefficients calculated for phantoms 1(a), 2(b), 3(c), 4(d), 5(e) and 6(f).

Chapter 5

Discussion

5.1 Source Validation

Validation of the modelled source was achieved by first comparing simulated photon spectra with results produced in a study conducted by Taylor and Rogers [1], and TG43 factors with recommended consensus data published by Perez et al. [13].

5.1.1 Spectrum Comparisons

Energy weighted spectra comparisons show there is good agreement with Taylor and Rogers results. Noticeable differences are seen at the lower end of the spectra which may be attributed to the different Ir-192 spectra attached to the core of each source model. In addition, an energy cut of 10 keV has been applied in all GATE simulations. The Ir192 spectrum used by Taylor and Rogers was taken from work done by Duchemin and Coursol [72], whereas this study used the spectrum provided by the NNDC [46]. A study done by Rivard et al. [24] showed that spectra used in both studies have minimal affect on TG43 parameter estimations. However, given that the NNDC spectrum is more recent and internationally evaluated, Rivard et al. suggest the NNDC Ir-192 spectrum be used for all medical physics applications.

5.1.2 TG43 Comparisons

TG43 parameters for the GammaMed Plus source have been extensively studied by both Ballester et al. [2] and Taylor and Rogers [1]. Ballester et al. conducted their study using Geant3 whereas Taylor and Rogers used EGSnrc. Although both studies produced comparable results, Taylor and Rogers results for the radial dose function were noisy. Dose rate constants reported in both studies were 1.118 ± 0.003 $\mathrm{cGy \cdot h^{-1} \cdot U^{-1}}$ [2] and 1.115 ± 0.003 $\mathrm{cGy \cdot h^{-1} \cdot U^{-1}}$ [1], where the average of these two values is used as ${}_{\mathrm{consensus}}\Lambda$. Due to the noisy results produced by Taylor and Rogers, Ballester et al. data was used as consensus data for the remaining TG43 parameters (${}_{\mathrm{consensus}}\mathrm{g_L(r)}$ and ${}_{\mathrm{consensus}}\mathrm{F(r,\theta)}$).

Perez et al. published a value of ${}_{\text{consensus}}\Lambda = 1.117 \pm 0.004$ cGy/hU for the DRC, while in this study the dose rate constant was estimated as $\Lambda = 1.123 \pm 0.033$ cGy/hU. The largest sources of uncertainty in this studies best estimation of the DRC were,

- the statistical uncertainty (type A) in measuring the dose rate at P(r_0, θ_0), and
- the estimated uncertainty (type B) in interpolating between data points when estimating the mass energy absorption coefficients for all energies.

The DRC estimated in this study is 0.57% higher than the consensus value but still agrees within the uncertainties.

Radial dose function values estimated in this study are in good agreement with consensus data values. All data points agreed within ±0.61%, with the largest differences being located at distances equal to 0.2 cm and 10 cm. A study done by Perez et al. [73] showed there is a relationship between phantom geometry and radial dose function and therefore a comparison was also made with Taylor and Rogers radial dose function results. Comparisons with Taylor and Rogers results agreed within ±0.29%, with the largest difference being located at a distance equal to 6 cm. Phantom geometry used across all three studies are different, with Ballester et al. using a 40 cm high solid cylinder with a 40 cm radius [74], Taylor and Rogers using a 30 x 30 x 30 cm^3 cube and a sphere with a 40 cm radius used in this study. The key result in comparing all three sets of data is that values estimated in this study are within the spread of estimations made in other certified studies.

Noticeable differences in anisotropy function comparisons were seen at points within 8 degrees of the source axis. Angles between 8 deg - 172 deg are in good agreement, with the majority of data points agreeing within 1%. Large differences near the source axis can be attributed to multiple factors. The first being a difference in source wire lengths modelled in both studies. Ballester et al. used a source wire length of 6 cm, where as a 2 mm source wire length was used in this study. Secondly, Ballester et al. scored dose instead of kerma. By doing this, Ballester et al. were able to present more accurate results near the long axis of the source [13]. Lastly, Ballester et al. included interpolated/extrapolated data for all points within the source (including the source wire).

Overall, comparisons with consensus data are in good agreement. Dose rate constant, radial dose function and for the most part anisotropy function estimations agree within 1%. These results demonstrate that the physics, actors, VRT's and source specifications have been accurately defined. Therefore, the GMP source modelled using the GATE toolkit accurately reflects what happens in the real world.

5.2 GATE vs BV Comparisons

The aim of this study was to assess the dose calculation accuracy of ABV in materials relevant to HDR brachytherapy. With the source validated, comparisons of ABV and GATE doses were executed using the following methods,

- Point-to-point profile comparisons
- 1D gamma analysis
- Correlation analysis

This section will discuss some of the common themes highlighted across all phantom comparisons.

5.2.1 Point-to-Point Profile Comparison

GATE and ABV doses agreed within uncertainty for the majority of data points in all profile comparisons (figure 4.4 - figure 4.9); however common trends seen in all case comparisons are the large differences seen at distances close to the source (i.e. r$\leq$0.6 cm) and in low density materials such as lung and air.

Large differences observed at close distances may be attributed to multiple factors, with the first being a lack of CPE. ABV assumes CPE exists at all points. In light of this, CPE may not exist at points within $\pm$0.6 cm of the source due to a nonuniform fluence [75], insufficient build up and an increase or decrease in backscatter. With high density materials such as stainless steel assigned to the source slab, differences in this region were reduced. Given the attenuation properties of materials like stainless steel, less build up material is required to reach CPE. Secondly, GATE and ABV doses may be pushed further apart due to voxel size effects in high dose gradient regions. A study conducted by Taylor and Rogers [76] showed that doses may be overestimated when using a large voxel calculation size.

Large differences were also seen when estimating doses in low density materials such as air and lung. This is illustrated by comparing doses in phantoms 1 and 3 (figure 4.4 and figure 4.6). ABV assumes all secondary electrons ranges are smaller than the voxel calculation size and deposit their energy locally (figure 5.1 [77]). Therefore in the context of cavity theory, ABV applies large cavity theory assumptions [8]. Stopping power data published by NIST [78] show that electrons with an initial kinetic energy of 0.3 MeV have a range of up to 0.842 mm in water, 3.27 mm in lung and 794 mm in air. Therefore, electron ranges will be much larger than the voxel calculation grid size and as a result $K_{coll} < D$. Energy deposited within these regions would be better described using small cavity theory, where dose is more accurately calculated using fluence and stopping powers [8]. Following these results, clinical recommendations would be to ensure that bolus, gauze and bladder filling protocols are utilised to reduce any gaps in and around the treatment area.

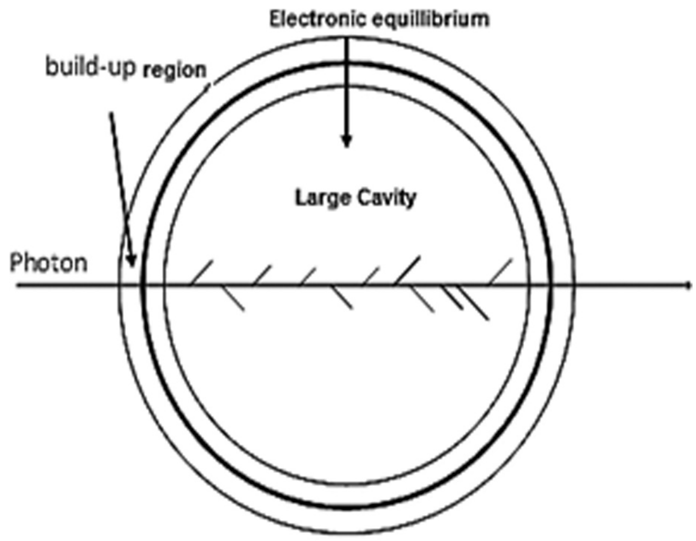

Figure 5.1: A schematic demonstrating large cavity theory, where secondary electron ranges are much smaller than the detection volume and deposit there dose locally.

5.2.2 1D Gamma Analysis

The most straightforward method for comparing profiles is a point-to-point comparison. However, it is method that can be very sensitive in high dose gradient regions [79]. As mentioned above, large differences were seen in all cases at points within close proximity of the source. Given the high dose gradients surrounding a brachytherapy source, a gamma analysis was applied to all profiles to collectively quantify the dose differences and spatial misalignment's at each data point.

The AAPM's report of TG186 [15] recognises the necessity of defining a gamma criteria specifically for brachytherapy and therefore proposed a gamma analysis pass criteria of 2%/2 mm with a ≥99% pass rate. TG186 also recognises that there is limited research on gamma criteria for brachytherapy and therefore understand that their proposed pass criteria may need to be adjusted depending on the case. Given the simplicity of the phantoms used in this study, a stricter gamma index criterion of 2%/1mm with a ≥ 99% was also used.

Among the 6 phantoms, phantoms 4, 5 and 6 produce gamma index pass rates of 100% for both pass criterion's used. However, phantoms 1, 2 and 3 produced varying results. Using a gamma index pass criteria of 2%/1 mm, phantoms 1, 2 and 3 produced passing rates of 43%, 86% and 57% respectively. Using TG186's proposed criteria, pass rates increased. Phantoms 1, 2 and 3 pass rates increased from 43%, 86% and 57% to 59%, 98% and 89% respectively. Given ABV's inability to accurately estimate doses in low density materials, low gamma index pass rates were to be expected for phantoms 1 and 3. The key finding in the gamma analysis results is that even with high density materials producing an excess in backscatter near the source, the spatial distribution of dose is within ±2 mm.

5.3 Clinical Implications

Within a clinical setting, the results presented in this study show that ABV can be used, but with caution. Simulated results show that ABV is unable to accurately calculate dose within and beyond low density materials. This is illustrated in phantoms 1 and 3 (figures 4.4 and 4.6). However, ABV demonstrates good accuracy when calculating doses in anatomical and applicator materials such as bone, cartilage, muscle, adipose, pmma, peek, titanium and stainless steel.

Given ABV demonstrates inaccuracies in low density materials, brachytherapy procedures should include identifying and minimising all air gaps immediately surrounding the source and volumes of interest. For gynaecological and prostate brachytherapy, the most common sites treated with brachytherapy at the WRCC, this is achieved using Vaseline gauze and bladder filling protocols [80, 81, 82].

Despite ABV's limitation in low density materials, it provides noticeable improvements when calculating dose in high density materials like stainless steel. This is illustrated in figure 5.2. For dose calculated in and beyond stainless steel, differences between GATE and TG43 doses ranged between -3.03 - -20.48 %, and gave an average difference of -8.59%; whereas differences between GATE and ABV doses ranged between -15.71 - 5.83 %, and gave an average difference of 0.8%. Therefore, this study's results showed that ABV is capable of providing more accurate dose calculations for plans including gynaecological applicators such the Fletcher-suit system [83].

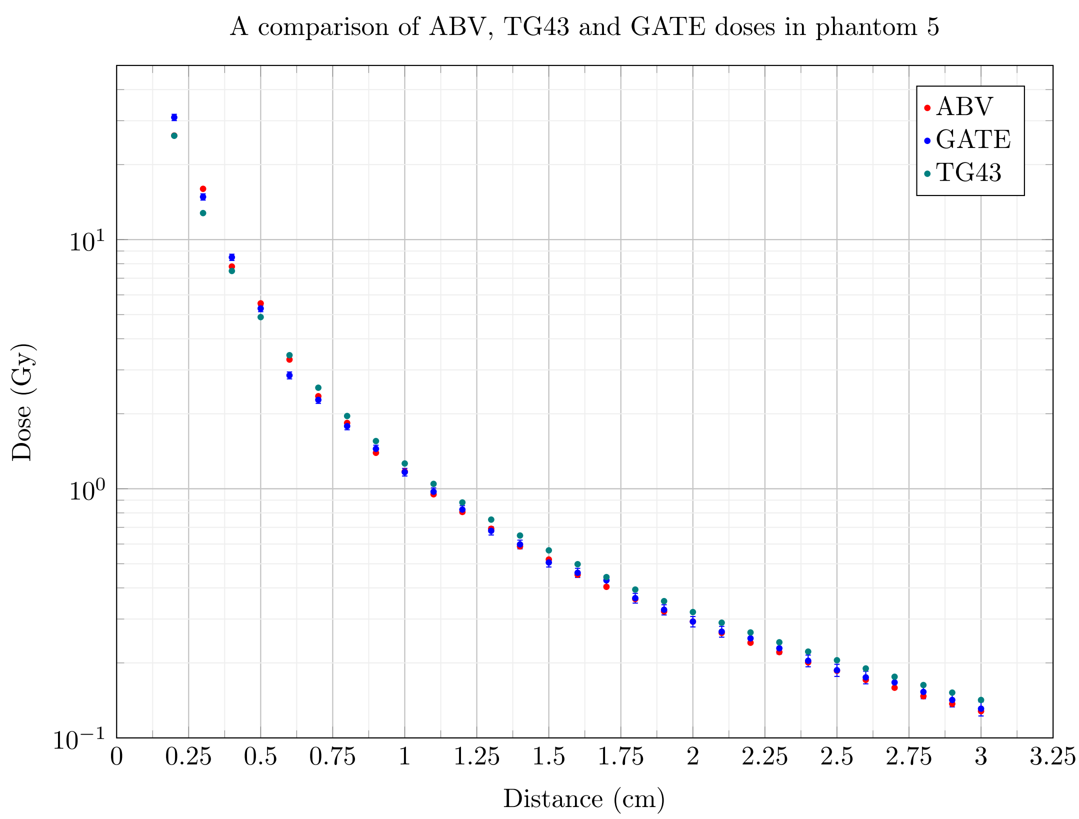

Figure 5.2: Point-to-point dose comparison between ABV, GATE and TG43.

Chapter 6

Conclusion

In first part of this study, Varian's Ir192 GammaMed Plus HDR source was modelled using the GATE MC toolkit. Geometry information published by Lopez et al. [45] and energy spectrum information provided by the NNDC [46] were combined to construct the source. Photon spectra and TG43 factors simulated in this study were compared to data published by Taylor and Rogers [1] Ballester et al. [2] and Perez et al. [13]. Output spectrum comparisons showed good agreement with minor differences seen at the lower end of the spectrum. TG43 comparisons also showed good agreement, with the DRC, radial dose function and anisotropy data points located between 8 deg - 172 deg agreeing within 1%.

The second part of this study was to compare GATE and ABV doses in a variety of materials relevant to HDR brachytherapy. Point-to-point comparisons showed large difference at distances close to the source (i.e. $r \leq 0.6$ cm). Notable differences were also observed in low density materials such as lung and air. It was proposed that these large differences arise due to a lack of CPE and secondary electrons escaping their local voxels.

1D gamma index analyses were evaluated for all phantoms. Using a gamma analysis pass criteria of 2%/1 mm produced pass rates for phantoms 1, 2, 3, 4, 5, 6 of 45%, 84%, 55%, 100%, 100% and 100% respectively. Using TG186's recommended pass criteria of 2%/2 mm produced increased pass rates of 59%, 100% and 88% for phantoms 1, 2 and 3 respectively. Although point-to-point comparisons showed large differences in the near source region, gamma analysis results show that the spatial distribution of dose in this region is within 2 mm.

Pearson correlation coefficients and their correlated p-values suggest that statistically there is no significant difference between MC and ABV doses. However, caution should be taken when interpreting correlation analysis due to its inability to detect causation.

The results presented in this study demonstrate that when applied correctly, ABV can produce accurate dose calculations. Caution must be taken when volumes of low density material are present, as ABV will underestimate doses in and beyond these regions. In contrast to this, ABV is highly capable of calculating doses in high density materials like steel and and bone. The clinical implications of this would mean that when compared to TG43, ABV would provide more accurate results.

6.1 Future Work

The results given in this study have shown that the GMP source has been modelled accurately and that ABV calculated doses are comparable with MC calculated doses except for in regions immediately surrounding the source. However, more research is required before ABV can be implemented clinically. Future work to improve and extend this study should firstly aim to develop a phantom for acquiring 2D dose distributions and point dose measurements. This will provide a means to compare simulated results with physical measurements and show that simulated results reflect what is happening in the real world. Following on from this, further comparisons must be made between MC and ABV. Comparisons need to be extended from 1D to 2D, and then to 3D using anatomical CT data sets that include target volumes and applicators.

Bibliography

[1] REP Taylor and DWO Rogers. “EGSnrc Monte Carlo calculated dosimetry parameters for and brachytherapy sources”. In: *Medical physics* 35.11 (2008), pp. 4933–4944.

[2] F Ballester et al. “Erratum:“Technical note: Monte-Carlo dosimetry of the HDR 12i and Plus sources”[Med. Phys. 28, 2586–2591 (2001)]”. In: *Medical Physics* 31.8 (2004), pp. 2372–2372.

[3] World Helath Organization. *World Health Organization: cancer*. `https://www.who.int/news-room/fact-sheets/detail/cancer`. Accessed: 22 January 2020.

[4] David A Jaffray and Mary K Gospodarowicz. “Radiation therapy for cancer”. In: *Disease Control Priorities,* 3 (2015), pp. 239–247.

[5] American Cancer Society. *American Cancer Society: Radiation Therapy*. `https://www.cancer.org/treatment/treatments-and-side-effects/treatment-types/radiation.html`. Accessed: 22 January 2020.

[6] Bradley J Stish et al. “Low dose rate prostate brachytherapy”. In: *Translational andrology and urology* 7.3 (2018), p. 341.

[7] FM Khan. *The physics of radiation therapy. 2010.*

[8] Philip Mayles, Alan Nahum, and Jean-Claude Rosenwald. *Handbook of radiotherapy physics: theory and practice*. CRC Press, 2007.

[9] Ravinder Nath et al. “Dosimetry of interstitial brachytherapy sources: recommendations of the AAPM Radiation Therapy Committee Task Group No. 43”. In: *Medical physics* 22.2 (1995), pp. 209–234.

[10] Gönül Kemikler. “History of Brachytherapy”. In: *Turkish Journal of Oncology* 34.1 (2019).

[11] FM Khan and BJ Gerbi. *Treatment planning in radiation oncology 2012.*

[12] Mark J Rivard et al. “Update of AAPM Task Group No. 43 Report: A revised AAPM protocol for brachytherapy dose calculations”. In: *Medical physics* 31.3 (2004), pp. 633–674.

[13] Jose Perez-Calatayud et al. “Dose calculation for photon-emitting brachytherapy sources with average energy higher than 50 keV: report of the AAPM and ESTRO”. In: *Medical physics* 39.5 (2012), pp. 2904–2929.

[14] Mark J Rivard, Luc Beaulieu, and Firas Mourtada. "Enhancements to commissioning techniques and quality assurance of brachytherapy treatment planning systems that use model-based dose calculation algorithmsa". In: *Medical physics* 37.6Part2 (2010), pp. 2645–2658.

[15] Luc Beaulieu et al. "Report of the Task Group 186 on model-based dose calculation methods in brachytherapy beyond the TG-43 formalism: current status and recommendations for clinical implementation". In: *Medical physics* 39.10 (2012), pp. 6208–6236.

[16] Mark J Rivard, Jack LM Venselaar, and Luc Beaulieu. "The evolution of brachytherapy treatment planning". In: *Medical physics* 36.6Part1 (2009), pp. 2136–2153.

[17] Varian Medical Systems. *Acuros BV Algorithm Reference Guide.* 2013.

[18] James L Bedford. "Calculation of absorbed dose in radiotherapy by solution of the linear Boltzmann transport equations". In: *Physics in medicine and biology* (2018).

[19] Kent A Gifford et al. "Comparison of a finite-element multigroup discrete-ordinates code with Monte Carlo for radiotherapy calculations". In: *Physics in Medicine & Biology* 51.9 (2006), p. 2253.

[20] Karl Bush et al. "Dosimetric validation of Acuros XB with Monte Carlo methods for photon dose calculations". In: *Medical physics* 38.4 (2011), pp. 2208–2221.

[21] Craig Edwards. *Fundamental quantities and units for ionizing radiation—ICRU report 60.* 1999.

[22] Wazir Muhammad, Amjad Hussain, and Muhammad Maqbool. "Basic Concepts in Radiation Dosimetry". In: *An Introduction to Medical Physics.* Springer, 2017, pp. 9–41.

[23] Ervin B Podgorsak et al. "Radiation oncology physics". In: *Vienna: International Atomic Energy Agency* (2005), pp. 123–271.

[24] Mark J Rivard et al. "Influence of photon energy spectra from brachytherapy sources on Monte Carlo simulations of kerma and dose rates in water and air". In: *Medical physics* 37.2 (2010), pp. 869–876.

[25] Elaine M Zeman, Eric C Schreiber, and Joel E Tepper. "Basics of radiation therapy". In: *Abeloff's Clinical Oncology.* Elsevier, 2020, pp. 431–460.

[26] Bryn Currie. *MDPH 403 Radiation Physics - Lecture 11-13: Charged Radiation.*

[27] Dirk Müssig. "Re-scanning in scanned ion beam therapy in the presence of organ motion". PhD thesis. Technische Universität, 2014.

[28] Eric J Hall and Amato J Giaccia. *Radiobiology for the Radiologist.* Vol. 6. Lippincott Williams & Wilkins, 2006.

[29] Frank Pajonk, Erina Vlashi, and William H McBride. "Radiation resistance of cancer stem cells: the 4 R's of radiobiology revisited". In: *Stem cells* 28.4 (2010), pp. 639–648.

[30] David J Brenner. "The linear-quadratic model is an appropriate methodology for determining isoeffective doses at large doses per fraction". In: *Seminars in radiation oncology.* Vol. 18. 4. Elsevier. 2008, pp. 234–239.

[31] DH Brand and JR Yarnold. "The Linear–Quadratic Model and Implications for Fractionation". In: *Clinical Oncology* 31.10 (2019), pp. 673–677.

[32] Michael D Chan et al. "Benign brain tumors: meningiomas and vestibular schwannomas". In: *Clinical Radiation Oncology*. Elsevier, 2016, pp. 483–501.

[33] Roukaya Keinj, Thierry Bastogne, and Pierre Vallois. "Multinomial model-based formulations of TCP and NTCP for radiotherapy treatment planning". In: *Journal of theoretical biology* 279.1 (2011), pp. 55–62.

[34] Murat Beyzadeoglu, Gokhan Ozyigit, and Cüneyt Ebruli. *Basic radiation oncology*. Springer Science & Business Media, 2010.

[35] Christopher R King, Thomas A DiPetrillo, and David E Wazer. "Optimal radiotherapy for prostate cancer: predictions for conventional external beam, imrt, and brachytherapy from radiobiologic models". In: *International Journal of Radiation Oncology* Biology* Physics* 46.1 (2000), pp. 165–172.

[36] American Cancer Society: Treatment for Cancer. *National Cancer Institute*. `https://www.cancer.gov/about-cancer/treatment`. Accessed: 22 January 2020.

[37] Faiz M Khan, John P Gibbons, and Paul W Sperduto. *Khan's Treatment Planning in Radiation Oncology*. Lippincott Williams & Wilkins, 2016.

[38] American Cancer Society. *Radiation Therapy for Cervical Cancer*. `https://www.cancer.org/cancer/cervical-cancer/treating/radiation.html`. Accessed: 04 April 2020.

[39] Joann I Prisciandaro. "From Licensing to QA, How to Implement HDR Brachytherapy Into Your Clinic". In: *Medical Physics*. Vol. 35. 6. WILEY 111 RIVER ST, HOBOKEN 07030-5774, NJ USA. 2008.

[40] Subir Nag. "High dose rate brachytherapy: its clinical applications and treatment guidelines". In: *Technology in cancer research & treatment* 3.3 (2004), pp. 269–287.

[41] Varian Medical Systems. *BrachyVision Reference Guide*. 2017.

[42] Ravinder Nath et al. "Recommendations of AAPM Task Group 32: Specification of Brachytherapy Source Strength (American Institute of Physics, New York, 1987)". In: (1995).

[43] Luc Beaulieu. *Model-Based Dose Calculation: An Introduction*. 2017. URL: `https://www.aapm.org/education/VL/vl.asp?id=11927`.

[44] K Zourari et al. "Dosimetric accuracy of a deterministic radiation transport based brachytherapy treatment planning system. Part I: Single sources and bounded homogeneous geometries". In: *Medical physics* 37.2 (2010), pp. 649–661.

[45] JF López, J Torres Donaire, and R Guerrero Alcalde. "Monte Carlo dosimetry of the most commonly used 192Ir high dose rate brachytherapy sources". In: *Rev Fis Med* 12.3 (2011), pp. 159–168.

[46] Brookhaven National Laboratory National Nuclear Data Center. *NUDAT 2.5*. `http://www.nndc.bnl.gov/nudat2/`. Accessed: 07 January 2020.

[47] Joao Seco and Frank Verhaegen. *Monte Carlo techniques in radiation therapy*. CRC/-Taylor & Francis, 2013.

[48] Ramses Herrera. *MCNP5 Monte Carlo based dosimetry for the nucletron iridium-192 high dose-rate brachytherapy source with tissue heterogeneity corrections.* Florida Atlantic University, 2012.

[49] JCGM JCGM et al. "Evaluation of measurement data—Guide to the expression of uncertainty in measurement". In: *Int. Organ. Stand. Geneva ISBN* 50 (2008), p. 134.

[50] Indrin J Chetty et al. "Reporting and analyzing statistical uncertainties in Monte Carlo–based treatment planning". In: *International Journal of Radiation Oncology* Biology* Physics* 65.4 (2006), pp. 1249–1259.

[51] F Smekens et al. "Split exponential track length estimator for Monte-Carlo simulations of small-animal radiation therapy". In: *Physics in Medicine & Biology* 59.24 (2014), p. 7703.

[52] John Allison et al. "Geant4 developments and applications". In: *IEEE Transactions on nuclear science* 53.1 (2006), pp. 270–278.

[53] David Sarrut et al. "A review of the use and potential of the GATE Monte Carlo simulation code for radiation therapy and dosimetry applications". In: *Medical physics* 41.6Part1 (2014).

[54] Sébastien Jan et al. "GATE: a simulation toolkit for PET and SPECT". In: *Physics in Medicine & Biology* 49.19 (2004), p. 4543.

[55] Albertine Dubios, David Sarrut, and Sebastien Jan. *Day 1: Main Principles of GATE.* 2018.

[56] Uwe Pietrzyk. *Users Guide V8.0.* 2017.

[57] F Baldacci et al. "A track length estimator method for dose calculations in low-energy X-ray irradiations: implementation, properties and performance". In: *Zeitschrift für Medizinische Physik* 25.1 (2015), pp. 36–47.

[58] CERN: Geant4 Collaboration. *EM Opt0.* http://geant4-userdoc.web.cern.ch/geant4-userdoc/UsersGuides/PhysicsListGuide/html/electromagnetic/Opt0.html.

[59] Makoto Matsumoto and Takuji Nishimura. "Mersenne twister: a 623-dimensionally equidistributed uniform pseudo-random number generator". In: *ACM Transactions on Modeling and Computer Simulation (TOMACS)* 8.1 (1998), pp. 3–30.

[60] Vadim Demchik. "Pseudo-random number generators for Monte Carlo simulations on ATI Graphics Processing Units". In: *Computer Physics Communications* 182.3 (2011), pp. 692–705.

[61] CO Thiam et al. "Validation of a dose deposited by low-energy photons using GATE/GEANT4". In: *Physics in Medicine & Biology* 53.11 (2008), p. 3039.

[62] Brian S Thomson. "On Riemann sums". In: *Real Analysis Exchange* 37.1 (2012), pp. 221–242.

[63] John H Hubbell and Stephen M Seltzer. *Tables of X-ray mass attenuation coefficients and mass energy-absorption coefficients 1 keV to 20 MeV for elements Z= 1 to 92 and 48 additional substances of dosimetric interest.* Tech. rep. National Inst. of Standards and Technology-PL, Gaithersburg, MD (United ..., 1995.

[64] Varian Medical Systems. *Varian Brachytherapy GammaMedplus iX Instructions for Use including the GammaMedplus 3/24 iX*. Varian Medical Systems, 2011.

[65] Daniel A Low et al. "A technique for the quantitative evaluation of dose distributions". In: *Medical physics* 25.5 (1998), pp. 656–661.

[66] Daniel Low. *Limitations of Gamma Analysis*. `https://www.aapm.org/education/VL/vl.asp?id=11122`. Accessed 17/03/2020. 2016.

[67] M Hussein, CH Clark, and Andrew Nisbet. "Challenges in calculation of the gamma index in radiotherapy–towards good practice". In: *Physica Medica* 36 (2017), pp. 1–11.

[68] Mark Geurts. *CalcGamma*. `https://github.com/mwgeurts/gamma`. Accessed 18/03/2020. 2015.

[69] David G Rees. *Essential statistics*. Vol. 50. CRC Press, 2000.

[70] Georgy L Shevlyakov and Hannu Oja. *Robust correlation: Theory and applications*. Vol. 3. John Wiley & Sons, 2016.

[71] Andrew A Jawlik. *Statistics from a to z: Confusing concepts clarified*. John Wiley & Sons, 2016.

[72] B Duchemin and N Coursol. "Reevalution de l'192Ir". In: *Technical Note LPRI/93/018, DAMRI, CEA, France* (1993).

[73] J Pérez-Calatayud, D Granero, and F Ballester. "Phantom size in brachytherapy source dosimetric studies". In: *Medical physics* 31.7 (2004), pp. 2075–2081.

[74] F Ballester et al. "Monte Carlo calculation of dose rate distributions around wires". In: *Medical physics* 24.8 (1997), pp. 1221–1228.

[75] Frank Herbert Attix. *Introduction to radiological physics and radiation dosimetry*. John Wiley & Sons, 2008.

[76] REP Taylor, G Yegin, and DWO Rogers. "Benchmarking brachydose: voxel based EGSnrc Monte Carlo calculations of TG-43 dosimetry parameters". In: *Medical physics* 34.2 (2007), pp. 445–457.

[77] Hossam Donya et al. "Prospective Monte Carlo Simulation for Choosing High Efficient Detectors for Small-Field Dosimetry". In: *Theory, Application, and Implementation of Monte Carlo Method in Science and Technology*. IntechOpen, 2019.

[78] MJ Berger et al. *Stopping-power and range tables for electrons, protons, and helium ions, NIST Standard Reference Database 124*. 2017.

[79] Moyed Miften et al. "Tolerance limits and methodologies for IMRT measurement-based verification QA: recommendations of AAPM Task Group No. 218". In: *Medical physics* 45.4 (2018), e53–e83.

[80] Radiation Oncology: Targeting Cancer. *Brachytherapy for Uterine Cancer*. `https://www.targetingcancer.com.au/radiation-therapy/brachytherapy/brachytherapy-for-uterine-cancer/`. Accessed 20/05/2020. 2019.

[81] Radiation Oncology: Targeting Cancer. *Brachytherapy for Cervix Cancer*. `https://www.targetingcancer.com.au/radiation-therapy/brachytherapy/brachytherapy-for-gynaecological-cancer/`. Accessed 20/05/2020. 2019.

[82] Radiation Oncology: Targeting Cancer. *Brachytherapy for Prostate Cancer*. https://www.targetingcancer.com.au/radiation-therapy/brachytherapy/brachytherapy-for-prostate-cancer/. Accessed 20/05/2020. 2019.

[83] Orau. *Fletcher-suit Afterloading Applicator (ca. 1960)*. https://www.orau.org/ptp/collection/brachytherapy/Fletcherafterloader.htm. Accessed 20/05/2020. 2010.

Appendix A

Appendix

A.1 GATE Code

A.1.1 GMP Geometry

```
####################################################    Source Capsule    ########################################

/gate/world/daughters/name          sc1
/gate/world/daughters/insert        cone
/gate/sc1/geometry/setRmin1         0 mm
/gate/sc1/geometry/setRmax1         0.45 mm
/gate/sc1/geometry/setRmin2         0 mm
/gate/sc1/geometry/setRmax2         0.175 mm
/gate/sc1/geometry/setHeight        0.155 mm
/gate/sc1/geometry/setPhiStart      0 deg
/gate/sc1/geometry/setDeltaPhi      360 deg
/gate/sc1/placement/setTranslation  0 0 2.3925 mm
/gate/sc1/setMaterial               316L
/gate/sc1/vis/setColor              red
/gate/sc1/vis/forceSolid            1

/gate/world/daughters/name          sc2
/gate/world/daughters/insert        cylinder
/gate/sc2/geometry/setRmin          0 mm
/gate/sc2/geometry/setRmax          0.45 mm
/gate/sc2/geometry/setHeight        0.465 mm
/gate/sc2/placement/setTranslation  0 0 2.0825 mm
/gate/sc2/setMaterial               316L
/gate/sc2/vis/setColor              red
/gate/sc2/vis/forceSolid            1

/gate/world/daughters/name          sc3
/gate/world/daughters/insert        cylinder
/gate/sc3/geometry/setRmin          0 mm
/gate/sc3/geometry/setRmax          0.35 mm
/gate/sc3/geometry/setHeight        0.1 mm
```

```
/gate/sc3/placement/setTranslation  0 0 1.8 mm
/gate/sc3/setMaterial               AirTG43U
/gate/sc3/vis/setColor              white

/gate/world/daughters/name          sc4
/gate/world/daughters/insert        cylinder
/gate/sc4/geometry/setRmin          0.35 mm
/gate/sc4/geometry/setRmax          0.45 mm
/gate/sc4/geometry/setHeight        0.1 mm
/gate/sc4/placement/setTranslation  0 0 1.8 mm
/gate/sc4/setMaterial               316L
/gate/sc4/vis/setColor              red
/gate/sc4/vis/forceSolid            1

/gate/world/daughters/name          sc5
/gate/world/daughters/insert        cylinder
/gate/sc5/geometry/setRmin          0.3 mm
/gate/sc5/geometry/setRmax          0.35 mm
/gate/sc5/geometry/setHeight        3.5 mm
/gate/sc5/placement/setTranslation  0 0 0 mm
/gate/sc5/setMaterial               AirTG43U
/gate/sc5/vis/setColor              white

/gate/world/daughters/name          sc6
/gate/world/daughters/insert        cylinder
/gate/sc6/geometry/setRmin          0.35 mm
/gate/sc6/geometry/setRmax          0.45 mm
/gate/sc6/geometry/setHeight        3.5 mm
/gate/sc6/placement/setTranslation  0 0 0 mm
/gate/sc6/setMaterial               316L
/gate/sc6/vis/setColor              red
/gate/sc6/vis/forceSolid            1

/gate/world/daughters/name          sc7
/gate/world/daughters/insert        cylinder
/gate/sc7/geometry/setRmin          0 mm
/gate/sc7/geometry/setRmax          0.45 mm
/gate/sc7/geometry/setHeight        0.3 mm
/gate/sc7/placement/setTranslation  0 0 -1.9 mm
/gate/sc7/setMaterial               316L
/gate/sc7/vis/setColor              red
/gate/sc7/vis/forceSolid            1

/gate/world/daughters/name          wire
/gate/world/daughters/insert        cylinder
/gate/wire/geometry/setRmin         0 mm
/gate/wire/geometry/setRmax         0.45 mm
/gate/wire/geometry/setHeight       2 mm
/gate/wire/placement/setTranslation 0 0 -3.05 mm
/gate/wire/setMaterial              304
/gate/wire/vis/setColor             blue
/gate/wire/vis/forceSolid           1


##################################################    source seed    ##################################################
```

```
/gate/world/daughters/name                 sourceSeed
/gate/world/daughters/insert               cylinder
/gate/sourceSeed/geometry/setRmin          0 mm
/gate/sourceSeed/geometry/setRmax          0.3 mm
/gate/sourceSeed/geometry/setHeight        3.5 mm
/gate/sourceSeed/placement/setTranslation  0 0 0 cm
/gate/sourceSeed/setMaterial               Seed192
/gate/sourceSeed/vis/setColor              blue
/gate/sourceSeed/vis/forceSolid            1
```

A.1.2 AKS and DRC

```
#=====================================================
# VISUALISATION
#=====================================================
#/control/execute    mac/vis.mac
#=====================================================
# MATERIALS
#=====================================================
#Define Materials Database
/gate/geometry/setMaterialDatabase data/MyMaterialDatabase.db

#=====================================================
# WORLD
#=====================================================
/gate/world/setMaterial               Vacuum
/gate/world/geometry/setXLength       10 m
/gate/world/geometry/setYLength       10 m
/gate/world/geometry/setZLength       10 m
#=====================================================
# GEOMETRY
#=====================================================

#calculation volume

/gate/world/daughters/name                          calcVolume
/gate/world/daughters/insert                        sphere
/gate/calcVolume/geometry/setRmin                   0 m
/gate/calcVolume/geometry/setRmax                   5 m
/gate/calcVolume/geometry/setPhiStart               0 deg
/gate/calcVolume/geometry/setDeltaPhi               360 deg
/gate/calcVolume/geometry/setThetaStart             0 deg
/gate/calcVolume/geometry/setDeltaTheta             360 deg
/gate/calcVolume/setMaterial                        Vacuum
/gate/calcVolume/vis/setColor                       blue

/control/execute                                    data/GMSource.mac

###################################################    Dose voxels    ###################################################
```

```
/gate/calcVolume/daughters/name                      d1
/gate/calcVolume/daughters/insert                    cylinder
/gate/d1/geometry/setRmin                            49.75 mm
/gate/d1/geometry/setRmax                            50.25 mm
/gate/d1/geometry/setHeight                          0.5 mm
/gate/d1/placement/setTranslation                    0 0 0 mm
/gate/d1/setMaterial                                 AirTG43U
/gate/d1/vis/setColor                                red

#------------------------------------------------

#=====================================================
# PHYSICS
#=====================================================
/gate/physics/addPhysicsList emstandard
#=============================================================================================
# customized CUTS
#=============================================================================================

/gate/physics/Gamma/SetCutInRegion                   calcVolume 10 keV
/gate/physics/Electron/SetCutInRegion                calcVolume 10 keV
/gate/physics/Positron/SetCutInRegion                calcVolume 10 keV

#=============================================================================================
# Additional processes not included in the list option 3
#=============================================================================================
/gate/physics/setEMin 10 keV
/gate/physics/setEMax 10 GeV
/gate/physics/setDEDXBinning 500
/gate/physics/setLambdaBinning 500

/gate/physics/processList Enabled
/gate/physics/processList Initialized

#=====================================================
# OUTPUT ACTORS
#=====================================================
#=====================================================
#ACTOR
#=====================================================

/gate/actor/addActor                                 EnergySpectrumActor Spectrum
/gate/actor/Spectrum/save                            output/AKStrength/spectrum_txt.txt
/gate/actor/Spectrum/save                            output/AKStrength/spectrum_root.root
/gate/actor/Spectrum/energySpectrum/setEmin          0.001 MeV
/gate/actor/Spectrum/energySpectrum/setEmax          0.885 MeV
/gate/actor/Spectrum/energySpectrum/setNumberOfBins  884
/gate/actor/Spectrum/attachTo                        d1

/gate/actor/addActor SimulationStatisticActor        statActor
/gate/actor/statActor/save                           output/AKStrength/stats.txt

#=====================================================
# END PHYSICS - Initialize before source definition
#=====================================================
# initialize
```

```
/gate/run/initialize
/gate/physics/print phys.txt

#=====================================================
# SOURCE
#=====================================================

/gate/source/addSource                      GammaMed1 gps
/gate/source/GammaMed1/gps/particle         gamma
/gate/source/GammaMed1/gps/energytype       UserSpectrum
/gate/source/GammaMed1/gps/setSpectrumFile  data/NUDATIridium192.txt
/gate/source/GammaMed1/gps/type             Volume
/gate/source/GammaMed1/attachTo             sourceSeed
/gate/source/GammaMed1/gps/shape            Cylinder
/gate/source/GammaMed1/gps/radius           0.3 mm
/gate/source/GammaMed1/gps/halfz            1.75 mm
/gate/source/GammaMed1/gps/angtype          iso

#Visualise the source
#/gate/source/GammaMed1/visualize           2000 yellow 3

#=====================================================#
# UNCOMMENT IF YOU WANT NO OUTPUT FROM SIMULATION
#=====================================================
#/gate/output/allowNoOutput

#=====================================================#
#   S T A R T   S I M U L A T I O N
#=====================================================#
/gate/random/setEngineName MersenneTwister
/gate/random/setEngineSeed auto
/gate/application/setNumberOfPrimariesPerRun        2100000000
/gate/application/start
exit
```

A.1.3 Radial Dose Function

```
#=====================================================
# VISUALISATION
#=====================================================
#/control/execute    mac/vis.mac
#=====================================================
# MATERIALS
#=====================================================
#Define Materials Database
/gate/geometry/setMaterialDatabase data/MyMaterialDatabase.db

#=====================================================
# WORLD
#=====================================================
/gate/world/setMaterial                   AirTG43U
```

```
/gate/world/geometry/setXLength           100 cm
/gate/world/geometry/setYLength           100 cm
/gate/world/geometry/setZLength           100 cm
#=====================================================
# GEOMETRY
#=====================================================

#calculation volume
/gate/world/daughters/name                calcVolume
/gate/world/daughters/insert              sphere
/gate/calcVolume/geometry/setRmin         0 mm
/gate/calcVolume/geometry/setRmax         40 cm
/gate/calcVolume/geometry/setPhiStart     0 deg
/gate/calcVolume/geometry/setDeltaPhi     360 deg
/gate/calcVolume/geometry/setThetaStart   0 deg
/gate/calcVolume/geometry/setDeltaTheta   360 deg
/gate/calcVolume/setMaterial              Water

#=====================================================
# source
#=====================================================
/control/execute  data/GMSource.mac


###################################################    Dose voxels    #################################################

/gate/calcVolume/daughters/name           d1
/gate/calcVolume/daughters/insert         cylinder
/gate/d1/geometry/setRmin                 1.95 mm
/gate/d1/geometry/setRmax                 2.05 mm
/gate/d1/geometry/setHeight               0.1 mm
/gate/d1/placement/setTranslation         0 0 0 cm
/gate/d1/setMaterial                      Water
/gate/d1/vis/setColor                     red

/gate/calcVolume/daughters/name           d2
/gate/calcVolume/daughters/insert         cylinder
/gate/d2/geometry/setRmin                 2.45 mm
/gate/d2/geometry/setRmax                 2.55 mm
/gate/d2/geometry/setHeight               0.1 mm
/gate/d2/placement/setTranslation         0 0 0 cm
/gate/d2/setMaterial                      Water
/gate/d2/vis/setColor                     red

/gate/calcVolume/daughters/name           d3
/gate/calcVolume/daughters/insert         cylinder
/gate/d3/geometry/setRmin                 4.95 mm
/gate/d3/geometry/setRmax                 5.05 mm
/gate/d3/geometry/setHeight               0.1 mm
/gate/d3/placement/setTranslation         0 0 0 cm
/gate/d3/setMaterial                      Water
/gate/d3/vis/setColor                     red

/gate/calcVolume/daughters/name           d4
/gate/calcVolume/daughters/insert         cylinder
/gate/d4/geometry/setRmin                 7.45 mm
```

```
/gate/d4/geometry/setRmax                  7.55 mm
/gate/d4/geometry/setHeight                0.1 mm
/gate/d4/placement/setTranslation          0 0 0 cm
/gate/d4/setMaterial                       Water
/gate/d4/vis/setColor                      red

/gate/calcVolume/daughters/name            d5
/gate/calcVolume/daughters/insert          cylinder
/gate/d5/geometry/setRmin                  9.95 mm
/gate/d5/geometry/setRmax                  10.05 mm
/gate/d5/geometry/setHeight                0.1 mm
/gate/d5/placement/setTranslation          0 0 0 cm
/gate/d5/setMaterial                       Water
/gate/d5/vis/setColor                      red

/gate/calcVolume/daughters/name            d6
/gate/calcVolume/daughters/insert          cylinder
/gate/d6/geometry/setRmin                  14.75 mm
/gate/d6/geometry/setRmax                  15.25 mm
/gate/d6/geometry/setHeight                0.5 mm
/gate/d6/placement/setTranslation          0 0 0 cm
/gate/d6/setMaterial                       Water
/gate/d6/vis/setColor                      red

/gate/calcVolume/daughters/name            d7
/gate/calcVolume/daughters/insert          cylinder
/gate/d7/geometry/setRmin                  19.75 mm
/gate/d7/geometry/setRmax                  20.25 mm
/gate/d7/geometry/setHeight                0.5 mm
/gate/d7/placement/setTranslation          0 0 0 cm
/gate/d7/setMaterial                       Water
/gate/d7/vis/setColor                      red

/gate/calcVolume/daughters/name            d8
/gate/calcVolume/daughters/insert          cylinder
/gate/d8/geometry/setRmin                  29.75 mm
/gate/d8/geometry/setRmax                  30.25 mm
/gate/d8/geometry/setHeight                0.5 mm
/gate/d8/placement/setTranslation          0 0 0 cm
/gate/d8/setMaterial                       Water
/gate/d8/vis/setColor                      red

/gate/calcVolume/daughters/name            d9
/gate/calcVolume/daughters/insert          cylinder
/gate/d9/geometry/setRmin                  39.75 mm
/gate/d9/geometry/setRmax                  40.25 mm
/gate/d9/geometry/setHeight                0.5 mm
/gate/d9/placement/setTranslation          0 0 0 cm
/gate/d9/setMaterial                       Water
/gate/d9/vis/setColor                      red

/gate/calcVolume/daughters/name            d10
/gate/calcVolume/daughters/insert          cylinder
/gate/d10/geometry/setRmin                 49.75 mm
/gate/d10/geometry/setRmax                 50.25 mm
/gate/d10/geometry/setHeight               0.5 mm
```

```
/gate/d10/placement/setTranslation        0 0 0 cm
/gate/d10/setMaterial                     Water
/gate/d10/vis/setColor                    red

/gate/calcVolume/daughters/name           d11
/gate/calcVolume/daughters/insert         cylinder
/gate/d11/geometry/setRmin                59.5 mm
/gate/d11/geometry/setRmax                60.5 mm
/gate/d11/geometry/setHeight              1 mm
/gate/d11/placement/setTranslation        0 0 0 cm
/gate/d11/setMaterial                     Water
/gate/d11/vis/setColor                    red

/gate/calcVolume/daughters/name           d12
/gate/calcVolume/daughters/insert         cylinder
/gate/d12/geometry/setRmin                79.5 mm
/gate/d12/geometry/setRmax                80.5 mm
/gate/d12/geometry/setHeight              1 mm
/gate/d12/placement/setTranslation        0 0 0 cm
/gate/d12/setMaterial                     Water
/gate/d12/vis/setColor                    red

/gate/calcVolume/daughters/name           d13
/gate/calcVolume/daughters/insert         cylinder
/gate/d13/geometry/setRmin                99.5 mm
/gate/d13/geometry/setRmax                100.5 mm
/gate/d13/geometry/setHeight              1 mm
/gate/d13/placement/setTranslation        0 0 0 cm
/gate/d13/setMaterial                     Water
/gate/d13/vis/setColor                    red


#------------------------------------------------

#=====================================================
# PHYSICS
#=====================================================
/gate/physics/addPhysicsList emstandard
#===============================================================================================
# customized CUTS
#===============================================================================================

/gate/physics/Gamma/SetCutInRegion        calcVolume 10 keV
/gate/physics/Electron/SetCutInRegion     calcVolume 10 keV
/gate/physics/Positron/SetCutInRegion     calcVolume 10 keV

#==============================================================================================
# Additional processes not included in the list option 3
#==============================================================================================
/gate/physics/setEMin 10 keV
/gate/physics/setEMax 10 GeV
/gate/physics/setDEDXBinning 500
/gate/physics/setLambdaBinning 500

/gate/physics/processList Enabled
/gate/physics/processList Initialized
```

```
#====================================================
# OUTPUT ACTORS
#====================================================
#====================================================
# DOSE ACTOR
#====================================================

/gate/actor/addActor                      TLEDoseActor dose1
/gate/actor/dose1/save                    output/radialDose/dose1.txt
/gate/actor/dose1/attachTo                d1
/gate/actor/dose1/stepHitType             random
/gate/actor/dose1/setResolution           1 1 1
/gate/actor/dose1/enableEdep              true
/gate/actor/dose1/enableDose              true
/gate/actor/dose1/enableUncertaintyDose   true
/gate/actor/dose1/enableUncertaintyEdep   true

/gate/actor/addActor                      TLEDoseActor dose2
/gate/actor/dose2/save                    output/radialDose/dose2.txt
/gate/actor/dose2/attachTo                d2
/gate/actor/dose2/stepHitType             random
/gate/actor/dose2/setResolution           1 1 1
/gate/actor/dose2/enableEdep              true
/gate/actor/dose2/enableDose              true
/gate/actor/dose2/enableUncertaintyDose   true
/gate/actor/dose2/enableUncertaintyEdep   true

/gate/actor/addActor                      TLEDoseActor dose3
/gate/actor/dose3/save                    output/radialDose/dose3.txt
/gate/actor/dose3/attachTo                d3
/gate/actor/dose3/stepHitType             random
/gate/actor/dose3/setResolution           1 1 1
/gate/actor/dose3/enableEdep              true
/gate/actor/dose3/enableDose              true
/gate/actor/dose3/enableUncertaintyDose   true
/gate/actor/dose3/enableUncertaintyEdep   true

/gate/actor/addActor                      TLEDoseActor dose4
/gate/actor/dose4/save                    output/radialDose/dose4.txt
/gate/actor/dose4/attachTo                d4
/gate/actor/dose4/stepHitType             random
/gate/actor/dose4/setResolution           1 1 1
/gate/actor/dose4/enableEdep              true
/gate/actor/dose4/enableDose              true
/gate/actor/dose4/enableUncertaintyDose   true
/gate/actor/dose4/enableUncertaintyEdep   true

/gate/actor/addActor                      TLEDoseActor dose5
/gate/actor/dose5/save                    output/radialDose/dose5.txt
/gate/actor/dose5/attachTo                d5
/gate/actor/dose5/stepHitType             random
/gate/actor/dose5/setResolution           1 1 1
/gate/actor/dose5/enableEdep              true
/gate/actor/dose5/enableDose              true
/gate/actor/dose5/enableUncertaintyDose   true
```

```
/gate/actor/dose5/enableUncertaintyEdep  true

/gate/actor/addActor                     TLEDoseActor dose6
/gate/actor/dose6/save                   output/radialDose/dose6.txt
/gate/actor/dose6/attachTo               d6
/gate/actor/dose6/stepHitType            random
/gate/actor/dose6/setResolution          1 1 1
/gate/actor/dose6/enableEdep             true
/gate/actor/dose6/enableDose             true
/gate/actor/dose6/enableUncertaintyDose  true
/gate/actor/dose6/enableUncertaintyEdep  true

/gate/actor/addActor                     TLEDoseActor dose7
/gate/actor/dose7/save                   output/radialDose/dose7.txt
/gate/actor/dose7/attachTo               d7
/gate/actor/dose7/stepHitType            random
/gate/actor/dose7/setResolution          1 1 1
/gate/actor/dose7/enableEdep             true
/gate/actor/dose7/enableDose             true
/gate/actor/dose7/enableUncertaintyDose  true
/gate/actor/dose7/enableUncertaintyEdep  true

/gate/actor/addActor                     TLEDoseActor dose8
/gate/actor/dose8/save                   output/radialDose/dose8.txt
/gate/actor/dose8/attachTo               d8
/gate/actor/dose8/stepHitType            random
/gate/actor/dose8/setResolution          1 1 1
/gate/actor/dose8/enableEdep             true
/gate/actor/dose8/enableDose             true
/gate/actor/dose8/enableUncertaintyDose  true
/gate/actor/dose8/enableUncertaintyEdep  true

/gate/actor/addActor                     TLEDoseActor dose9
/gate/actor/dose9/save                   output/radialDose/dose9.txt
/gate/actor/dose9/attachTo               d9
/gate/actor/dose9/stepHitType            random
/gate/actor/dose9/setResolution          1 1 1
/gate/actor/dose9/enableEdep             true
/gate/actor/dose9/enableDose             true
/gate/actor/dose9/enableUncertaintyDose  true
/gate/actor/dose9/enableUncertaintyEdep  true

/gate/actor/addActor                     TLEDoseActor dose10
/gate/actor/dose10/save                  output/radialDose/dose10.txt
/gate/actor/dose10/attachTo              d10
/gate/actor/dose10/stepHitType           random
/gate/actor/dose10/setResolution         1 1 1
/gate/actor/dose10/enableEdep            true
/gate/actor/dose10/enableDose            true
/gate/actor/dose10/enableUncertaintyDose true
/gate/actor/dose10/enableUncertaintyEdep true

/gate/actor/addActor                     TLEDoseActor dose11
/gate/actor/dose11/save                  output/radialDose/dose11.txt
/gate/actor/dose11/attachTo              d11
/gate/actor/dose11/stepHitType           random
```

```
/gate/actor/dose11/setResolution         1 1 1
/gate/actor/dose11/enableEdep            true
/gate/actor/dose11/enableDose            true
/gate/actor/dose11/enableUncertaintyDose true
/gate/actor/dose11/enableUncertaintyEdep true

/gate/actor/addActor                    TLEDoseActor dose12
/gate/actor/dose12/save                  output/radialDose/dose12.txt
/gate/actor/dose12/attachTo             d12
/gate/actor/dose12/stepHitType           random
/gate/actor/dose12/setResolution         1 1 1
/gate/actor/dose12/enableEdep            true
/gate/actor/dose12/enableDose            true
/gate/actor/dose12/enableUncertaintyDose true
/gate/actor/dose12/enableUncertaintyEdep true

/gate/actor/addActor                    TLEDoseActor dose13
/gate/actor/dose13/save                  output/radialDose/dose13.txt
/gate/actor/dose13/attachTo             d13
/gate/actor/dose13/stepHitType           random
/gate/actor/dose13/setResolution         1 1 1
/gate/actor/dose13/enableEdep            true
/gate/actor/dose13/enableDose            true
/gate/actor/dose13/enableUncertaintyDose true
/gate/actor/dose13/enableUncertaintyEdep true

/gate/actor/addActor SimulationStatisticActor  statActor
/gate/actor/statActor/save                     output/radialDose/stats.txt

#=====================================================
# END PHYSICS - Initialize before source definition
#=====================================================
# initialize
/gate/run/initialize
/gate/physics/print phys.txt

#=====================================================
# SOURCE
#=====================================================

/gate/source/addSource                     GammaMed1 gps
/gate/source/GammaMed1/gps/particle        gamma
/gate/source/GammaMed1/gps/energytype      UserSpectrum
/gate/source/GammaMed1/gps/setSpectrumFile  data/NUDATIridium192.txt
/gate/source/GammaMed1/gps/type            Volume
/gate/source/GammaMed1/attachTo            sourceSeed
/gate/source/GammaMed1/gps/shape           Cylinder
/gate/source/GammaMed1/gps/radius          0.3 mm
/gate/source/GammaMed1/gps/halfz           1.75 mm
/gate/source/GammaMed1/gps/angtype         iso

#Visualise the source
#/gate/source/GammaMed1/visualize          2000 yellow 3

#=====================================================#
# UNCOMMENT IF YOU WANT NO OUTPUT FROM SIMULATION
```

```
#=====================================================
#/gate/output/allowNoOutput

#=====================================================#
#  S T A R T   S I M U L A T I O N
#=====================================================#
/gate/random/setEngineName MersenneTwister
/gate/random/setEngineSeed auto
/gate/application/setNumberOfPrimariesPerRun        2100000000
/gate/application/start
exit
```

A.1.4 2D Anisotropy Function

```
#=====================================================
# VISUALISATION
#=====================================================
#/control/execute    mac/vis.mac
#=====================================================
# MATERIALS
#=====================================================
#Define Materials Database
/gate/geometry/setMaterialDatabase data/MyMaterialDatabase.db

#=====================================================
# WORLD
#=====================================================
/gate/world/setMaterial                   AirTG43U
/gate/world/geometry/setXLength           100 cm
/gate/world/geometry/setYLength           100 cm
/gate/world/geometry/setZLength           100 cm
#=====================================================
# GEOMETRY
#=====================================================

#calculation volume
/gate/world/daughters/name                calcVolume
/gate/world/daughters/insert              sphere
/gate/calcVolume/geometry/setRmin         0 mm
/gate/calcVolume/geometry/setRmax         40 cm
/gate/calcVolume/geometry/setPhiStart     0 deg
/gate/calcVolume/geometry/setDeltaPhi     360 deg
/gate/calcVolume/geometry/setThetaStart   0 deg
/gate/calcVolume/geometry/setDeltaTheta   360 deg
/gate/calcVolume/setMaterial              Water

/control/execute  data/GMSource.mac

###################################################    Dose voxels    #################################################

/gate/calcVolume/daughters/name           d0
```

```
/gate/calcVolume/daughters/insert          box
/gate/d0/geometry/setXLength               x mm
/gate/d0/geometry/setYLength               y mm
/gate/d0/geometry/setZLength               z mm
/gate/d0/placement/setTranslation          0 0 Z mm
/gate/d0/setMaterial                       Water
/gate/d0/vis/setColor                      red

/gate/calcVolume/daughters/name            d2
/gate/calcVolume/daughters/insert          cylinder
/gate/d2/geometry/setRmin                  ID
/gate/d2/geometry/setRmax                  OD
/gate/d2/geometry/setHeight                h
/gate/d2/placement/setTranslation          0 0 Z
/gate/d2/setMaterial                       Water
/gate/d2/vis/setColor                      red

/gate/calcVolume/daughters/name            d4
/gate/calcVolume/daughters/insert          cylinder
/gate/d4/geometry/setRmin                  ID
/gate/d4/geometry/setRmax                  OD
/gate/d4/geometry/setHeight                h
/gate/d4/placement/setTranslation          0 0 Z
/gate/d4/setMaterial                       Water
/gate/d4/vis/setColor                      red

/gate/calcVolume/daughters/name            d6
/gate/calcVolume/daughters/insert          cylinder
/gate/d6/geometry/setRmin                  ID
/gate/d6/geometry/setRmax                  OD
/gate/d6/geometry/setHeight                h
/gate/d6/placement/setTranslation          0 0 Z
/gate/d6/setMaterial                       Water
/gate/d6/vis/setColor                      red

/gate/calcVolume/daughters/name            d8
/gate/calcVolume/daughters/insert          cylinder
/gate/d8/geometry/setRmin                  ID
/gate/d8/geometry/setRmax                  OD
/gate/d8/geometry/setHeight                h
/gate/d8/placement/setTranslation          0 0 Z
/gate/d8/setMaterial                       Water
/gate/d8/vis/setColor                      red

/gate/calcVolume/daughters/name            d10
/gate/calcVolume/daughters/insert          cylinder
/gate/d10/geometry/setRmin                 ID
/gate/d10/geometry/setRmax                 OD
/gate/d10/geometry/setHeight               h
/gate/d10/placement/setTranslation         0 0 Z
/gate/d10/setMaterial                      Water
/gate/d10/vis/setColor                     red

/gate/calcVolume/daughters/name            d20
/gate/calcVolume/daughters/insert          cylinder
/gate/d20/geometry/setRmin                 ID
```

```
/gate/d20/geometry/setRmax              OD
/gate/d20/geometry/setHeight            h
/gate/d20/placement/setTranslation      0 0 Z
/gate/d20/setMaterial                   Water
/gate/d20/vis/setColor                  red

/gate/calcVolume/daughters/name         d30
/gate/calcVolume/daughters/insert       cylinder
/gate/d30/geometry/setRmin              ID
/gate/d30/geometry/setRmax              OD
/gate/d30/geometry/setHeight            h
/gate/d30/placement/setTranslation      0 0 Z
/gate/d30/setMaterial                   Water
/gate/d30/vis/setColor                  red

/gate/calcVolume/daughters/name         d40
/gate/calcVolume/daughters/insert       cylinder
/gate/d40/geometry/setRmin              ID
/gate/d40/geometry/setRmax              OD
/gate/d40/geometry/setHeight            h
/gate/d40/placement/setTranslation      0 0 Z
/gate/d40/setMaterial                   Water
/gate/d40/vis/setColor                  red

/gate/calcVolume/daughters/name         d50
/gate/calcVolume/daughters/insert       cylinder
/gate/d50/geometry/setRmin              ID
/gate/d50/geometry/setRmax              OD
/gate/d50/geometry/setHeight            h
/gate/d50/placement/setTranslation      0 0 Z
/gate/d50/setMaterial                   Water
/gate/d50/vis/setColor                  red

/gate/calcVolume/daughters/name         d60
/gate/calcVolume/daughters/insert       cylinder
/gate/d60/geometry/setRmin              ID
/gate/d60/geometry/setRmax              OD
/gate/d60/geometry/setHeight            h
/gate/d60/placement/setTranslation      0 0 Z
/gate/d60/setMaterial                   Water
/gate/d60/vis/setColor                  red

/gate/calcVolume/daughters/name         d70
/gate/calcVolume/daughters/insert       cylinder
/gate/d70/geometry/setRmin              ID
/gate/d70/geometry/setRmax              OD
/gate/d70/geometry/setHeight            h
/gate/d70/placement/setTranslation      0 0 Z
/gate/d70/setMaterial                   Water
/gate/d70/vis/setColor                  red

/gate/calcVolume/daughters/name         d80
/gate/calcVolume/daughters/insert       cylinder
/gate/d80/geometry/setRmin              ID
/gate/d80/geometry/setRmax              OD
/gate/d80/geometry/setHeight            h
```

```
/gate/d80/placement/setTranslation       0 0 Z
/gate/d80/setMaterial                    Water
/gate/d80/vis/setColor                   red

/gate/calcVolume/daughters/name          d90
/gate/calcVolume/daughters/insert        cylinder
/gate/d90/geometry/setRmin               ID
/gate/d90/geometry/setRmax               OD
/gate/d90/geometry/setHeight             h
/gate/d90/placement/setTranslation       0 0 0
/gate/d90/setMaterial                    Water
/gate/d90/vis/setColor                   red

/gate/calcVolume/daughters/name          d100
/gate/calcVolume/daughters/insert        cylinder
/gate/d100/geometry/setRmin              ID
/gate/d100/geometry/setRmax              OD
/gate/d100/geometry/setHeight            h
/gate/d100/placement/setTranslation      0 0 Z
/gate/d100/setMaterial                   Water
/gate/d100/vis/setColor                  red

/gate/calcVolume/daughters/name          d110
/gate/calcVolume/daughters/insert        cylinder
/gate/d110/geometry/setRmin              ID
/gate/d110/geometry/setRmax              OD
/gate/d110/geometry/setHeight            h
/gate/d110/placement/setTranslation      0 0 Z
/gate/d110/setMaterial                   Water
/gate/d110/vis/setColor                  red

/gate/calcVolume/daughters/name          d120
/gate/calcVolume/daughters/insert        cylinder
/gate/d120/geometry/setRmin              ID
/gate/d120/geometry/setRmax              OD
/gate/d120/geometry/setHeight            h
/gate/d120/placement/setTranslation      0 0 Z
/gate/d120/setMaterial                   Water
/gate/d120/vis/setColor                  red

/gate/calcVolume/daughters/name          d130
/gate/calcVolume/daughters/insert        cylinder
/gate/d130/geometry/setRmin              ID
/gate/d130/geometry/setRmax              OD
/gate/d130/geometry/setHeight            h
/gate/d130/placement/setTranslation      0 0 Z
/gate/d130/setMaterial                   Water
/gate/d130/vis/setColor                  red

/gate/calcVolume/daughters/name          d140
/gate/calcVolume/daughters/insert        cylinder
/gate/d140/geometry/setRmin              ID
/gate/d140/geometry/setRmax              OD
/gate/d140/geometry/setHeight            h
/gate/d140/placement/setTranslation      0 0 Z
/gate/d140/setMaterial                   Water
```

```
/gate/d140/vis/setColor                  red

/gate/calcVolume/daughters/name          d150
/gate/calcVolume/daughters/insert        cylinder
/gate/d150/geometry/setRmin              ID
/gate/d150/geometry/setRmax              OD
/gate/d150/geometry/setHeight            h
/gate/d150/placement/setTranslation      0 0 Z
/gate/d150/setMaterial                   Water
/gate/d150/vis/setColor                  red

/gate/calcVolume/daughters/name          d160
/gate/calcVolume/daughters/insert        cylinder
/gate/d160/geometry/setRmin              ID
/gate/d160/geometry/setRmax              OD
/gate/d160/geometry/setHeight            h
/gate/d160/placement/setTranslation      0 0 Z
/gate/d160/setMaterial                   Water
/gate/d160/vis/setColor                  red

/gate/calcVolume/daughters/name          d170
/gate/calcVolume/daughters/insert        cylinder
/gate/d170/geometry/setRmin              ID
/gate/d170/geometry/setRmax              OD
/gate/d170/geometry/setHeight            h
/gate/d170/placement/setTranslation      0 0 Z
/gate/d170/setMaterial                   Water
/gate/d170/vis/setColor                  red

/gate/calcVolume/daughters/name          d172
/gate/calcVolume/daughters/insert        cylinder
/gate/d172/geometry/setRmin              ID
/gate/d172/geometry/setRmax              OD
/gate/d172/geometry/setHeight            h
/gate/d172/placement/setTranslation      0 0 Z
/gate/d172/setMaterial                   Water
/gate/d172/vis/setColor                  red

/gate/calcVolume/daughters/name          d174
/gate/calcVolume/daughters/insert        cylinder
/gate/d174/geometry/setRmin              ID
/gate/d174/geometry/setRmax              OD
/gate/d174/geometry/setHeight            h
/gate/d174/placement/setTranslation      0 0 Z
/gate/d174/setMaterial                   Water
/gate/d174/vis/setColor                  red

/gate/calcVolume/daughters/name         d176
/gate/calcVolume/daughters/insert       cylinder
/gate/d176/geometry/setRmin             ID
/gate/d176/geometry/setRmax             OD
/gate/d176/geometry/setHeight           h
/gate/d176/placement/setTranslation     0 0 Z
/gate/d176/setMaterial                  Water
/gate/d176/vis/setColor                 red
```

```
/gate/calcVolume/daughters/name          d178
/gate/calcVolume/daughters/insert        cylinder
/gate/d178/geometry/setRmin              ID
/gate/d178/geometry/setRmax              OD
/gate/d178/geometry/setHeight            h
/gate/d178/placement/setTranslation      0 0 Z
/gate/d178/setMaterial                   Water
/gate/d178/vis/setColor                   red

/gate/calcVolume/daughters/name           d180
/gate/calcVolume/daughters/insert         box
/gate/d180/geometry/setXLength            x
/gate/d180/geometry/setYLength            y
/gate/d180/geometry/setZLength            z
/gate/d180/placement/setTranslation       0 0 Z
/gate/d180/setMaterial                    Water
/gate/d180/vis/setColor                   red


#-----------------------------------------------

#=====================================================
# PHYSICS
#=====================================================
/gate/physics/addPhysicsList emstandard
#===================================================================================================
# customized CUTS
#===================================================================================================

/gate/physics/Gamma/SetCutInRegion        calcVolume 10 keV
/gate/physics/Electron/SetCutInRegion     calcVolume 10 keV
/gate/physics/Positron/SetCutInRegion     calcVolume 10 keV

#==================================================================================================
# Additional processes not included in the list option 3
#==================================================================================================
/gate/physics/setEMin 10 keV
/gate/physics/setEMax 10 GeV
/gate/physics/setDEDXBinning 500
/gate/physics/setLambdaBinning 500

/gate/physics/processList Enabled
/gate/physics/processList Initialized

#=====================================================
# OUTPUT ACTORS
#=====================================================
#=====================================================
# DOSE ACTOR
#=====================================================
/gate/actor/addActor                      TLEDoseActor dose0
/gate/actor/dose0/save                    output/anisotropy4mm/dose0.txt
/gate/actor/dose0/attachTo                d0
/gate/actor/dose0/setResolution           1 1 1
/gate/actor/dose0/stepHitType             random
/gate/actor/dose0/enableEdep              true
```

```
/gate/actor/dose0/enableDose                true
/gate/actor/dose0/enableUncertaintyDose     true
/gate/actor/dose0/enableSquaredEdep         true
/gate/actor/dose0/enableSquaredDose         true
/gate/actor/dose0/enableUncertaintyEdep     true

/gate/actor/addActor                        TLEDoseActor dose2
/gate/actor/dose2/save                      output/anisotropy4mm/dose2.txt
/gate/actor/dose2/attachTo                  d2
/gate/actor/dose2/setResolution             1 1 1
/gate/actor/dose2/stepHitType               random
/gate/actor/dose2/enableEdep                true
/gate/actor/dose2/enableDose                true
/gate/actor/dose2/enableUncertaintyDose     true
/gate/actor/dose2/enableSquaredEdep         true
/gate/actor/dose2/enableSquaredDose         true
/gate/actor/dose2/enableUncertaintyEdep     true

/gate/actor/addActor                        TLEDoseActor dose4
/gate/actor/dose4/save                      output/anisotropy4mm/dose4.txt
/gate/actor/dose4/attachTo                  d4
/gate/actor/dose4/setResolution             1 1 1
/gate/actor/dose4/stepHitType               random
/gate/actor/dose4/enableEdep                true
/gate/actor/dose4/enableDose                true
/gate/actor/dose4/enableUncertaintyDose     true
/gate/actor/dose4/enableSquaredEdep         true
/gate/actor/dose4/enableSquaredDose         true
/gate/actor/dose4/enableUncertaintyEdep     true

/gate/actor/addActor                        TLEDoseActor dose6
/gate/actor/dose6/save                      output/anisotropy4mm/dose6.txt
/gate/actor/dose6/attachTo                  d6
/gate/actor/dose6/setResolution             1 1 1
/gate/actor/dose6/stepHitType               random
/gate/actor/dose6/enableEdep                true
/gate/actor/dose6/enableDose                true
/gate/actor/dose6/enableUncertaintyDose     true
/gate/actor/dose6/enableSquaredEdep         true
/gate/actor/dose6/enableSquaredDose         true
/gate/actor/dose6/enableUncertaintyEdep     true

/gate/actor/addActor                        TLEDoseActor dose8
/gate/actor/dose8/save                      output/anisotropy4mm/dose8.txt
/gate/actor/dose8/attachTo                  d8
/gate/actor/dose8/setResolution             1 1 1
/gate/actor/dose8/stepHitType               random
/gate/actor/dose8/enableEdep                true
/gate/actor/dose8/enableDose                true
/gate/actor/dose8/enableUncertaintyDose     true
/gate/actor/dose8/enableSquaredEdep         true
/gate/actor/dose8/enableSquaredDose         true
/gate/actor/dose8/enableUncertaintyEdep     true

/gate/actor/addActor                         TLEDoseActor dose10
/gate/actor/dose10/save                      output/anisotropy4mm/dose10.txt
```

```
/gate/actor/dose10/attachTo                 d10
/gate/actor/dose10/setResolution            1 1 1
/gate/actor/dose10/stepHitType              random
/gate/actor/dose10/enableEdep               true
/gate/actor/dose10/enableDose               true
/gate/actor/dose10/enableUncertaintyDose    true
/gate/actor/dose10/enableSquaredEdep        true
/gate/actor/dose10/enableSquaredDose        true
/gate/actor/dose10/enableUncertaintyEdep    true

/gate/actor/addActor                        TLEDoseActor dose20
/gate/actor/dose20/save                     output/anisotropy4mm/dose20.txt
/gate/actor/dose20/attachTo                 d20
/gate/actor/dose20/setResolution            1 1 1
/gate/actor/dose20/stepHitType              random
/gate/actor/dose20/enableEdep               true
/gate/actor/dose20/enableDose               true
/gate/actor/dose20/enableUncertaintyDose    true
/gate/actor/dose20/enableSquaredEdep        true
/gate/actor/dose20/enableSquaredDose        true
/gate/actor/dose20/enableUncertaintyEdep    true

/gate/actor/addActor                        TLEDoseActor dose30
/gate/actor/dose30/save                     output/anisotropy4mm/dose30.txt
/gate/actor/dose30/attachTo                 d30
/gate/actor/dose30/setResolution            1 1 1
/gate/actor/dose30/stepHitType              random
/gate/actor/dose30/enableEdep               true
/gate/actor/dose30/enableDose               true
/gate/actor/dose30/enableUncertaintyDose    true
/gate/actor/dose30/enableSquaredEdep        true
/gate/actor/dose30/enableSquaredDose        true
/gate/actor/dose30/enableUncertaintyEdep    true

/gate/actor/addActor                        TLEDoseActor dose40
/gate/actor/dose40/save                     output/anisotropy4mm/dose40.txt
/gate/actor/dose40/attachTo                 d40
/gate/actor/dose40/setResolution            1 1 1
/gate/actor/dose40/stepHitType              random
/gate/actor/dose40/enableEdep               true
/gate/actor/dose40/enableDose               true
/gate/actor/dose40/enableUncertaintyDose    true
/gate/actor/dose40/enableSquaredEdep        true
/gate/actor/dose40/enableSquaredDose        true
/gate/actor/dose40/enableUncertaintyEdep    true

/gate/actor/addActor                        TLEDoseActor dose50
/gate/actor/dose50/save                     output/anisotropy4mm/dose50.txt
/gate/actor/dose50/attachTo                 d50
/gate/actor/dose50/setResolution            1 1 1
/gate/actor/dose50/stepHitType              random
/gate/actor/dose50/enableEdep               true
/gate/actor/dose50/enableDose               true
/gate/actor/dose50/enableUncertaintyDose    true
/gate/actor/dose50/enableSquaredEdep        true
/gate/actor/dose50/enableSquaredDose        true
```

```
/gate/actor/dose50/enableUncertaintyEdep   true

/gate/actor/addActor                       TLEDoseActor dose60
/gate/actor/dose60/save                    output/anisotropy4mm/dose60.txt
/gate/actor/dose60/attachTo                d60
/gate/actor/dose60/setResolution           1 1 1
/gate/actor/dose60/stepHitType             random
/gate/actor/dose60/enableEdep              true
/gate/actor/dose60/enableDose              true
/gate/actor/dose60/enableUncertaintyDose   true
/gate/actor/dose60/enableSquaredEdep       true
/gate/actor/dose60/enableSquaredDose       true
/gate/actor/dose60/enableUncertaintyEdep   true

/gate/actor/addActor                      TLEDoseActor dose70
/gate/actor/dose70/save                    output/anisotropy4mm/dose70.txt
/gate/actor/dose70/attachTo                d70
/gate/actor/dose70/setResolution           1 1 1
/gate/actor/dose70/stepHitType             random
/gate/actor/dose70/enableEdep              true
/gate/actor/dose70/enableDose              true
/gate/actor/dose70/enableUncertaintyDose   true
/gate/actor/dose70/enableSquaredEdep       true
/gate/actor/dose70/enableSquaredDose       true
/gate/actor/dose70/enableUncertaintyEdep   true

/gate/actor/addActor                       TLEDoseActor dose80
/gate/actor/dose80/save                    output/anisotropy4mm/dose80.txt
/gate/actor/dose80/attachTo                d80
/gate/actor/dose80/setResolution           1 1 1
/gate/actor/dose80/stepHitType             random
/gate/actor/dose80/enableEdep              true
/gate/actor/dose80/enableDose              true
/gate/actor/dose80/enableUncertaintyDose   true
/gate/actor/dose80/enableSquaredEdep       true
/gate/actor/dose80/enableSquaredDose       true
/gate/actor/dose80/enableUncertaintyEdep   true

/gate/actor/addActor                       TLEDoseActor dose90
/gate/actor/dose90/save                    output/anisotropy4mm/dose90.txt
/gate/actor/dose90/attachTo                d90
/gate/actor/dose90/setResolution           1 1 1
/gate/actor/dose90/stepHitType             random
/gate/actor/dose90/enableEdep              true
/gate/actor/dose90/enableDose              true
/gate/actor/dose90/enableUncertaintyDose   true
/gate/actor/dose90/enableSquaredEdep       true
/gate/actor/dose90/enableSquaredDose       true
/gate/actor/dose90/enableUncertaintyEdep   true

/gate/actor/addActor                       TLEDoseActor dose100
/gate/actor/dose100/save                   output/anisotropy4mm/dose100.txt
/gate/actor/dose100/attachTo               d100
/gate/actor/dose100/setResolution          1 1 1
/gate/actor/dose100/stepHitType            random
/gate/actor/dose100/enableEdep             true
```

```
/gate/actor/dose100/enableDose              true
/gate/actor/dose100/enableUncertaintyDose  true
/gate/actor/dose100/enableSquaredEdep      true
/gate/actor/dose100/enableSquaredDose      true
/gate/actor/dose100/enableUncertaintyEdep  true

/gate/actor/addActor                        TLEDoseActor dose110
/gate/actor/dose110/save                    output/anisotropy4mm/dose110.txt
/gate/actor/dose110/attachTo                d110
/gate/actor/dose110/setResolution           1 1 1
/gate/actor/dose110/stepHitType             random
/gate/actor/dose110/enableEdep              true
/gate/actor/dose110/enableDose              true
/gate/actor/dose110/enableUncertaintyDose  true
/gate/actor/dose110/enableSquaredEdep      true
/gate/actor/dose110/enableSquaredDose      true
/gate/actor/dose110/enableUncertaintyEdep  true

/gate/actor/addActor                        TLEDoseActor dose120
/gate/actor/dose120/save                    output/anisotropy4mm/dose120.txt
/gate/actor/dose120/attachTo                d120
/gate/actor/dose120/setResolution           1 1 1
/gate/actor/dose120/stepHitType             random
/gate/actor/dose120/enableEdep              true
/gate/actor/dose120/enableDose              true
/gate/actor/dose120/enableUncertaintyDose  true
/gate/actor/dose120/enableSquaredEdep      true
/gate/actor/dose120/enableSquaredDose      true
/gate/actor/dose120/enableUncertaintyEdep  true

/gate/actor/addActor                        TLEDoseActor dose130
/gate/actor/dose130/save                    output/anisotropy4mm/dose130.txt
/gate/actor/dose130/attachTo                d130
/gate/actor/dose130/setResolution           1 1 1
/gate/actor/dose130/stepHitType             random
/gate/actor/dose130/enableEdep              true
/gate/actor/dose130/enableDose              true
/gate/actor/dose130/enableUncertaintyDose  true
/gate/actor/dose130/enableSquaredEdep      true
/gate/actor/dose130/enableSquaredDose      true
/gate/actor/dose130/enableUncertaintyEdep  true

/gate/actor/addActor                        TLEDoseActor dose140
/gate/actor/dose140/save                    output/anisotropy4mm/dose140.txt
/gate/actor/dose140/attachTo                d140
/gate/actor/dose140/setResolution           1 1 1
/gate/actor/dose140/stepHitType             random
/gate/actor/dose140/enableEdep              true
/gate/actor/dose140/enableDose              true
/gate/actor/dose140/enableUncertaintyDose  true
/gate/actor/dose140/enableSquaredEdep      true
/gate/actor/dose140/enableSquaredDose      true
/gate/actor/dose140/enableUncertaintyEdep  true

/gate/actor/addActor                        TLEDoseActor dose150
/gate/actor/dose150/save                    output/anisotropy4mm/dose150.txt
```

```
/gate/actor/dose150/attachTo               d150
/gate/actor/dose150/setResolution          1 1 1
/gate/actor/dose150/stepHitType            random
/gate/actor/dose150/enableEdep             true
/gate/actor/dose150/enableDose             true
/gate/actor/dose150/enableUncertaintyDose  true
/gate/actor/dose150/enableSquaredEdep      true
/gate/actor/dose150/enableSquaredDose      true
/gate/actor/dose150/enableUncertaintyEdep  true

/gate/actor/addActor                       TLEDoseActor dose160
/gate/actor/dose160/save                   output/anisotropy4mm/dose160.txt
/gate/actor/dose160/attachTo               d160
/gate/actor/dose160/setResolution          1 1 1
/gate/actor/dose160/stepHitType            random
/gate/actor/dose160/enableEdep             true
/gate/actor/dose160/enableDose             true
/gate/actor/dose160/enableUncertaintyDose  true
/gate/actor/dose160/enableSquaredEdep      true
/gate/actor/dose160/enableSquaredDose      true
/gate/actor/dose160/enableUncertaintyEdep  true

/gate/actor/addActor                       TLEDoseActor dose170
/gate/actor/dose170/save                   output/anisotropy4mm/dose170.txt
/gate/actor/dose170/attachTo               d170
/gate/actor/dose170/setResolution          1 1 1
/gate/actor/dose170/stepHitType            random
/gate/actor/dose170/enableEdep             true
/gate/actor/dose170/enableDose             true
/gate/actor/dose170/enableUncertaintyDose  true
/gate/actor/dose170/enableSquaredEdep      true
/gate/actor/dose170/enableSquaredDose      true
/gate/actor/dose170/enableUncertaintyEdep  true

/gate/actor/addActor                       TLEDoseActor dose172
/gate/actor/dose172/save                   output/anisotropy4mm/dose172.txt
/gate/actor/dose172/attachTo               d172
/gate/actor/dose172/setResolution          1 1 1
/gate/actor/dose172/stepHitType            random
/gate/actor/dose172/enableEdep             true
/gate/actor/dose172/enableDose             true
/gate/actor/dose172/enableUncertaintyDose  true
/gate/actor/dose172/enableSquaredEdep      true
/gate/actor/dose172/enableSquaredDose      true
/gate/actor/dose172/enableUncertaintyEdep  true

/gate/actor/addActor                       TLEDoseActor dose174
/gate/actor/dose174/save                   output/anisotropy4mm/dose174.txt
/gate/actor/dose174/attachTo               d174
/gate/actor/dose174/setResolution          1 1 1
/gate/actor/dose174/stepHitType            random
/gate/actor/dose174/enableEdep             true
/gate/actor/dose174/enableDose             true
/gate/actor/dose174/enableUncertaintyDose  true
/gate/actor/dose174/enableSquaredEdep      true
/gate/actor/dose174/enableSquaredDose      true
```

```
/gate/actor/dose174/enableUncertaintyEdep  true

/gate/actor/addActor                       TLEDoseActor dose176
/gate/actor/dose176/save                   output/anisotropy4mm/dose176.txt
/gate/actor/dose176/attachTo               d176
/gate/actor/dose176/setResolution          1 1 1
/gate/actor/dose176/stepHitType            random
/gate/actor/dose176/enableEdep             true
/gate/actor/dose176/enableDose             true
/gate/actor/dose176/enableUncertaintyDose  true
/gate/actor/dose176/enableSquaredEdep      true
/gate/actor/dose176/enableSquaredDose      true
/gate/actor/dose176/enableUncertaintyEdep  true

/gate/actor/addActor                       TLEDoseActor dose178
/gate/actor/dose178/save                   output/anisotropy4mm/dose178.txt
/gate/actor/dose178/attachTo               d178
/gate/actor/dose178/setResolution          1 1 1
/gate/actor/dose178/stepHitType            random
/gate/actor/dose178/enableEdep             true
/gate/actor/dose178/enableDose             true
/gate/actor/dose178/enableUncertaintyDose  true
/gate/actor/dose178/enableSquaredEdep      true
/gate/actor/dose178/enableSquaredDose      true
/gate/actor/dose178/enableUncertaintyEdep  true

/gate/actor/addActor                       TLEDoseActor dose180
/gate/actor/dose180/save                   output/anisotropy4mm/dose180.txt
/gate/actor/dose180/attachTo               d180
/gate/actor/dose180/setResolution          1 1 1
/gate/actor/dose180/stepHitType            random
/gate/actor/dose180/enableEdep             true
/gate/actor/dose180/enableDose             true
/gate/actor/dose180/enableUncertaintyDose  true
/gate/actor/dose180/enableSquaredEdep      true
/gate/actor/dose180/enableSquaredDose      true
/gate/actor/dose180/enableUncertaintyEdep  true


/gate/actor/addActor                       SimulationStatisticActor statActor
/gate/actor/statActor/save                 output/anisotropy4mm/stats4mm.txt


#=====================================================
# END PHYSICS - Initialize before source definition
#=====================================================
# initialize
/gate/run/initialize
/gate/physics/print phys.txt

#=====================================================
# SOURCE
#=====================================================

/gate/source/addSource                      GammaMed1 gps
/gate/source/GammaMed1/gps/particle         gamma
```

```
/gate/source/GammaMed1/gps/energytype       UserSpectrum
/gate/source/GammaMed1/gps/setSpectrumFile  data/NUDATIridium192.txt
/gate/source/GammaMed1/gps/type             Volume
/gate/source/GammaMed1/attachTo             sourceSeed
/gate/source/GammaMed1/gps/shape            Cylinder
/gate/source/GammaMed1/gps/radius           0.3 mm
/gate/source/GammaMed1/gps/halfz            1.75 mm
/gate/source/GammaMed1/gps/angtype          iso


#Visualise the source
#/gate/source/GammaMed1/visualize           2000 yellow 3

#=====================================================#
# UNCOMMENT IF YOU WANT NO OUTPUT FROM SIMULATION
#=====================================================
#/gate/output/allowNoOutput

#=====================================================#
#  S T A R T  S I M U L A T I O N
#=====================================================#
/gate/random/setEngineName MersenneTwister
/gate/random/setEngineSeed auto
/gate/application/setNumberOfPrimariesPerRun        2100000000
/gate/application/start
exit
```

A.1.5 Material Compisition Data

```
[Elements]
Hydrogen:     S= H  ; Z= 1.  ; A=  1.01    g/mole
Helium:       S= He ; Z= 2.  ; A=  4.003   g/mole
Lithium:      S= Li ; Z= 3.  ; A=  6.941   g/mole
Beryllium:    S= Be ; Z= 4.  ; A=  9.012   g/mole
Boron:        S= B  ; Z= 5.  ; A=  10.811  g/mole
Carbon:       S= C  ; Z= 6.  ; A=  12.01   g/mole
Nitrogen:     S= N  ; Z= 7.  ; A=  14.01   g/mole
Oxygen:       S= O  ; Z= 8.  ; A=  16.00   g/mole
Fluorine:     S= F  ; Z= 9.  ; A=  18.998  g/mole
Neon:         S= Ne ; Z= 10. ; A=  20.180  g/mole
Sodium:       S= Na ; Z= 11. ; A=  22.99   g/mole
Magnesium:    S= Mg ; Z= 12. ; A=  24.305  g/mole
Aluminium:    S= Al ; Z= 13. ; A=  26.98   g/mole
Silicon:      S= Si ; Z= 14. ; A=  28.09   g/mole
Phosphor:     S= P  ; Z= 15. ; A=  30.97   g/mole
Sulfur:       S= S  ; Z= 16. ; A=  32.066  g/mole
Chlorine:     S= Cl ; Z= 17. ; A=  35.45   g/mole
Argon:        S= Ar ; Z= 18. ; A=  39.95   g/mole
Potassium:    S= K  ; Z= 19. ; A=  39.098  g/mole
Calcium:      S= Ca ; Z= 20. ; A=  40.08   g/mole
Scandium:     S= Sc ; Z= 21. ; A=  44.956  g/mole
```

```
Titanium:      S= Ti ; Z= 22. ; A=  47.867  g/mole
Vandium:       S= V  ; Z =23. ; A=  50.942  g/mole
Chromium:      S= Cr ; Z= 24. ; A=  51.996  g/mole
Manganese:     S= Mn ; Z= 25. ; A=  54.938  g/mole
Iron:          S= Fe ; Z= 26. ; A=  55.845  g/mole
Cobalt:        S= Co ; Z= 27. ; A=  58.933  g/mole
Nickel:        S= Ni ; Z= 28. ; A=  58.693  g/mole
Copper:        S= Cu ; Z= 29. ; A=  63.39   g/mole
Zinc:          S= Zn ; Z= 30. ; A=  65.39   g/mole
Gallium:       S= Ga ; Z= 31. ; A=  69.723  g/mole
Germanium:     S= Ge ; Z= 32. ; A=  72.61   g/mole
Yttrium:       S= Y  ; Z= 39. ; A=  88.91   g/mole
Silver:        S= Ag ; Z= 47. ; A=  107.868 g/mole
Cadmium:       S= Cd ; Z= 48. ; A=  112.41  g/mole
Tin:           S= Sn ; Z= 50. ; A=  118.71  g/mole
Antimony:      S= Sb ; Z= 51. ; A=  121.76  g/mole
Tellurium:     S= Te ; Z= 52. ; A=  127.6   g/mole
Iodine:        S= I  ; Z= 53. ; A=  126.90  g/mole
Cesium:        S= Cs ; Z= 55. ; A=  132.905 g/mole
Gadolinium:    S= Gd ; Z= 64. ; A=  157.25  g/mole
Lutetium:      S= Lu ; Z= 71. ; A=  174.97  g/mole
Tungsten:      S= W  ; Z= 74. ; A=  183.84  g/mole
Gold:          S= Au ; Z= 79. ; A=  196.967 g/mole
Thallium:      S= Tl ; Z= 81. ; A=  204.37  g/mole
Lead:          S= Pb ; Z= 82. ; A=  207.20  g/mole
Bismuth:       S= Bi ; Z= 83. ; A=  208.98  g/mole
Uranium:       S= U  ; Z= 92. ; A=  238.03  g/mole
Molybdenum:    S= Mo ; Z= 42. ; A=  95.94   g/mole
Iridium:       S= Ir ; Z= 77  ; A=  192.217 g/mole
Platinum:      S= Pt ; Z= 78  ; A=  195.078 g/mole

[Materials]
Water: d=1 g/cm3 ; n=1
+el: name=Hydrogen   ; f=0.111894
+el: name=Oxygen     ; f=0.888106


Seed192: d=22.42 g/cm3 ; n=1
+el: name=Iridium    ; n=1

TitaniumBV: d=4.42 g/cm3 ; n=3
+el: name=Aluminium  ; f=0.06
+el: name=Titanium   ; f=0.9
+el: name=Vandium    ; f=0.04

Vacuum: d=0.000001 mg/cm3 ; n=1
+el: name=Hydrogen   ; n=1

AirTG43U: d=0.0012 g/cm3 ; n=4
+el: name=Nitrogen   ; f=0.750325
+el: name=Oxygen     ; f=0.236077
+el: name=Argon      ; f=0.012743
+el: name=Carbon     ; f=0.000123
+el: name=Hydrogen   ; f=0.000732

LungBV: d=0.26 g/cm3 ; n=13
```

```
+el: name=Hydrogen   ; f=0.101278
+el: name=Carbon     ; f=0.102310
+el: name=Nitrogen   ; f=0.028650
+el: name=Oxygen     ; f=0.757072
+el: name=Sodium     ; f=0.001840
+el: name=Magnesium  ; f=0.000730
+el: name=Phosphor   ; f=0.000800
+el: name=Sulfur     ; f=0.002250
+el: name=Chlorine   ; f=0.002660
+el: name=Potassium  ; f=0.001940
+el: name=Calcium    ; f=0.000090
+el: name=Iron       ; f=0.000370
+el: name=Zinc       ; f=0.000010

MuscleBV: d=1.05 g/cm3 ; n=13
+el: name=Hydrogen   ; f=0.100637
+el: name=Carbon     ; f=0.10783
+el: name=Nitrogen   ; f=0.027680
+el: name=Oxygen     ; f=0.754773
+el: name=Sodium     ; f=0.00075
+el: name=Magnesium  ; f=0.000190
+el: name=Phosphor   ; f=0.0018
+el: name=Sulfur     ; f=0.00241
+el: name=Chlorine   ; f=0.00079
+el: name=Potassium  ; f=0.00302
+el: name=Calcium    ; f=0.00003
+el: name=Iron       ; f=0.00004
+el: name=Zinc       ; f=0.00005



BoneBV: d=1.92 g/cm3 ; n=9
+el: name=Hydrogen   ; f=0.047234
+el: name=Carbon     ; f=0.14433
+el: name=Nitrogen   ; f=0.04199
+el: name=Oxygen     ; f=0.446096
+el: name=Magnesium  ; f=0.0022
+el: name=Phosphor   ; f=0.10497
+el: name=Sulfur     ; f=0.00315
+el: name=Calcium    ; f=0.20993
+el: name=Zinc       ; f=0.0001

AdiposeBV: d=0.92 g/cm3 ; n=11
+el: name=Hydrogen   ; f=0.119477
+el: name=Carbon     ; f=0.637240
+el: name=Nitrogen   ; f=0.007970
+el: name=Oxygen     ; f=0.232333
+el: name=Sodium     ; f=0.0005
+el: name=Magnesium  ; f=0.00002
+el: name=Phosphor   ; f=0.00016
+el: name=Sulfur     ; f=0.00073
+el: name=Chlorine   ; f=0.00119
+el: name=Potassium  ; f=0.00032
+el: name=Calcium    ; f=0.00002
+el: name=Iron       ; f=0.00002
+el: name=Zinc       ; f=0.00002
```

```
CartilageBV: d=1.10 g/cm3 ; n=11
+el: name=Hydrogen   ; f=0.096
+el: name=Carbon     ; f=0.099
+el: name=Nitrogen   ; f=0.022
+el: name=Oxygen     ; f=0.744
+el: name=Sodium     ; f=0.005
+el: name=Phosphor   ; f=0.022
+el: name=Sulfur     ; f=0.009
+el: name=Chlorine   ; f=0.003
+el: name=Argon      ; f=0.0
+el: name=Potassium  ; f=0.0
+el: name=Calcium    ; f=0.0

316L: d=8.03 g/cm3 ; n=10;
+el: name=Carbon     ; f=0.0003
+el: name=Nitrogen   ; f=0.001
+el: name=Silicon    ; f=0.0075
+el: name=Phosphor   ; f=0.00045
+el: name=Sulfur     ; f=0.0003
+el: name=Chromium   ; f=0.17
+el: name=Manganese  ; f=0.02
+el: name=Iron       ; f=0.65545
+el: name=Nickel     ; f=0.12
+el: name=Molybdenu  ; f=0.025

304: d=5.6 g/cm3 ; n=9
+el: name=Carbon     ; f=0.0008
+el: name=Nitrogen   ; f=0.001
+el: name=Silicon    ; f=0.0075
+el: name=Phosphor   ; f=0.00045
+el: name=Sulfu      ; f=0.0003
+el: name=Chromium   ; f=0.19
+el: name=Manganese  ; f=0.02
+el: name=Iron       ; f=0.68745
+el: name=Nickel     ; f=0.0925

SSBV: d=8 g/cm3 ; n=7
+el: name=Carbon     ; f=0.0008
+el: name=Silicon    ; f=0.01
+el: name=Phosphor   ; f=0.00045
+el: name=Chromium   ; f=0.19
+el: name=Manganese  ; f=0.02
+el: name=Iron       ; f=0.68375
+el: name=Nickel     ; f=0.095

PeekBV: d=1.31 g/cm3 ; n=3
+el: name=Hydrogen   ; f=0.041954
+el: name=Carbon     ; f=0.791557
+el: name=Oxygen     ; f=0.166489

PMMABV: d=1.19 g/cm3 ; n=3
+el: name=Hydrogen   ; f=0.080542
+el: name=Carbon     ; f=0.59984
+el: name=Oxygen     ; f=0.319618
```

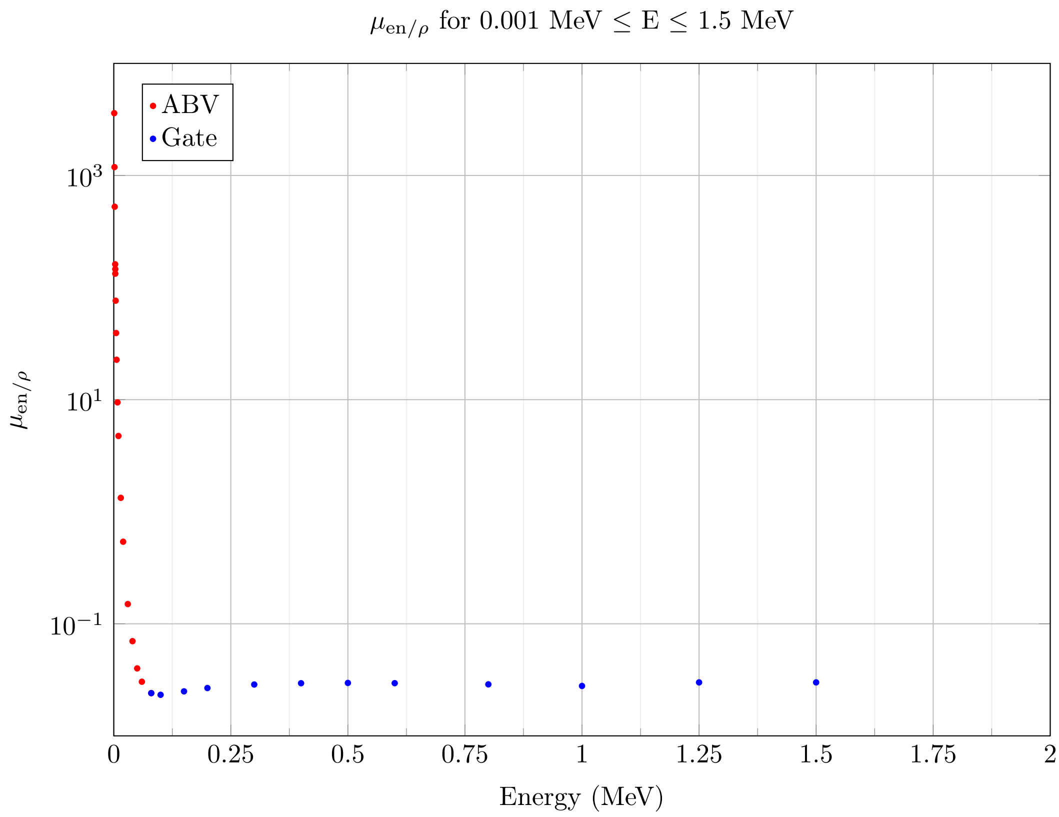

Figure A.1: Mass energy absorption coefficient plot for photons with energies 0.001 MeV $\leq$ E $\leq$ 1.5 MeV.

A.2 Tables and Figures

A.2.1 Air KERMA Strength S_k and Dose Rate Constant Λ

A.2.2 Geometry Function

θ (°)	r (cm) 0	0.1	0.2	0.25	0.3	0.4	0.5	0.6	0.7	0.75	0.8	0.9	1
0	-32.653	-4.85E+01	1.07E+02	3.14E+01	1.68E+01	7.73E+00	4.56E+00	3.04E+00	2.18E+00	1.88E+00	1.64E+00	1.28E+00	1.03E+00
1	-	5.09E+03	1.06E+02	3.13E+01	1.68E+01	7.73E+00	4.56E+00	3.04E+00	2.18E+00	1.88E+00	2.19E+00	1.28E+00	1.03E+00
2	-	2.52E+03	1.04E+02	3.13E+01	1.68E+01	7.73E+00	4.56E+00	3.04E+00	2.18E+00	1.88E+00	2.19E+00	1.28E+00	1.03E+00
3	-	1.67E+03	1.02E+02	3.12E+01	1.68E+01	7.72E+00	4.56E+00	3.03E+00	2.18E+00	1.88E+00	2.19E+00	1.28E+00	1.03E+00
4	-	1.24E+03	9.83E+01	3.10E+01	1.68E+01	7.71E+00	4.55E+00	3.03E+00	2.18E+00	1.88E+00	2.19E+00	1.28E+00	1.03E+00
5	-	9.82E+02	9.46E+01	3.08E+01	1.67E+01	7.71E+00	4.55E+00	3.03E+00	2.18E+00	1.88E+00	2.19E+00	1.28E+00	1.03E+00
6	-	8.11E+02	9.06E+01	3.06E+01	1.67E+01	7.70E+00	4.55E+00	3.03E+00	2.17E+00	1.88E+00	2.19E+00	1.28E+00	1.03E+00
7	-	6.89E+02	8.65E+01	3.03E+01	1.66E+01	7.69E+00	4.54E+00	3.03E+00	2.17E+00	1.88E+00	2.19E+00	1.28E+00	1.03E+00
8	-	5.97E+02	8.26E+01	3.00E+01	1.65E+01	7.67E+00	4.54E+00	3.03E+00	2.17E+00	1.88E+00	2.19E+00	1.28E+00	1.03E+00
9	-	5.26E+02	7.88E+01	2.96E+01	1.64E+01	7.66E+00	4.53E+00	3.03E+00	2.17E+00	1.88E+00	2.18E+00	1.28E+00	1.03E+00
10	-	4.70E+02	7.52E+01	2.93E+01	1.63E+01	7.64E+00	4.53E+00	3.02E+00	2.17E+00	1.88E+00	2.18E+00	1.28E+00	1.03E+00
15	-	3.01E+02	6.03E+01	2.73E+01	1.58E+01	7.54E+00	4.50E+00	3.01E+00	2.16E+00	1.87E+00	2.18E+00	1.28E+00	1.03E+00
20	-	2.19E+02	5.00E+01	2.52E+01	1.51E+01	7.40E+00	4.45E+00	2.99E+00	2.15E+00	1.86E+00	2.17E+00	1.27E+00	1.03E+00
30	-	1.39E+02	3.74E+01	2.15E+01	1.38E+01	7.09E+00	4.34E+00	2.94E+00	2.13E+00	1.84E+00	2.15E+00	1.27E+00	1.02E+00
40	-	1.03E+02	3.03E+01	1.88E+01	1.26E+01	6.75E+00	4.21E+00	2.88E+00	2.10E+00	1.82E+00	2.13E+00	1.26E+00	1.01E+00
50	-	8.30E+01	2.61E+01	1.68E+01	1.16E+01	6.45E+00	4.09E+00	2.82E+00	2.07E+00	1.80E+00	2.10E+00	1.24E+00	1.01E+00
60	-	7.15E+01	2.34E+01	1.55E+01	1.09E+01	6.21E+00	3.99E+00	2.77E+00	2.04E+00	1.78E+00	2.08E+00	1.23E+00	1.00E+00
70	-	6.48E+01	2.17E+01	1.46E+01	1.04E+01	6.03E+00	3.91E+00	2.74E+00	2.02E+00	1.76E+00	2.07E+00	1.23E+00	9.95E-01
80	-	6.12E+01	2.08E+01	1.41E+01	1.02E+01	5.93E+00	3.86E+00	2.71E+00	2.00E+00	1.75E+00	2.05E+00	1.22E+00	9.91E-01
90	-	6.01E+01	2.05E+01	1.40E+01	1.01E+01	5.89E+00	3.85E+00	2.70E+00	2.00E+00	1.75E+00	2.05E+00	1.22E+00	9.90E-01
100	-	6.12E+01	2.08E+01	1.41E+01	1.02E+01	5.93E+00	3.86E+00	2.71E+00	2.00E+00	1.75E+00	2.05E+00	1.22E+00	9.91E-01
110	-	6.48E+01	2.17E+01	1.46E+01	1.04E+01	6.03E+00	3.91E+00	2.74E+00	2.02E+00	1.76E+00	2.07E+00	1.23E+00	9.95E-01
120	-	7.15E+01	2.34E+01	1.55E+01	1.09E+01	6.21E+00	3.99E+00	2.77E+00	2.04E+00	1.78E+00	2.08E+00	1.23E+00	1.00E+00
130	-	8.30E+01	2.61E+01	1.68E+01	1.16E+01	6.45E+00	4.09E+00	2.82E+00	2.07E+00	1.80E+00	2.10E+00	1.24E+00	1.01E+00
140	-	1.03E+02	3.03E+01	1.88E+01	1.26E+01	6.75E+00	4.21E+00	2.88E+00	2.10E+00	1.82E+00	2.13E+00	1.26E+00	1.01E+00
150	-	1.39E+02	3.74E+01	2.15E+01	1.38E+01	7.09E+00	4.34E+00	2.94E+00	2.13E+00	1.84E+00	2.15E+00	1.27E+00	1.02E+00
160	-	2.19E+02	5.00E+01	2.52E+01	1.51E+01	7.40E+00	4.45E+00	2.99E+00	2.15E+00	1.86E+00	2.17E+00	1.27E+00	1.03E+00
165	-	3.01E+02	6.03E+01	2.73E+01	1.58E+01	7.54E+00	4.50E+00	3.01E+00	2.16E+00	1.87E+00	2.18E+00	1.28E+00	1.03E+00
170	-	4.70E+02	7.52E+01	2.93E+01	1.63E+01	7.64E+00	4.53E+00	3.02E+00	2.17E+00	1.88E+00	2.18E+00	1.28E+00	1.03E+00
171	-	5.26E+02	7.88E+01	2.96E+01	1.64E+01	7.66E+00	4.53E+00	3.03E+00	2.17E+00	1.88E+00	2.18E+00	1.28E+00	1.03E+00
172	-	5.97E+02	8.26E+01	3.00E+01	1.65E+01	7.67E+00	4.54E+00	3.03E+00	2.17E+00	1.88E+00	2.19E+00	1.28E+00	1.03E+00
173	-	6.89E+02	8.65E+01	3.03E+01	1.66E+01	7.69E+00	4.54E+00	3.03E+00	2.17E+00	1.88E+00	2.19E+00	1.28E+00	1.03E+00
174	-	8.11E+02	9.06E+01	3.06E+01	1.67E+01	7.70E+00	4.55E+00	3.03E+00	2.17E+00	1.88E+00	2.19E+00	1.28E+00	1.03E+00
175	-	9.82E+02	9.46E+01	3.08E+01	1.67E+01	7.71E+00	4.55E+00	3.03E+00	2.18E+00	1.88E+00	2.19E+00	1.28E+00	1.03E+00
176	-	1.24E+03	9.83E+01	3.10E+01	1.68E+01	7.71E+00	4.55E+00	3.03E+00	2.18E+00	1.88E+00	2.19E+00	1.28E+00	1.03E+00
177	-	1.67E+03	1.02E+02	3.12E+01	1.68E+01	7.72E+00	4.56E+00	3.03E+00	2.18E+00	1.88E+00	2.19E+00	1.28E+00	1.03E+00
178	-	2.52E+03	1.04E+02	3.13E+01	1.68E+01	7.73E+00	4.56E+00	3.04E+00	2.18E+00	1.88E+00	2.19E+00	1.28E+00	1.03E+00
179	-	5.09E+03	1.06E+02	3.13E+01	1.68E+01	7.73E+00	4.56E+00	3.04E+00	2.18E+00	1.88E+00	2.19E+00	1.28E+00	1.03E+00
180	-32.653	-4.85E+01	1.07E+02	3.14E+01	1.68E+01	7.73E+00	4.56E+00	3.04E+00	2.18E+00	1.88E+00	1.64E+00	1.28E+00	1.03E+00

θ (°)	r (cm) 1.25	1.50	1.75	2	2.5	3	3.5	4	4.5	5	6	7	8	9	10
0	6.53E-01	4.51E-01	3.30E-01	2.52E-01	1.61E-01	1.11E-01	8.18E-02	6.26E-02	4.95E-02	4.00E-02	2.78E-02	2.04E-02	1.56E-02	1.24E-02	1.00E-02
1	6.53E-01	4.51E-01	2.89E-01	2.52E-01	1.61E-01	1.11E-01	8.18E-02	6.26E-02	4.95E-02	4.00E-02	2.78E-02	2.04E-02	1.56E-02	1.24E-02	1.00E-02
2	6.53E-01	4.51E-01	2.89E-01	2.52E-01	1.61E-01	1.11E-01	8.18E-02	6.26E-02	4.95E-02	4.00E-02	2.78E-02	2.04E-02	1.56E-02	1.24E-02	1.00E-02
3	6.53E-01	4.51E-01	2.89E-01	2.52E-01	1.61E-01	1.11E-01	8.18E-02	6.26E-02	4.95E-02	4.00E-02	2.78E-02	2.04E-02	1.56E-02	1.24E-02	1.00E-02
4	6.53E-01	4.51E-01	2.89E-01	2.52E-01	1.61E-01	1.11E-01	8.18E-02	6.26E-02	4.95E-02	4.00E-02	2.78E-02	2.04E-02	1.56E-02	1.24E-02	1.00E-02
5	6.53E-01	4.51E-01	2.89E-01	2.52E-01	1.61E-01	1.11E-01	8.18E-02	6.26E-02	4.95E-02	4.00E-02	2.78E-02	2.04E-02	1.56E-02	1.24E-02	1.00E-02
6	6.53E-01	4.50E-01	2.89E-01	2.52E-01	1.61E-01	1.11E-01	8.18E-02	6.26E-02	4.95E-02	4.00E-02	2.78E-02	2.04E-02	1.56E-02	1.24E-02	1.00E-02
7	6.53E-01	4.50E-01	2.89E-01	2.52E-01	1.61E-01	1.11E-01	8.18E-02	6.26E-02	4.95E-02	4.00E-02	2.78E-02	2.04E-02	1.56E-02	1.24E-02	1.00E-02
8	6.52E-01	4.50E-01	2.89E-01	2.52E-01	1.61E-01	1.11E-01	8.18E-02	6.26E-02	4.95E-02	4.00E-02	2.78E-02	2.04E-02	1.56E-02	1.24E-02	1.00E-02
9	6.52E-01	4.50E-01	2.89E-01	2.52E-01	1.61E-01	1.11E-01	8.18E-02	6.26E-02	4.95E-02	4.00E-02	2.78E-02	2.04E-02	1.56E-02	1.24E-02	1.00E-02
10	6.52E-01	4.50E-01	2.88E-01	2.52E-01	1.61E-01	1.11E-01	8.18E-02	6.26E-02	4.95E-02	4.00E-02	2.78E-02	2.04E-02	1.56E-02	1.24E-02	1.00E-02
15	6.52E-01	4.50E-01	2.88E-01	2.52E-01	1.61E-01	1.11E-01	8.18E-02	6.26E-02	4.95E-02	4.00E-02	2.78E-02	2.04E-02	1.56E-02	1.23E-02	1.00E-02
20	6.51E-01	4.50E-01	2.88E-01	2.52E-01	1.61E-01	1.11E-01	8.18E-02	6.26E-02	4.94E-02	4.00E-02	2.78E-02	2.04E-02	1.56E-02	1.23E-02	1.00E-02
30	6.48E-01	4.48E-01	2.88E-01	2.51E-01	1.61E-01	1.11E-01	8.18E-02	6.26E-02	4.94E-02	4.00E-02	2.78E-02	2.04E-02	1.56E-02	1.23E-02	1.00E-02
40	6.46E-01	4.47E-01	2.87E-01	2.51E-01	1.60E-01	1.11E-01	8.17E-02	6.26E-02	4.94E-02	4.00E-02	2.78E-02	2.04E-02	1.56E-02	1.23E-02	1.00E-02
50	6.43E-01	4.46E-01	2.86E-01	2.50E-01	1.60E-01	1.11E-01	8.17E-02	6.25E-02	4.94E-02	4.00E-02	2.78E-02	2.04E-02	1.56E-02	1.23E-02	1.00E-02
60	6.40E-01	4.44E-01	2.86E-01	2.50E-01	1.60E-01	1.11E-01	8.16E-02	6.25E-02	4.94E-02	4.00E-02	2.78E-02	2.04E-02	1.56E-02	1.23E-02	1.00E-02
70	6.38E-01	4.43E-01	2.85E-01	2.50E-01	1.60E-01	1.11E-01	8.16E-02	6.25E-02	4.94E-02	4.00E-02	2.78E-02	2.04E-02	1.56E-02	1.23E-02	1.00E-02
80	6.36E-01	4.43E-01	2.85E-01	2.49E-01	1.60E-01	1.11E-01	8.16E-02	6.25E-02	4.94E-02	4.00E-02	2.78E-02	2.04E-02	1.56E-02	1.23E-02	1.00E-02
90	6.36E-01	4.42E-01	2.85E-01	2.49E-01	1.60E-01	1.11E-01	8.16E-02	6.25E-02	4.94E-02	4.00E-02	2.78E-02	2.04E-02	1.56E-02	1.23E-02	1.00E-02
100	6.36E-01	4.43E-01	2.85E-01	2.49E-01	1.60E-01	1.11E-01	8.16E-02	6.25E-02	4.94E-02	4.00E-02	2.78E-02	2.04E-02	1.56E-02	1.23E-02	1.00E-02
110	6.38E-01	4.43E-01	2.85E-01	2.50E-01	1.60E-01	1.11E-01	8.16E-02	6.25E-02	4.94E-02	4.00E-02	2.78E-02	2.04E-02	1.56E-02	1.23E-02	1.00E-02
120	6.40E-01	4.44E-01	2.86E-01	2.50E-01	1.60E-01	1.11E-01	8.16E-02	6.25E-02	4.94E-02	4.00E-02	2.78E-02	2.04E-02	1.56E-02	1.23E-02	1.00E-02
130	6.43E-01	4.46E-01	2.86E-01	2.50E-01	1.60E-01	1.11E-01	8.17E-02	6.25E-02	4.94E-02	4.00E-02	2.78E-02	2.04E-02	1.56E-02	1.23E-02	1.00E-02
140	6.46E-01	4.47E-01	2.87E-01	2.51E-01	1.60E-01	1.11E-01	8.17E-02	6.26E-02	4.94E-02	4.00E-02	2.78E-02	2.04E-02	1.56E-02	1.23E-02	1.00E-02
150	6.48E-01	4.48E-01	2.88E-01	2.51E-01	1.61E-01	1.11E-01	8.18E-02	6.26E-02	4.94E-02	4.00E-02	2.78E-02	2.04E-02	1.56E-02	1.23E-02	1.00E-02
160	6.51E-01	4.50E-01	2.88E-01	2.52E-01	1.61E-01	1.11E-01	8.18E-02	6.26E-02	4.94E-02	4.00E-02	2.78E-02	2.04E-02	1.56E-02	1.23E-02	1.00E-02
165	6.52E-01	4.50E-01	2.88E-01	2.52E-01	1.61E-01	1.11E-01	8.18E-02	6.26E-02	4.95E-02	4.00E-02	2.78E-02	2.04E-02	1.56E-02	1.23E-02	1.00E-02
170	6.52E-01	4.50E-01	2.88E-01	2.52E-01	1.61E-01	1.11E-01	8.18E-02	6.26E-02	4.95E-02	4.00E-02	2.78E-02	2.04E-02	1.56E-02	1.24E-02	1.00E-02
171	6.52E-01	4.50E-01	2.89E-01	2.52E-01	1.61E-01	1.11E-01	8.18E-02	6.26E-02	4.95E-02	4.00E-02	2.78E-02	2.04E-02	1.56E-02	1.24E-02	1.00E-02
172	6.52E-01	4.50E-01	2.89E-01	2.52E-01	1.61E-01	1.11E-01	8.18E-02	6.26E-02	4.95E-02	4.00E-02	2.78E-02	2.04E-02	1.56E-02	1.24E-02	1.00E-02
173	6.53E-01	4.50E-01	2.89E-01	2.52E-01	1.61E-01	1.11E-01	8.18E-02	6.26E-02	4.95E-02	4.00E-02	2.78E-02	2.04E-02	1.56E-02	1.24E-02	1.00E-02
174	6.53E-01	4.50E-01	2.89E-01	2.52E-01	1.61E-01	1.11E-01	8.18E-02	6.26E-02	4.95E-02	4.00E-02	2.78E-02	2.04E-02	1.56E-02	1.24E-02	1.00E-02
175	6.53E-01	4.51E-01	2.89E-01	2.52E-01	1.61E-01	1.11E-01	8.18E-02	6.26E-02	4.95E-02	4.00E-02	2.78E-02	2.04E-02	1.56E-02	1.24E-02	1.00E-02
176	6.53E-01	4.51E-01	2.89E-01	2.52E-01	1.61E-01	1.11E-01	8.18E-02	6.26E-02	4.95E-02	4.00E-02	2.78E-02	2.04E-02	1.56E-02	1.24E-02	1.00E-02
177	6.53E-01	4.51E-01	2.89E-01	2.52E-01	1.61E-01	1.11E-01	8.18E-02	6.26E-02	4.95E-02	4.00E-02	2.78E-02	2.04E-02	1.56E-02	1.24E-02	1.00E-02
178	6.53E-01	4.51E-01	2.89E-01	2.52E-01	1.61E-01	1.11E-01	8.18E-02	6.26E-02	4.95E-02	4.00E-02	2.78E-02	2.04E-02	1.56E-02	1.24E-02	1.00E-02
179	6.53E-01	4.51E-01	2.89E-01	2.52E-01	1.61E-01	1.11E-01	8.18E-02	6.26E-02	4.95E-02	4.00E-02	2.78E-02	2.04E-02	1.56E-02	1.24E-02	1.00E-02
180	6.53E-01	4.51E-01	3.30E-01	2.52E-01	1.61E-01	1.11E-01	8.18E-02	6.26E-02	4.95E-02	4.00E-02	2.78E-02	2.04E-02	1.56E-02	1.24E-02	1.00E-02

Figure A.2: Geometry function

A.2.3 Radial Dose Function

Table A.1: Ring dimensions used for g(r) measurements

Ring Dimensions				
r (cm)	OD (cm)	ID (cm)	Height (cm)	Volume (cm^3)
0.2	0.195	0.205	0.1	0.126
0.25	0.255	0.245	0.1	0.157
0.5	0.505	0.495	0.1	0.314
0.75	0.755	0.745	0.1	0.471
1	1.005	0.995	0.1	0.628
1.5	1.525	1.475	0.5	23.562
2	2.025	1.975	0.5	31.416
3	3.025	2.975	0.5	47.124
4	4.025	3.975	0.5	62.832
5	5.025	4.975	0.5	78.540
6	6.05	5.95	1	376.991
8	8.05	7.95	1	502.655
10	10.05	9.95	1	628.319

A.2.4 2D Anisotropy Function

Table A.2: Cylinder dimensions used for F(r = 4mm, θ) measurements, where h=0.1mm

Cylinder Dimensions for r = 4 mm			
θ	OD (mm)	ID (mm)	Z = r Cos(θ) (mm)
90 ± 88	0.19	0.09	∓3.998
90 ± 86	0.33	0.23	∓3.990
90 ± 84	0.47	0.37	∓3.978
90 ± 82	0.61	0.51	∓3.961
90 ± 80	0.74	0.64	∓3.939
90 ± 70	1.42	1.32	∓3.759
90 ± 60	2.05	1.95	∓3.464
90 ± 50	2.62	2.52	∓3.064
90 ± 40	3.11	3.01	∓2.571
90 ± 30	3.51	3.41	∓2.000
90 ± 20	3.81	3.71	∓1.368
90 ± 10	3.99	3.89	∓0.695
90 ± 0	4.05	3.95	0
90 ± 90	Cube dimensions 0.1 mm x 0.1 mm x 0.1 mm		

Table A.3: Cylinder dimensions used for F(r = 6mm, θ) measurements, where h=0.1mm

Cylinder Dimensions for r = 6 mm			
θ	OD (mm)	ID (mm)	Z = r Cos(θ) (mm)
90 ± 88	0.26	0.16	∓5.996
90 ± 86	0.47	0.37	∓5.985
90 ± 84	0.68	0.58	∓5.967
90 ± 82	0.89	0.79	∓5.942
90 ± 80	1.09	0.99	∓5.909
90 ± 70	2.10	2.00	∓5.638
90 ± 60	3.05	2.95	∓5.196
90 ± 50	3.91	3.81	∓4.596
90 ± 40	4.65	4.55	∓3.857
90 ± 30	5.25	5.15	∓3.000
90 ± 20	5.69	5.59	∓2.052
90 ± 10	5.96	5.86	∓1.042
90 ± 0	6.05	5.95	0
90 ± 90	Cube dimensions 0.1 mm x 0.1 mm x 0.1 mm		

Table A.4: Cylinder dimensions used for F(r = 10mm, θ) measurements, where h=0.1mm

Cylinder Dimensions for r = 10 mm			
θ	OD (mm)	ID (mm)	Z = r Cos(θ) (mm)
90 ± 88	0.4	0.3	$\mp$9.994
90 ± 86	0.75	0.65	$\mp$9.976
90 ± 84	1.1	1.00	$\mp$9.945
90 ± 82	1.44	1.34	$\mp$9.903
90 ± 80	1.79	1.69	$\mp$9.848
90 ± 70	3.47	3.37	$\mp$9.397
90 ± 60	5.05	4.95	$\mp$8.660
90 ± 50	6.48	6.38	$\mp$7.660
90 ± 40	7.71	7.61	$\mp$6.428
90 ± 30	8.71	8.61	$\mp$5.000
90 ± 20	9.45	9.35	$\mp$3.420
90 ± 10	9.90	9.80	$\mp$1.736
90 ± 0	10.05	9.98	0
90 ± 90	Cube dimensions 0.1 mm x 0.1 mm x 0.1 mm		

Table A.5: Cylinder dimensions used for F(r = 35mm, θ) measurements, where h=0.5mm

Cylinder Dimensions for r = 35 mm			
θ	OD (mm)	ID (mm)	Z = r Cos(θ) (mm)
90 ± 88	1.47	0.97	$\mp$34.979
90 ± 86	2.69	2.17	$\mp$34.915
90 ± 84	3.91	3.41	$\mp$34.808
90 ± 82	5.12	4.62	$\mp$34.659
90 ± 80	6.33	5.83	$\mp$34.468
90 ± 70	12.22	11.72	$\mp$32.889
90 ± 60	17.75	17.25	$\mp$30.311
90 ± 50	22.75	22.25	$\mp$26.812
90 ± 40	27.06	26.56	$\mp$22.498
90 ± 30	30.56	30.06	$\mp$17.5
90 ± 20	33.14	32.64	$\mp$11.971
90 ± 10	34.72	34.22	$\mp$6.078
90 ± 0	35.25	34.75	0
90 ± 90	Cube dimensions 0.5 mm x 0.5 mm x 0.5 mm		

Table A.6: Cylinder dimensions used for F(r = 60mm, θ) measurements, where h=1mm

Cylinder Dimensions for r = 60 mm			
θ	OD (mm)	ID (mm)	Z = r Cos(θ) (mm)
90 $\pm$ 88	2.59	1.59	$\mp$59.963
90 $\pm$ 86	4.69	3.69	$\mp$59.854
90 $\pm$ 84	6.77	5.77	$\mp$59.671
90 $\pm$ 82	8.85	7.85	$\mp$59.416
90 $\pm$ 80	10.92	9.92	$\mp$59.088
90 $\pm$ 70	21.00	20.02	$\mp$56.382
90 $\pm$ 60	30.50	29.50	$\mp$51.962
90 $\pm$ 50	39.07	38.07	$\mp$45.963
90 $\pm$ 40	46.46	45.46	$\mp$38.567
90 $\pm$ 30	52.46	51.46	$\mp$30.00
90 $\pm$ 20	56.88	55.88	$\mp$20.521
90 $\pm$ 10	59.59	58.59	$\mp$10.419
90 $\pm$ 0	60.50	59.50	0
90 $\pm$ 90	Cube dimensions 1 mm x 1 mm x 1 mm		

Table A.7: Cylinder dimensions used for F(r = 100mm, θ) measurements, where h=1mm

Cylinder Dimensions for r = 100 mm			
θ	OD (mm)	ID (mm)	Z = r Cos(θ) (mm)
90 $\pm$ 88	3.99	2.99	$\mp$99.939
90 $\pm$ 86	7.48	6.48	$\mp$99.756
90 $\pm$ 84	10.95	9.95	$\mp$99.452
90 $\pm$ 82	14.42	13.42	$\mp$99.027
90 $\pm$ 80	17.86	16.86	$\mp$98.481
90 $\pm$ 70	34.70	33.70	$\mp$93.969
90 $\pm$ 60	50.50	49.50	$\mp$86.603
90 $\pm$ 50	64.78	63.78	$\mp$76.064
90 $\pm$ 40	77.10	76.10	$\mp$64.279
90 $\pm$ 30	87.10	86.10	$\mp$50.000
90 $\pm$ 20	94.47	93.47	$\mp$34.202
90 $\pm$ 10	98.98	97.98	$\mp$517.365
90 $\pm$ 0	100.50	99.5	0
90 $\pm$ 90	Cube dimensions 1 mm x 1 mm x 1 mm		